



University of  
New Hampshire

# WAVE ENERGY CONVERSION BUOY

For deployment at the Appledore Island site off the  
Isle of Shoals

Nate Bent  
Nathaniel Brown  
Corin Craig  
Molly Curran  
Pedro Da Masceno  
Andrew Diorro  
Kaare Francis  
Ryan Kirby  
John Pauley  
Jeff Sweeny

Advisors:  
Kenneth Baldwin  
M. Robinson Swift  
Corey Sullivan  
Special thanks to:  
Matt Rowell  
Prof. Carlos Andre Dias Bezerra



4/24/15

## **Acknowledgments**

Our appreciation goes out to the individuals and organizations that helped facilitate and fund our project. We would like to extend our gratitude to Professor M. Robinson Swift and Professor Kenneth Baldwin who were our advisers, along with our graduate advisor Corey Sullivan. Without their enthusiasm and input, this project would not have been as successful. We would also like to thank Matt Rowell for sharing his input on our mooring design and helping us coordinate with the UNH boat captains, Scott Cambell and Drummond Byles for their help in the machine shop and UNH boat captains for help deploying our buoy. Lastly, we would like to thank the OE and ME Departments and NH Sea Grant Foundation for funding our project.

# Table of Contents

Acknowledgments.....	1
Abstract.....	3
Introduction.....	4
Preliminary Field Test.....	5
Mooring.....	5
Transportation.....	6
Deployment & Recovery.....	6
Follower Buoy and Spar System.....	7
Heave plate design.....	13
Power Take Off System (PTO).....	15
PTO Design.....	26
Data Acquisition.....	28
Pressure Sensor Data.....	28
On-board Data Acquisition System.....	33
Final Design.....	35
Field Test.....	40
Conclusion.....	44
References.....	45
Appendix.....	46
Future Work.....	46
Budget.....	47
Part Locations.....	48
Matlab Code.....	49
PTO.....	49
Pressure transducer analysis code.....	52
Arduino Code.....	54
Procedures.....	60
Assembly Procedure.....	60

## **Abstract**

The Wave Energy Conversion Buoy (WECB) is a senior design project in the Undergraduate Ocean Research Program (TECH 797). The WECB team's goal is to design and construct a point absorber wave energy device, which will generate electrical power from ocean waves. A point absorber buoy generates power by using the relative motion between two buoys (the middle spar buoy and the follower "donut" buoy) to drive a dual rack and pinion gear system that in turn spins a generator. The intent of the project is to demonstrate wave energy as a viable source of renewable energy for powering the Shoals Marine Laboratory located on Appledore Island, Isles of Shoals, off the coast of Maine and New Hampshire.

The power take off was designed using a dual rack and pinion system utilizing clutch bearings and a flywheel to keep the generator spinning the same direction along the entire period of the passing wave. The follower buoy dimensions were optimized measuring 5' in diameter and 18" high that resulted in a 1.9 second damped natural period average in order to increase the responsiveness. An onboard and remote data acquisition system was developed to record power output of generator onto an SD card via an Arduino Uno and a GSM shield was utilized to also remotely monitor the power output of the generator during deployments.

The 2013/2014 WECB was deployed to test its performance as well as a mooring system that consisted of a pressure transducer which was used to calculate an energy spectra to compare the available power in the waves to the power output by the generator. Those parameters were used to calculate a water to wire efficiency. The 2014/2015 WECB was later deployed using the NOAA vessel, Cocheco. The buoy was towed during transportation which resulted in a mechanical failure making the first deployment unsuccessful. A 2nd deployment will be scheduled making sure the buoy is deployed via a vessel equipped with an A-frame. The 2014/2015 WECB goal is to reach a 20% water to wire efficiency.

## Introduction

In a day and age where substantial energy is consumed due to an increasing population and advancement in technology, alternative energy sources are in high demand. There are many different renewable energy sectors currently being researched, such as solar, wind, geothermal, wave energy, etc. Wave energy has potential for providing a virtually unlimited, clean energy source while having little negative side effects. This process is conducted by capturing and converting available energy from swells and wind waves into a usable form of work, such as electricity. While there are many different designs of wave energy converters, which each utilize a different method of energy extraction and generation, the focus on this project was to efficiently design and innovate an existing Point Absorber Wave Energy Buoy.

A Point Absorber Wave Energy Buoy is a device that utilizes the relative vertical motion between a wave-activated float on the sea surface and a long cylindrical spar to drive a three phase generator. The relative linear motion is then converted into rotational motion through a dual rack and pinion system, which generates rotational torque on the up and down stroke. The angular velocity is increased through a gear ratio of 5:1, in order to meet the required startup torque for the generator. In order to successfully design a WEC, the deployment site location's characteristics must be carefully determined in order to reach acceptable efficiencies. The main characteristics of the ocean that affect the available energy are the height, length, and frequency of the waves.

The Wave Energy Conversion Buoy team from the previous school year paved the way for the design and construction of a point absorber wave energy buoy. The team designed a buoy for a wave height and period of 2 feet and 4 seconds, respectively. The buoy was tested in the Chase Ocean Engineering Laboratory to record power output from the generator. The tank was operated at a 20 centimeter wave height with a 2 second period. Under the specified conditions, the buoy generated approximately 12.5 Watts, producing a water-to-wire efficiency of approximately 14.6%. While the system was functional, there were many improvements necessary to be completed in order to increase the overall power output and efficiency of the buoy.

To improve the Wave Energy Conversion Buoy, the 2015 buoy team focused on optimizing the hydrostatics of the point absorber system to maximize efficiencies. Since the previous buoy was donated from a third party, the geometry was not ideal. Through careful calculation and experimentation, the correct geometry was determined, and a new buoy was manufactured to the correct design specifications. Additionally, the spar length and buoyancy were modified, as well as the power take off design and enclosed housing. The goal of the energy generated within the buoy was to assist offsetting the power consumption by the diesel generators used on Appledore Island at the Isle of Shoals. This would be accomplished though the generator being connected to the battery bank on the island that is currently installed. Since there is a laboratory on shore, having a point absorber buoy deployed would be a valuable asset in the goal of making the island a more self-sustainable entity.

## Preliminary Field Test

The group was requested to perform a field test in order to prove the 2014 groups design. This test was held on October 31, 2014 using the UNH Research Vessel Gulf Challenger. The buoy was deployed at Isle of Shoals area at an approximate depth of 80ft.

## Mooring

An essential part of the deployment was to design the mooring system which should be easy to deploy and reliable. The mooring should be able to hold the WECB in place but with enough room to move around. The end was result satisfied both criteria while being reliable and easy to deploy.

The designed mooring system can be easily explained by splitting it in half, the buoy side and the pressure transducer side as shown in *figure 1*. The buoy side, as named, is the side that the buoy was placed; there were four sets of ropes connected with shackles, in a total length of 220ft, one end connected to the buoy and the second end connected to a chain of eight 25 lb. stud-links. The chain was connected to a 150 ft. rope that went through the bottom and connected to two of the 25lb chain stud-links, the beginning of the pressure transducer side. This side was composed by an upright tensioned rope - one end connected to the chain and the other end to a pressure transducer. A buoy for retrieval was on the top of the pressure transducer side and a second buoy was used to keep the sensor upright.

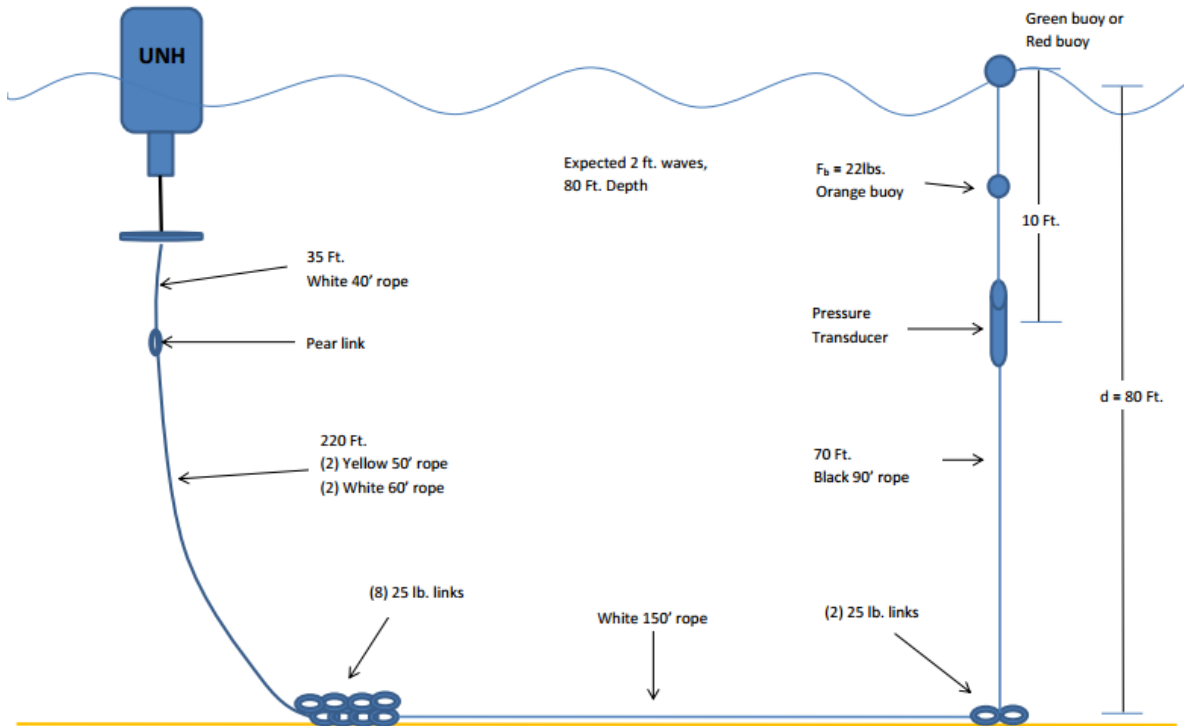


Figure 1 - Mooring System Schematic

## **Transportation**

A transportation plan had to be organized in order to transport the buoy to the UNH Pier at New Castle - NH, where the R/V Gulf Challenger was docked.

Two options were proposed, tow it using a boat trailer or transport the buoy disassembled to the pier. To save time and avoid any surprise during the assembly on the dock, it was fastened on a trailer using cargo straps and wooden blocks to avoid lateral movement.

All the mooring materials, data acquisition and spare hardware were loaded inside a pick-up truck, in an organized way to facilitate the deployment on the deck.

## **Deployment & Recovery**

The buoy was deployed at the Isle of Shoals area at an approximate depth of 80 ft. It was deployed in three steps: buoy, mooring and pressure transducer.

During the first step, the team used the R/V Gulf Challenger A-Frame to deploy the buoy in the water. One requirement to deploy the buoy was that it needed be lifted at a certain angle in order to not flood the PTO and the sensors, so a dedicated lifting rigging was designed to keep the needed angle.

The second step was to deploy the mooring system. In order to assure no issues with the ropes during the mooring deployment, all the ropes were stretched on the deck to ensure that there was no entanglement between the parts.

The third and final step of the deployment was to deploy the pressure transducer and two buoys. This step was changing since the team had to shorten the rope to a certain length to ensure that the pressure transducer was 10ft below the water line.

The buoy recovery took more time and attention from the team and the crew since the work had to be done close to the edge of the boat. Similar to the deployment, the recovery was split in three main steps but in the opposite direction. The first part that came onboard was the pressure transducer and the buoys; after that, the mooring lines and the chains, and then finally the buoy.

## Follower Buoy and Spar System

One of the main aspects of the project was the redesign of the float follower buoy. The purpose of the float is to be extremely responsive to the waves in order to achieve maximum relative motion between the spar buoy and the float buoy. In order to attain this, the buoy must have a small natural period, specifically smaller than the proposed average wave periods of the desired deployment location. The average wave period north east of Appledore Island in the Isle of Shoals was found to be approximately 4 seconds from a site study conducted by the 2013 UNH wave energy team. The buoy from the 2013-2014 Wave Energy Conversion Team was donated to them thus the dimensions of the float were not optimal for the wave conditions at the deployment site. Both experimental tests and theoretical calculations were performed to determine that the surface plane area must be increased and the mass must be decreased in order to increase the natural frequency which is inversely related to the natural period. The final design of the float which has a 5 foot diameter and is 18 inches in height with an expected natural period of 1.88 seconds. After optimizing the dimensions of float, several options were considered for the fabrication of the buoy. After considering factors such as quality, cost, and production time, the Gilman Corporation was chosen to fabricate the buoy. The Buoy was created from a strong Solflite Ionomer closed cell foam which was extruded as continuous flat sheets wound cylindrically and densified using heat and pressure.

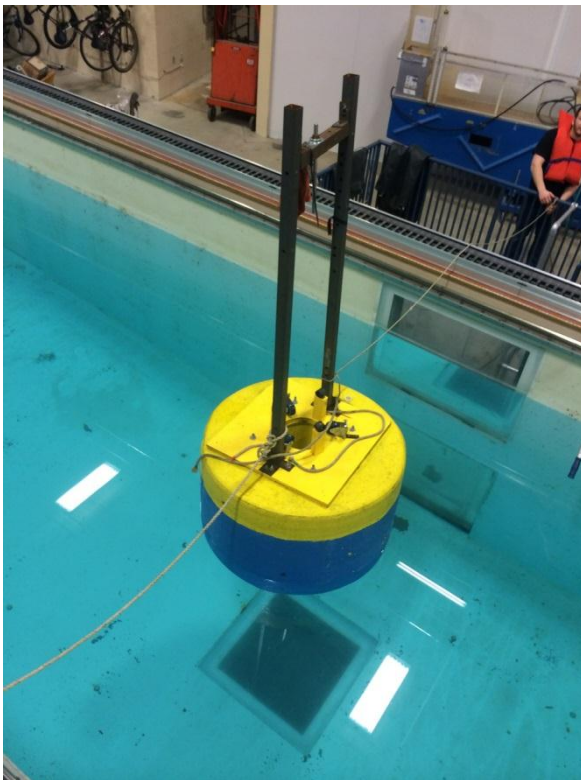


*Figure 2: Photo from the experimental push test of the 2013/14 float in the Jere A. Chase Ocean Engineering facility.*

The 2013/14 follower buoy was tested in the Jere E. Chase Ocean Engineering Laboratory on December 4<sup>th</sup>, 2014, as shown in *figure 2*. The natural period of the buoy was investigated by exciting the buoy in the water and tracking its motion. Because the draft of this particular buoy is so small, a typical drop test could not be executed. Instead, the buoy was displaced by forcing it underwater an arbitrary distance and releasing it. The dynamic response was recorded using Optical Positioning Instrumentation and Evaluation System (OPIE) and evaluated using MATLAB. The software operates by tracking black dots on the buoy with a high speed digital camera, plotting the motion of the dots at 30 frames per second. The data of the two points that were tracked is shown below in *figure 5*. While *figures 3 and 4* show the photos OPIE took to track the motion of the float. The natural period of the 2013/14 follower buoy was found to be 3.1 seconds, which serves as a comparison for other designs.





Figure 3: OPIE image of the 2013/14 float with the black dots used for tracking.



Figure 4: OPIE image of the 1/10<sup>th</sup> scaled model buoy with the black dots used for tracking.

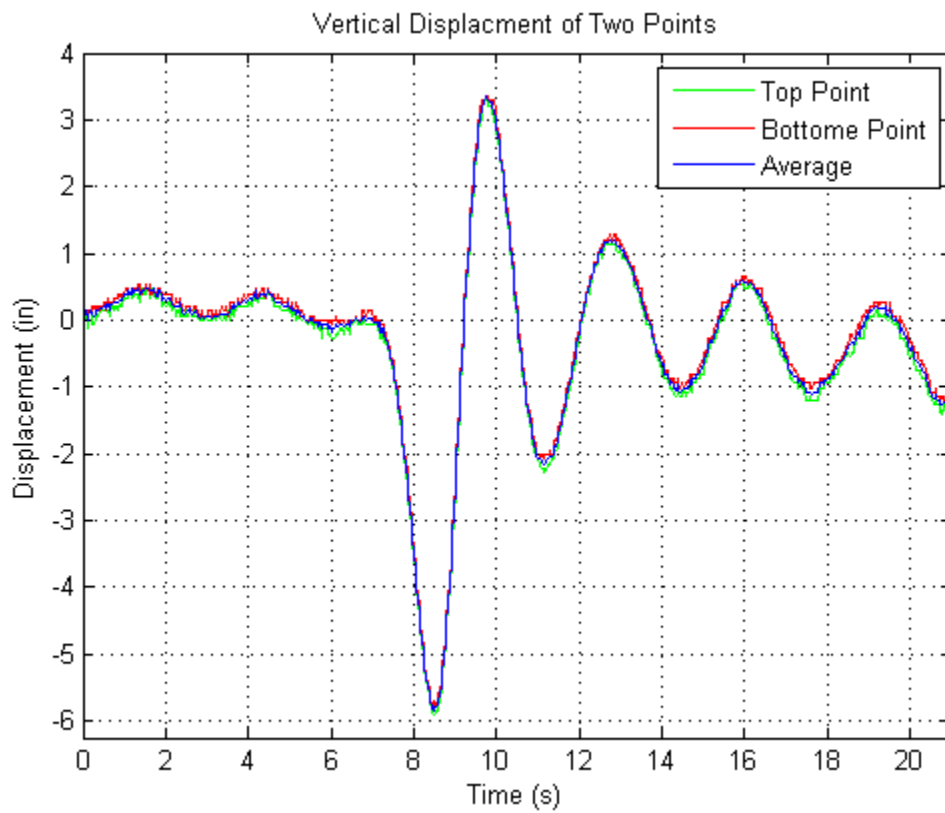


Figure 5: Data achieved from the push test of the 2013/13 float using OPIE and Matlab programming,

An analytical approach was used in attempting to optimize the follower buoy starting with basic concepts of hydrostatics. When a buoyant object sits in water, the weight is balanced by an upward

buoyant force. A static force balance is achieved by a buoyant force  $B$  that is equal to the follower buoy weight  $W$ . The force balance is represented in *equation 1*

$$W = B = \rho g A_p d \quad (1)$$

Where  $\rho$  is the water density assumed as  $1000 \text{ kg/m}^3$  in the laboratory,  $g$  is the gravitational constant  $9.81 \text{ m/s}^2$ ,  $A_p$  is the water plane area, and  $d$  is the draft, which is described as the vertical displacement of the follower buoy below the waterline. The resultant of these terms is a force that is equal to the weight of the displaced water.

When the draft is changing while the follower buoy is moving, it then becomes a dynamic system, such that equations of motion can be determined. Taking a dynamic force balance, the motion is characterized by the vertical displacement  $x$  from the waterline. The buoyant force  $B$  subtracted by the weight force  $W$  reduces to a second order system in the form

$$m_v \frac{dx^2}{dt^2} + \rho g A_p x = 0 \quad (2)$$

Where the coefficients in front of the  $x$  term represent a restoring force to changes in the buoy's equilibrium position. The second order term characterizes a force that is proportional to the acceleration of the buoy. In a real world system, there is also a damping force proportional to the velocity. The damping is investigated with experimental data taken from the buoy.

The term  $m_v$  represents a quantity referred to as the virtual mass. The virtual mass is equal to the force of the follower buoy mass  $m$  plus the added mass  $m_a$ . This added mass value is represented as an additional component of inertia resulting from the follower buoy displacing a certain volume of water as it moves. Putting the system in the necessary form, it can be described in terms of natural frequency  $w_o$

$$\frac{dx^2}{dt^2} + w_o^2 x = 0 \quad (3)$$

Where

$$w_o = \sqrt{\frac{\rho g A_p}{m_a + m}} \quad (4)$$

Since is the added mass is the only unknown in this equation, a natural period can be estimated by applying a relationship to between the follower buoy mass  $m$  and the added mass  $m_a$ . For a follower buoy of this geometry, this relation is approximated as by *Berteaux [4]* in *equation 5*.

$$m_a \cong \frac{m}{2} \quad (5)$$

There are multiple limiting factors in designing the follower buoy, as it is one part of a more complicated mechanical design. The stroke length, which is the vertical range of motion the follower buoy has between the bottom and top stops on the spar, is limited by the follower buoy height. While there was consideration of expanding the length of the spar which was ultimately done, it is useful to design with optimal stroke length in mind. However, as the follower buoy height decreases, increasing the stroke length, there is another physical limitation that the spar could become misaligned and buckle in its guide-hole. A larger follower buoy height supports the spar at points that are more contingent to stability.

With these design parameters, it was concluded that a wider, shorter follower buoy is the optimal design. The width can be approximated based on what is a practical size for the given system. The height needs to work well with the constraints of the spar and yield a draft that is not too large. Values of 5 feet for the buoy diameter and 18 inches for the height were chosen to reflect changes in buoy geometry that will, in theory, decrease the natural period. With these values of height and width, the dynamics of the system can be modeled just as the 2013/14 follower buoy was modeled.

To obtain an understanding of the physical parameters of a new design, a 1/10<sup>th</sup> scale model was constructed and tested in a similar way the 2013/14 buoy was tested. Given a scaled frequency, a technique known as Froude scaling is applied to obtain the characteristics of a full scale model.

The Froude number is a dimensionless number that describes a fluid flow similar to the concept of the Reynolds number. The Froude number  $F$  is the ratio of the inertial forces of the flow to the gravitational forces of the flow. It is assumed that the Froude number is constant for objects of similar geometric and dynamic characteristics. Setting the Froude number of the small and full scale model equal, the timescale relationship for a 1/10<sup>th</sup> scale experiment is given by *equation 6*.

$$\frac{time_{full\ scale}}{time_{model\ scale}} = \sqrt{\frac{d_{full\ model}}{d_{model\ scale}}} = \sqrt{10} \quad (6)$$

Therefore, while the physical parameters of the designed follower buoy are ten times that of the scale model, time is scaled by the square root of ten in testing.

The scale model was constructed with a diameter of 6 inches and a height of 1.8 inches, and was made with Styrofoam, which has a density ( $\rho_{buoy}$ ) of  $27.49\ kg/m^3$ . It was evaluated by performing a push test, and the response was recorded using Optical Positioning Instrumentation and Evaluation System (OPIE) and MATLAB. The raw data of the two points that were tracked is shown below in *figure 6*.

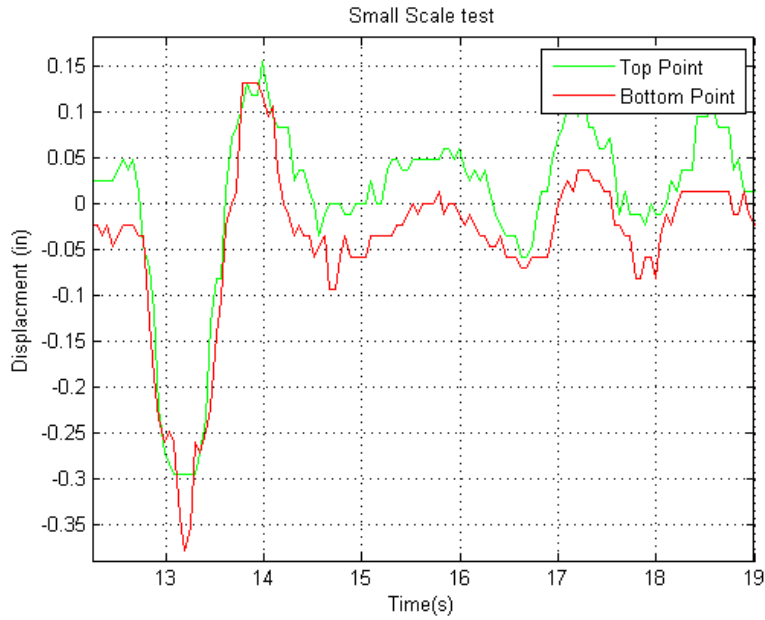


Figure 6: Raw data from the small scale test.

Due to the small nature of the experiment, the noise in the data is a significant. To improve the signal, the two points tracked were averaged and that average was run through a moving average digital filter in Matlab. The best parameters to use with the filter function were determined iteratively. The filtered data is shown below in *figure 7*.

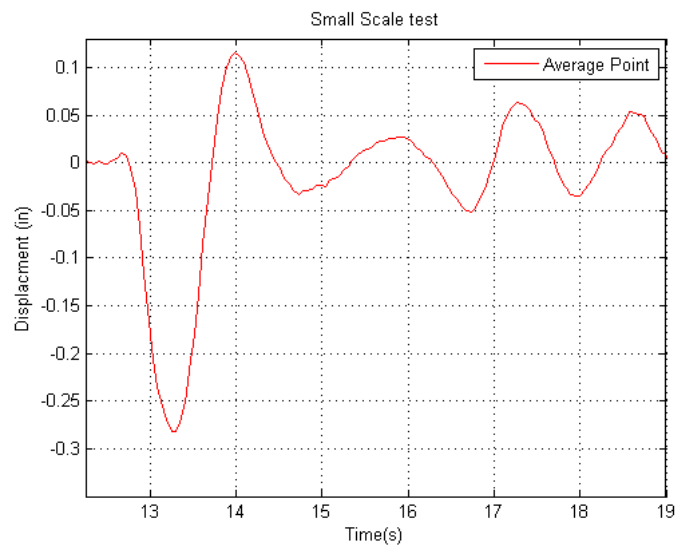
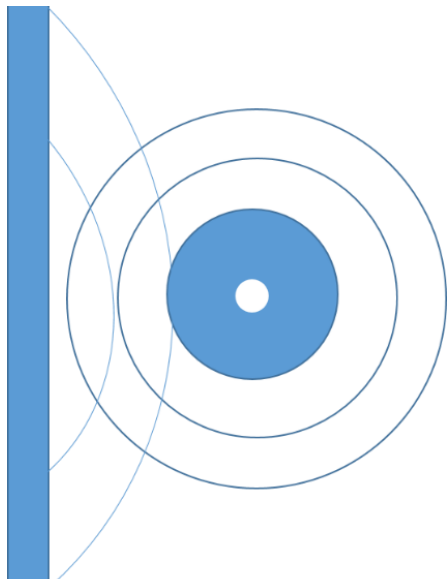


Figure 7: Data from the small scale test, averaged and filtered

Interpreting this motion, the first trough represents an initial displacement. The transient response in question begins when the follower buoy is released and becomes dynamic, represented by

subsequent oscillations. However, it is noticed that the third peak in the oscillations is greater in magnitude than the second. This is inconsistent with a standard second order system and is due to the reflection of the initial wave off of the side of the tank becoming an excitation to the system. This phenomena is represented in *figure 6*.



*Figure 6: Diagram of reflected waves interfering with follower buoy motion*

This interaction with reflected waves was not an issue for the large scale experiment because the large scale follower buoy was farther from the side of the tank and inherently has a greater resistance to wave motion given its greater mass.

Although it is normally beneficial to evaluate the damping ratio and natural period at multiple points, it is determined that follower buoy data becomes unusable when the follower buoy is forced by other means. For this reason, only the first two peaks were used to determine the dynamic characteristics. A natural period of the scale model was calculated as 0.59 seconds. Froude scaling techniques were applied and a natural period of 1.88 seconds was determined for a full scale model.

The decrease in natural period from 3.1 seconds to 1.88 seconds for the follower buoy design demonstrates a rise in the responsiveness of the buoy. It was proven that by decreasing the mass while increasing the water plane area, the natural period of the system would decrease. These findings led to a final follower buoy design being 5 feet in diameter and 18 inches high.

After determining the design of the buoy, the method of fabrication was controversial and varied between several options. The first option for the creation of the float was to create a mold out of different material and pour our own two part foam into the mold and allow it to expand. After speaking with several experienced Ocean Engineering professors, we were informed that pouring foam for such a big design would be a very difficult and precise process, because of the large volume that would have to be filled, the timing and mixing of the two parts that needed to be combined to form the expanding reaction would require much precision. It was determined that with the expensive price of the self-pour foam and the possibility of incorrectly pouring it, therefore was not chosen for fabrication. The second option considered for fabrication was to buy marine grade Styrofoam and cut pieces to the proper shape. Two problems arose from this option. First, the difficulty involved in finding blocks of foam on the order of 5 feet. The second problem was that if being unable to find foam large enough, there is no precise way of cutting something so large. Heat cutting was considered but it was not a strong option.

After doing a great deal of research, considering quality, cost, time, and ease, the Gilman Corporation based out of Gilman Connecticut was chosen to fabricate the buoy. The Gilman Corporation offered the team a significant discount since the buoy was a student research project. It was important that the buoy would be delivered in a timely matter as the team had field

deployments planned for the beginning of April. The company could deliver the buoy free of cost within two weeks and guaranteed a quality product, as they also make buoys for the United States Coast Guard.

The buoy was created out of Softlite Ionomer Foam developed by the Gilman Corporation. When the resin is extruded as foam, the Ionomer properties yield to a product with extraordinary performance. The foam is closed cell, thick walled, low weight, low density, durable, and tough. The foam was extruded as flat sheets and was spirally wound to create the cylindrical shape of the buoy, seen in *figure 8*. Heat and pressure were used to create the structured homogenous buoy and heat cutting was used to achieve the desired shape. The surfaces were then densified using heat and pressure creating a tough, abrasive resistant outer layer. The 9” diameter inner hole and frame upright slots and the threaded rod slots were created with a .06” tolerance, as shown in *figure 7*.



*Figure 7: Picture of the buoy float showing the inner diameter hole, the 4 slotted rod holes, and the 2 frame through holes.*



*Figure 8: Photo from the fabrication process of the buoy float representing that foam sheets wound cylindrically to form the buoy shape.*

### **Heave plate design**

Possibly one of the most important components of the wave energy buoy was the heave plate. The heave plate is what allows for the spar and the follower buoy to have relative motion between each other. The heave plate acts as a sail in a section of water that has a much lower vertical motion than the surface. As the heave plate is placed in lower sections of the water column, the vertical fluid motion decreases in a logarithmic scale. The equation for this reduction in vertical movement is shown below.

$$\xi = \frac{H}{2} \frac{\sinh\left[\frac{2\pi}{L}(h+z)\right]}{\sinh\left(\frac{2\pi}{L}\right)} \quad (7)$$

Because of the logarithmic scale at which fluid motion decreases, it would have been unreasonable to lower the heave plate to a point at which the fluid motion is completely zero. It was decided that a 90% reduction would be reasonable. If fluid motion is equal to 10% of the surface fluid motion,

then  $\xi=H/20$ . The depth at which the heave plate needed to be located is shown below and is equal to at least 16.88 feet below the surface of the water.

$$\frac{H}{20} = \frac{H}{2} \frac{\sinh\left[\frac{2\pi}{46.08ft}(80ft+z)\right]}{\sinh\left(\frac{2\pi}{46.08ft}\right)} \quad z = -16.88 ft$$

The wavelength of 46.08 ft. was found using the dispersion relation. The spar sits approximately 10 feet below the surface of the water. This meant that an extension needed to be added to reach the goal of approximately 17 feet deep. It was decided that an 8 foot galvanized steel pipe would act as an extension for the heave plate. This allowed the heave plate to sit at a depth of 18 feet, reaching the goal of at least 17 feet. The heave plate itself was made of a 4 foot in diameter wooden piece of plywood. This was then covered in a water resistant paint in order to increase the durability.

Now knowing how long the extension need to being the best method of attaching the heave plate need to be determined. Originally the heave plate was connected to the bottom end of the spar through a thread. This thread connection was not the best option to be use since it is not reliable, took a lot of time to assembly and need special tools (pipe wrench) to make the connection.

After some research it was determined that a pin connection would be a good option to be used since it is reliable, safe and the assembly is simple. The best option to attach the heave extension to the spar was to use a flange with a thorough hole where the pin would pass through. After the new connection decision, FEA (finite elements analyses) was performed using SolidWorks. It was also necessary to perform FEA on the heave plate extension to ensure that it would not fail during operation.

Some of the analyses results are shown below.

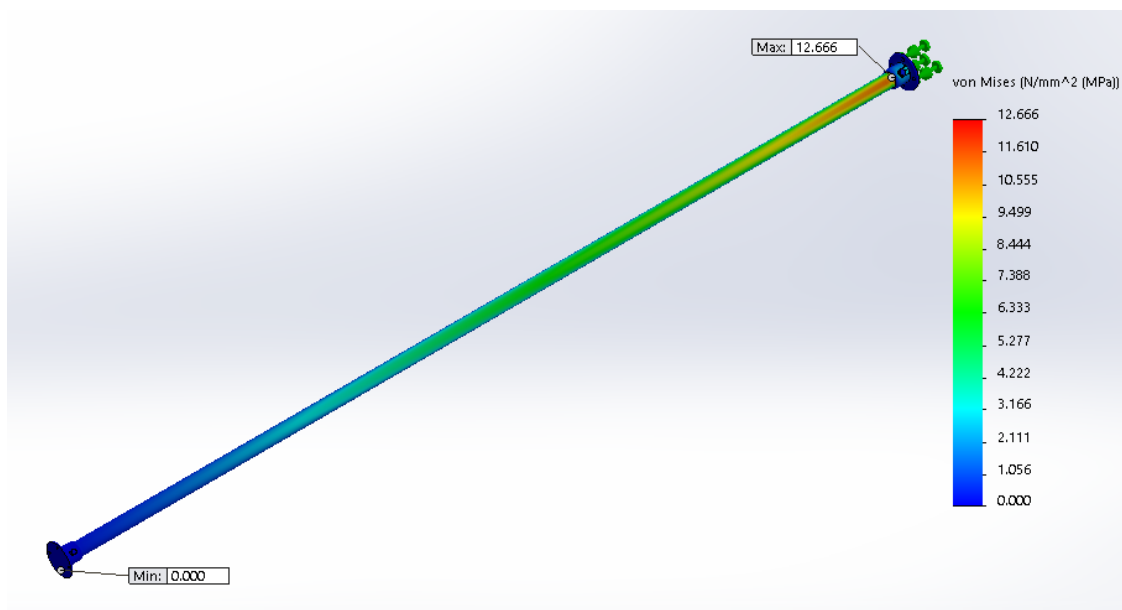


Figure 9 - Von Mises Stress Analysis

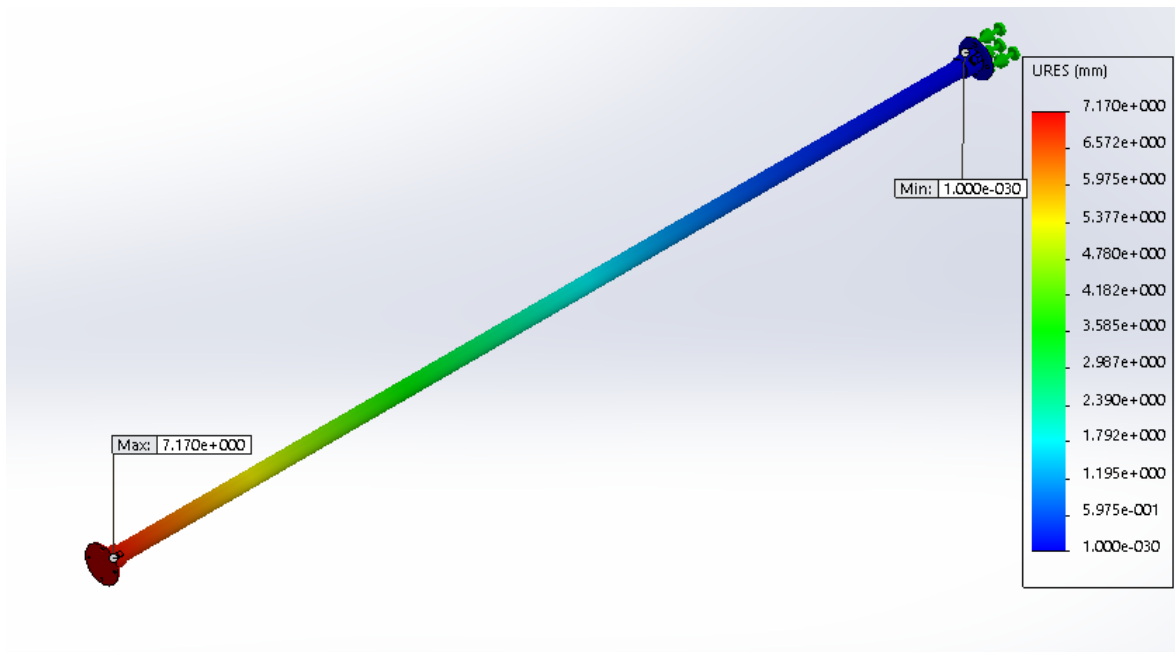


Figure 10 - Displacement Analysis

## Power Take Off System (PTO)

When trying to create the electro mechanical system referred to as the power take off or PTO arguably the most important part of the system is the generator that turns the mechanical motion into electrical power. The generator used by the wave energy buoy team last year was analyzed for a better understanding of it. The generator is a three phase alternator passing through a diode rectifying circuit with a dc output. Three-phase alternators are a suitable choice for small wave energy buoys and wind turbines due to their high efficiencies and lower costs. An inexpensive three-phase alternator was purchased last year for the Wave Energy Buoy team. No specifications were shipped with the product and as a result, analysis was required. The application for this generator is much different than a wind turbine because the generator is powered by the motion of random seas in short intervals, not by constant wind. Since the ocean produces random waves with different velocities it is important to know how the generator will act when encountering a wide range of wave heights. The efficiency of the generator will depend on the angular velocity of the input shaft. By changing the resistance on the output of the generator it will change the amount of torque needed to spin the shaft and therefore control the speed at which the generator spins. The motivation of this experiment was to determine the generators efficiency and optimum resistive load for different angular velocities as well as the motor constants.

The analytical model of the alternator after it passes through the rectifying circuit was found to look at motor constant values as well as torque. To find the efficiency of the generator it was attached to a lathe and spun at different angular velocities. Different resistance loads were placed across the output of the generator with each RPM. The voltage and current output of the generator were recorded so that power output could be calculated and compared to the input power to find the efficiency. To compare the torque to the analytical model a load cell was attached to the end of a lever arm and attached to the generator. The load cell was pinned against the side of the lathe



so that when the generator spun the load cell voltage could be recorded after passing through an amplifier. All the values were recorded using multimeters and a potentiometer was used to control the load on the output. The major results of the experiment are shown below in *table 1*.

Table 1: Major Results of Lathe Experiment

$K_a$	1.1770 ft-lbs/amp
$K_b$	0.1537 V/rpm
Most Efficient Range of Resistive Load	100 ohm – 120 ohm
Most Efficient Rotational Speed of Motor	302 RPM

Due to varying wave conditions, the velocity of the generators shaft can vary drastically. An approximation was made by using linear wave theory and historical buoy data at the proposed wave energy buoys test site to find appropriate wave velocities. At the test site the average wave heights range from 0.5 ft. waves to 4 ft. waves. This is the range of velocities that will be used. The average vertical wave velocity of the follower buoy can be found using the following equation:

$$v = \frac{H}{T} \quad (8)$$

Where is  $H$  the wave height and  $T$  is the wave period. This equation is an estimate of the average vertical velocity that will be seen by the racks of the power take off system shown below which will have the same angular velocity as the large gear shown as  $r_2$  in the *figure 11* below.

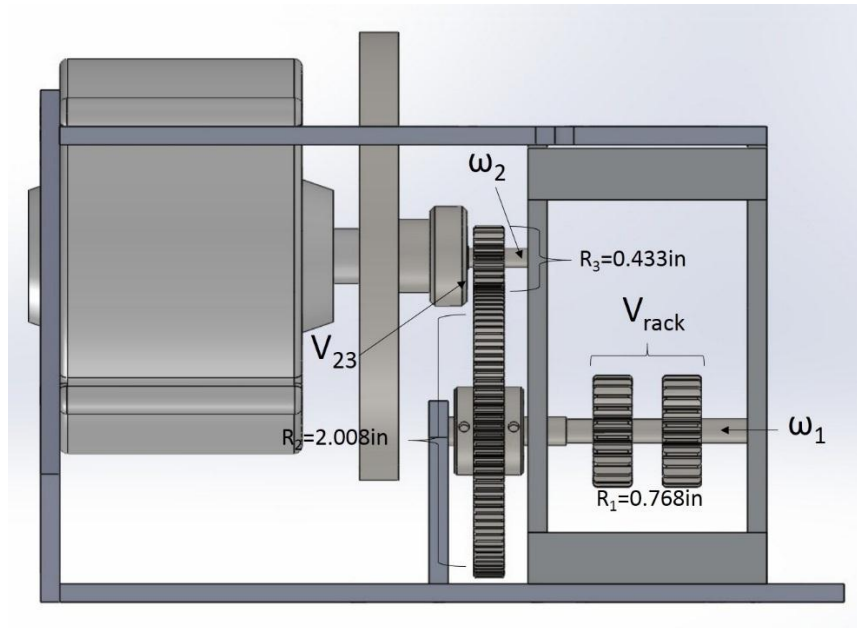


Figure 11: Rack and Pinion gear system

Knowing that the vertical velocity between meshing gears must be the same it is possible to find  $\omega_3$  using the simple relationship:

$$\omega_a r_a = \omega_b r_b \quad (9)$$

Where the subscript ‘a’ denotes one gear meshing with the other gear denoted by subscript b. It is important to note that the angular velocities found are in rad/s and need to be converted to rpm.

Knowing the rpm range that is needed to simulate the wave conditions an experiment could now be designed. A lathe was used to back drive the motor with a constant rotational velocity. With the lathe the input shaft of the generator could easily be placed inside the chuck to hold it steady. The output of the generator was measured using digital handheld multimeters. In order to find the efficiency of the generator, the input power needs to be known which was found knowing the torque input and the input rpm. A strobe tachometer was used to find the rpm. The torque was found by using a load cell to measure the force on the end of a moment arm placed across the backside of the generator. Knowing the length of the arm, force is easily converted into input torque. The output of the load cell could now be measured using an amplifier and hooked up to a hand held multimeter. A potentiometer was chosen to serve as the resistive load because it is easily adjusted and covers a large range of resistances. The potentiometer also had a higher amperage rating than many resistors.

Since the lathe had fixed speeds, intervals between 50-265 rpm were chosen to closely match the rpm values for the different wave heights. Although these were the stated speeds on the lathe, an Omegaette HHT-1500 optical tachometer was used to capture the actual speed. A piece of reflective tape was fixed to the lathes spindle which the optical tachometer used to read the output rpm.

A Kent TRL-13X40 lathe was used to power the generator. To acquire torque, a lever arm was machined from a piece of aluminum stock with a 100 lbf Interface load cell bolted to the end as shown in *figure 12*. A flat spot on the lathe acted as a stop for the load cell. The initial value from the load cell was recorded each time the lathe was turned on to neglect the force of gravity. Since the aluminum lever arm passed straight through the center of the generator, the measurement was simply taken from the center of the generator to where the nut on the load cell made contact with the lathe.

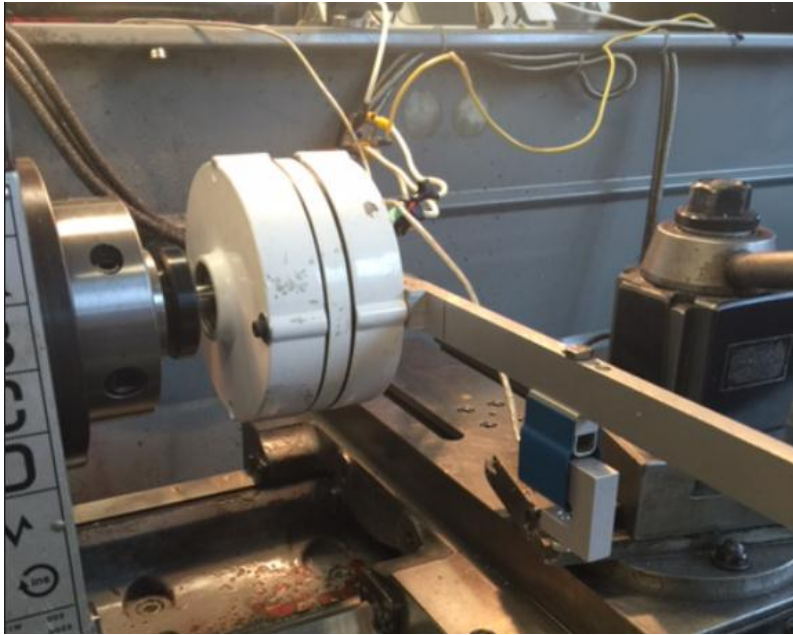


*Figure 12: The generator, load cell, and lathe*

The load cell output was hooked up to an AD-620 amplifier with a gain of 1000 as well as a multimeter. The amplifier was powered by 4.96 volts which was supplied by the power bread board.

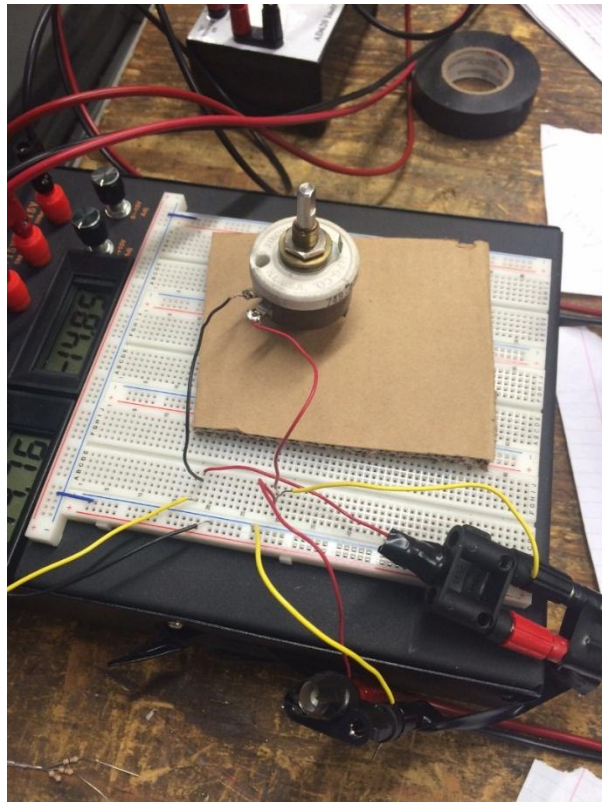


*Figure 13: Breadboard circuit and potentiometer*

The output of the generator was alternating current (AC), which was rectified to direct current (DC). The output from the rectifier circuit was then connected to a power bread board which provided +/- 15 volts. The potentiometer was also chosen since it could handle a higher current (.22 amps) than the small resistors commonly found in the lab. A multimeter was hooked up to record the current from the generator and addition multimeters was used to record the voltage across each resistor.

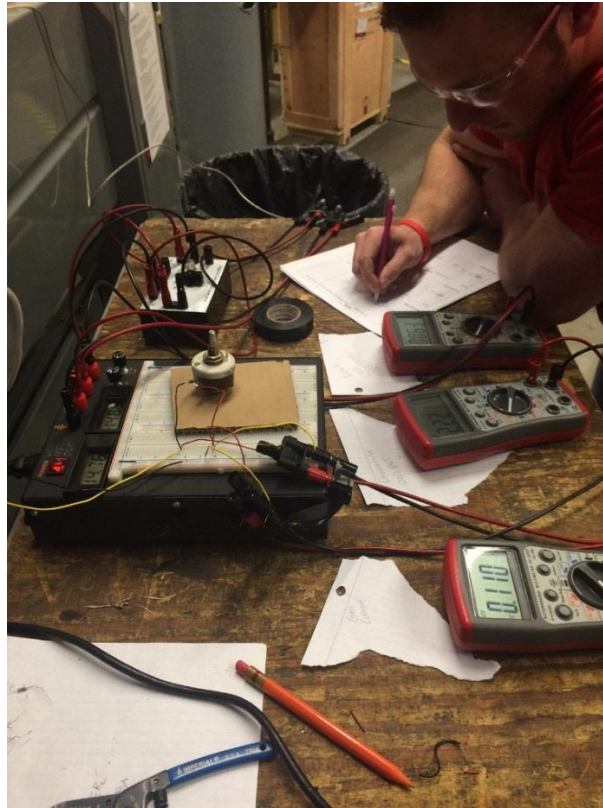


Figure 14: Complete electrical portion of experiment

The AC brushless three phase alternator can be modeled as a simple DC motor because the output was being passed through a rectifying circuit. The rectifying circuit takes the alternating current, which changes direction as it flows, and converts it to flow in a single direction, or direct current. The schematic of the model is shown below in *figure 15*.

The

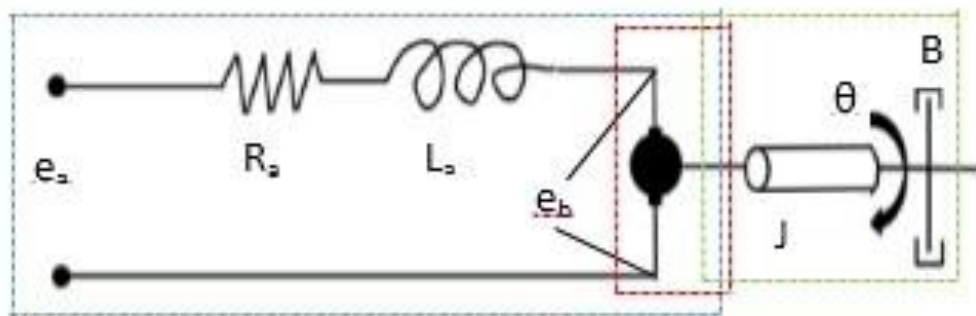


Figure 15: Model of a DC motor

electrical equation of motion for the system can be found using Kirchhoff's Voltage Law (KVL)

around the inside loop of the circuit shown in the blue dashed box. The electrical equation of motion is shown below:

$$e_a - R_a i_a - L_a \frac{da}{dt} = e_b \quad (10)$$

The mechanical equation of motion was found by summing the torques in the mechanical system shown by the green dashed box.

$$J\ddot{\theta} + B\dot{\theta} = T \quad (11)$$

The last sub system to look at is the interaction between the electrical system and the mechanical system shown in the red dashed box, where  $k_a$  and  $k_b$  are properties of the motor that remain constant.

$$e_b = k_b \dot{\theta} \quad (12)$$

$$T = k_a i_a \quad (13)$$

In normal circumstances the two motor constants mentioned above are given to the user in the motor spec sheet. These constants allow the user to closely estimate the back emf constant given a known rotational velocity as an input. The alternator that was used was bought cheaply from China and did not have a spec sheet or any documentation included with it. Thus, the motor constants were not known and had to be experimentally determined.

The back emf voltage was determined by removing the resistance from the circuit, allowing the voltage to freely flow directly from the generator to the multi meter. This voltage was measured at varying rotational speeds and plotted to produce the graph shown in *figure 16* below.

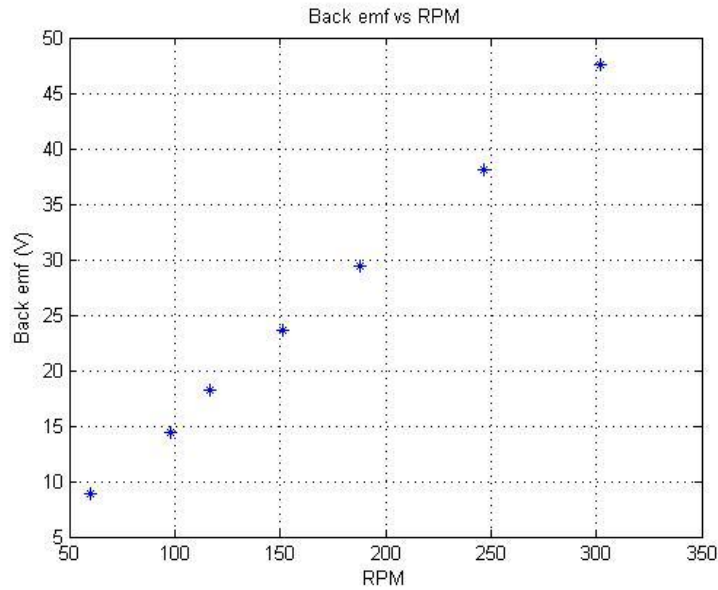


Figure 16: Back emf versus RPM

From the previous data above, it was possible to solve for the motor constant  $k_b$  by dividing the back emf by the RPM. This produced an average value of 0.1537 V/RPM for  $k_b$ .

The 100 lb. load cell that was used to measure torque gave an output voltage that was converted to a force by using *equation 14*, shown below, where the full load refers to the full load of the load cell (100 lbs.), the gain is that of the amplifier (1000),  $V_{in}$  is the excitation voltage (4.97 V), and the sensitivity (3.25001 mV/V). The value of 1000 in the denominator converts the millivolts to volts.

$$F = \frac{(Full\ Load) * V_o * Gain}{V_{in} * Sensitivity * 1000} \quad (14)$$

It was then necessary to multiply this force by the moment arm (0.65 ft) to calculate the torque. *Figure 17 and 18* below show the torque and power of the generator versus the RPM, at 100 ohms and 200 ohms respectively.

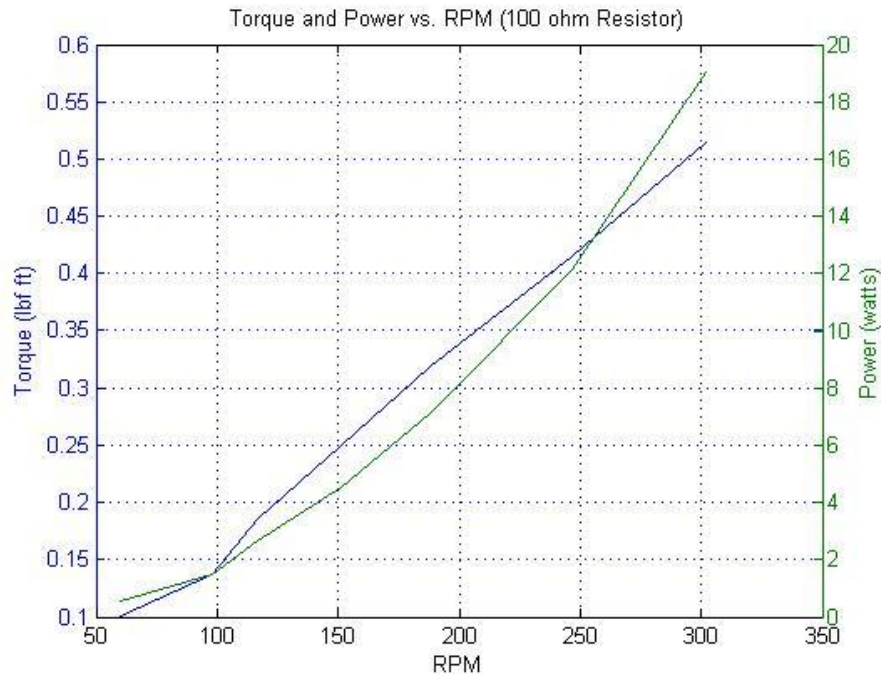


Figure 17: 100 ohm torque and power

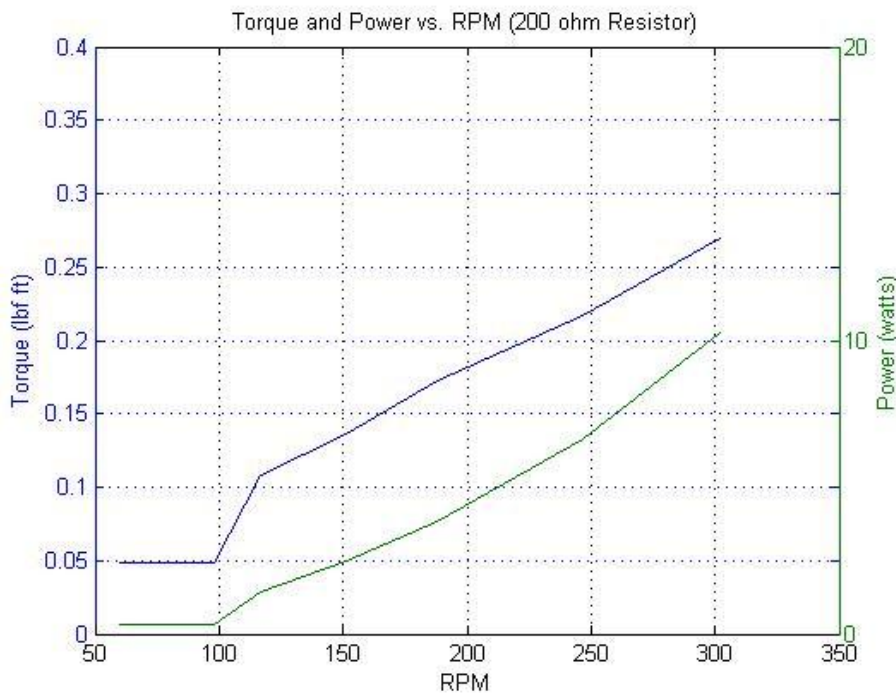


Figure 18: 200 ohm torque and power

When comparing the two graphs of torque and power versus the rotational speed it is evident that greater torque and power is generated with a lower resistive load applied to the system.

The motor constant  $k_a$  was experimentally calculated with the use of *equation 13* and by measuring the torque and current. *Figure 19* below helps to show the relationship between torque and current.

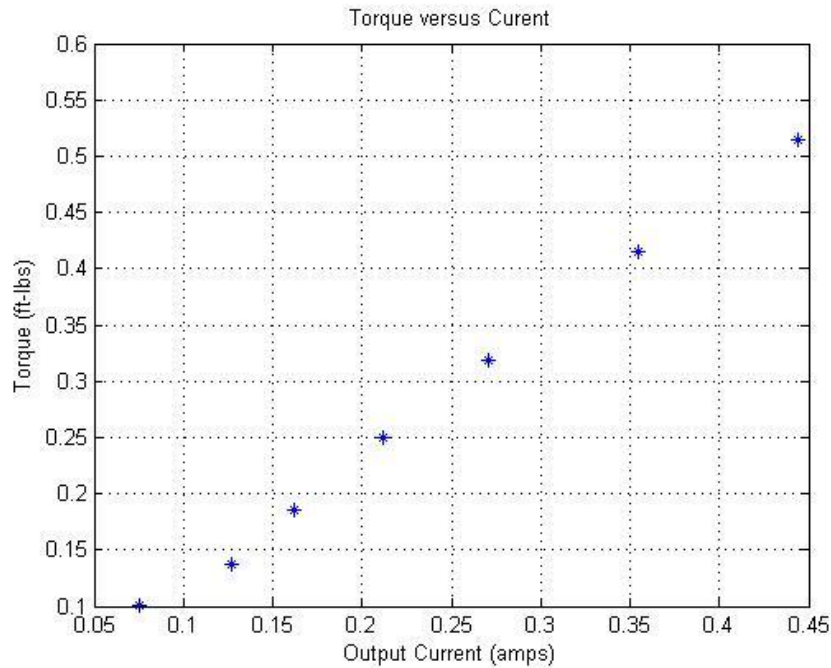


Figure 19: Output current of the generator against input torque

Using the data above, it was possible to solve for  $k_a$  by dividing torque by the current. The average value of  $k_a$  was determined to be 1.1770 ft.-lbs/amp.

The most important aspect of this experiment was to measure and record the power generated by the alternator at various speeds, under different resistive loads. Power can be calculated using either a combination of voltage and resistance, or current and resistance. These equations are shown below.

$$Power = \frac{V^2}{R} \quad (15)$$

$$Power = I^2R \quad (16)$$

With the chosen electrical setup, the voltage is measured before the current. This means that there is a very small amount of internal resistance inside the multi meter that measured the voltage. Therefore using equation 16 will produce a slightly more accurate result than equation 15.



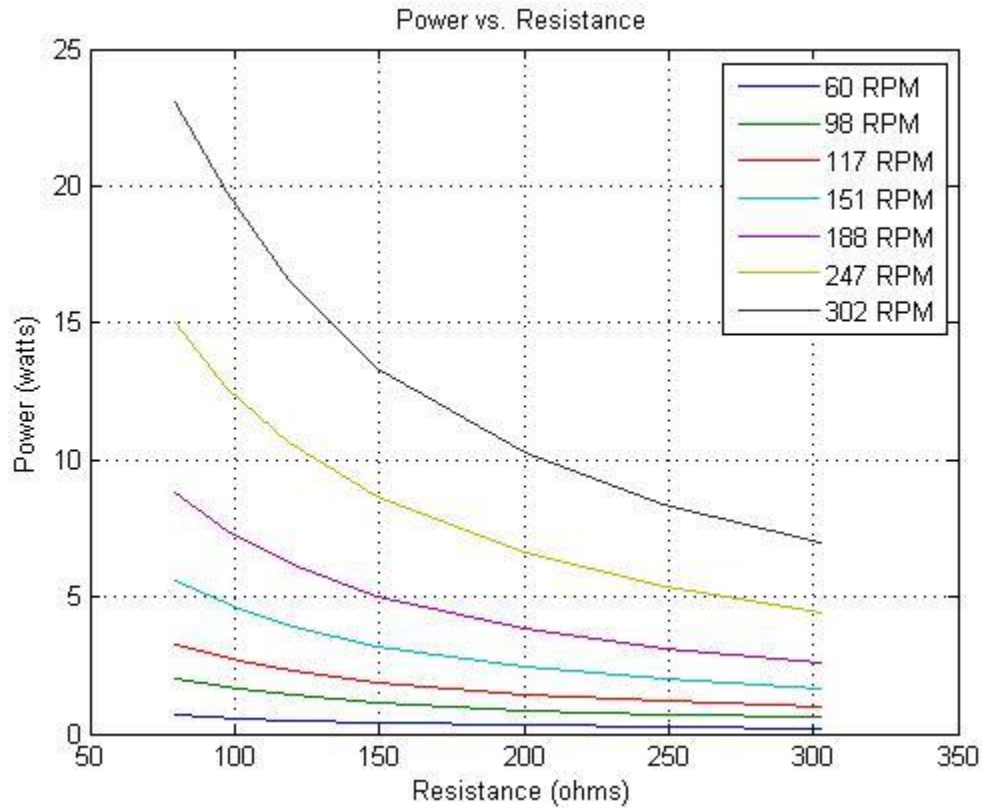


Figure 20: Power versus Resistance

The output power of the generator is plotted as a function of resistance at a series of RPMs in figure 20. It is evident from the plot that in order to acquire the most power, it should have a low resistive load and a high RPM. In reality, this is not possible because if too much power is being transferred through a resistor, it will burn up. Another factor to consider is to make sure that the shaft of the generator maintains a high enough torque to keep it rotating, and generating power.

$$Eff = \frac{P_{electric}}{P_{Mechanical}} \quad (17)$$

The efficiency of the generator at different resistive loads and rotational speeds was also calculated, using *equation 17* above. This was done by taking the power output of the generator and dividing it by the power input. This relationship can be seen in *figure 21* below.

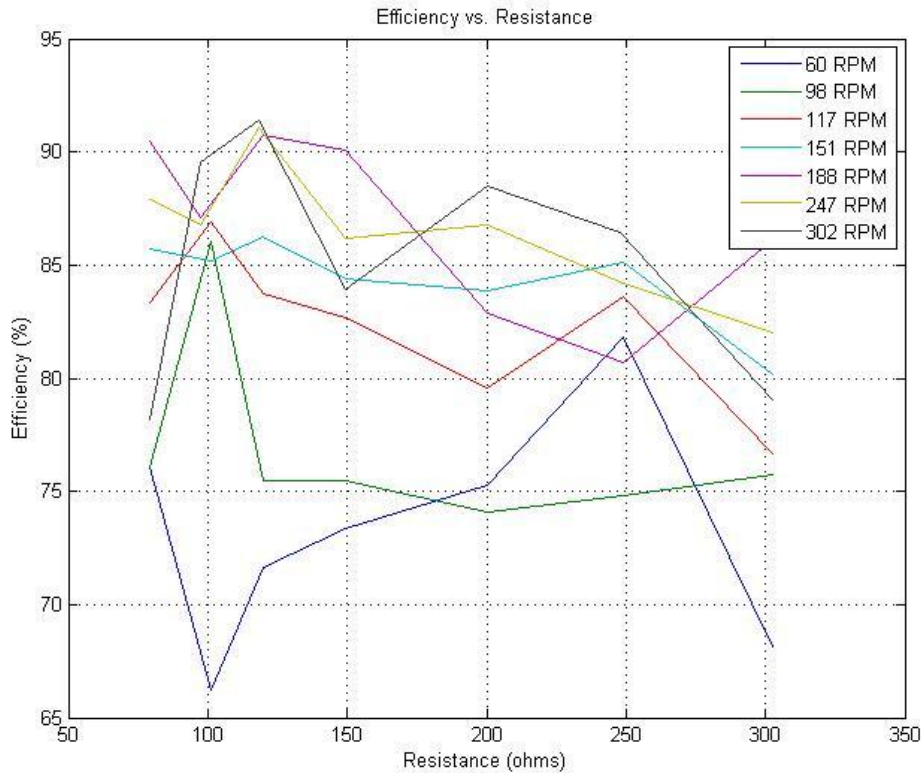


Figure 21: Efficiency versus resistance

The plot shows that the most efficient resistance for speeds greater than 150 RPM was 120 ohms and that the most efficient resistance for 98 RPM and 117 RPM was 100 ohms. For the low speed of 60 RPM, the results was an outlier and it did not follow any trend.

This experiment showed that by using a resistance of 120 ohms at high speeds (greater than 150 RPM), a high efficiency of up to 91% can be achieved. This is purely the efficiency of the generator and not of the entire system (which will be much lower). It is evident that the generator becomes more efficient as the rotational speed of the shaft reaches 300 RPM. Because this is the average rotational speeds that the buoy will encounter when it is put into the ocean, the generator will be efficient in the given operating range.

Although the average speeds that the generator will encounter were considered in this experiment, much higher speeds will be reached for brief periods of time throughout the period of a wave. This experiment needs to be continued with higher input speeds to see if the efficiency continues to rise while increasing the speed or if the efficiency will plateau. The issue that will have to be overcome in doing so is finding resistors that can handle the amount of power that will be surging through them. Once a speed is determined that has the absolute peak efficiency, the entire power take-off can be designed to maintain this speed throughout most of the period of wave with proper gear ratios and by incorporating a transmission into the system.

## PTO Design

In order to convert the linear motion between the follower buoy and the spar into rotational motion, a dual rack and pinion gear system was designed. This system included two 48 x ½ inch, 20° pressure angle racks, two 20° pressure angle pinion gears and 2 one way bearings as shown in *Figure 22*. Both the racks and gears were made from hardened alloy steel and were held in place by 4 black delrin guide blocks. Both gears were press fit onto one way bearings (clutch bearings), which were then press fit onto a shaft. These bearings engage in the counterclockwise direction and free wheel in the clockwise direction. On the up stroke, one bearing engages while other free wheels. The opposite is true on the down stroke. This ensured that the shaft always spin in the same direction on both the up stroke and down stroke (*Figure 21*).

Mounted to the end of this shaft was a 4" gear sandwiched between two aluminum collars. Each collar had two set screws which were used to prevent the 4" gear from spinning on the shaft since it had to be a slip fit for assembly. To maximize the power output, a 5:1 gear ratio was used to spin the generator at an ideal rpm which was determined by the generator analysis.

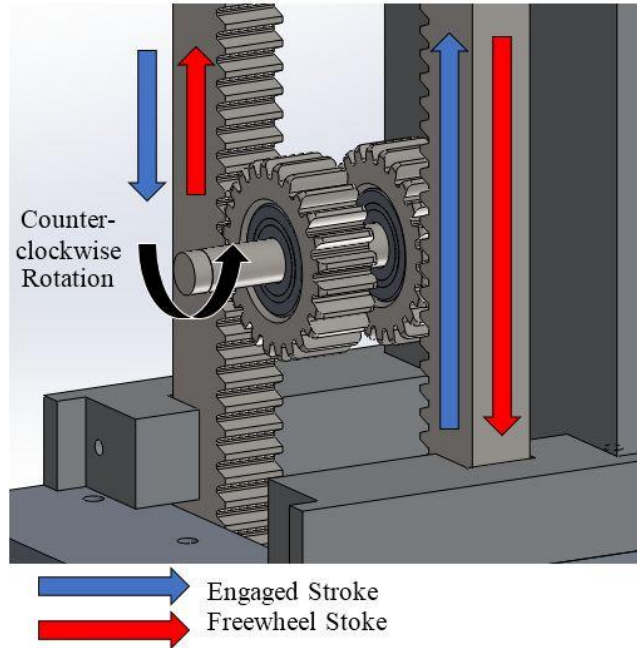


*Figure 22: Dual rack and pinion system*

At the peak and trough of the wave there is an instantaneous point where the follower buoy has no vertical motion. To overcome this problem a flywheel made from 4140 steel was incorporated. After the 5:1 gear ratio a clutch bearing was press fit onto the end of the shaft. The clutch bearing was then slip fit into a 4140 steel coupler which held the outer race of the bearing in place with a set screw. The coupler was then threaded onto the generator shaft. When the dual rack and pinion system is engaged, the clutch bearing inside the coupler engages which spins the generator shaft. At the top and bottom of the wave the rotational energy of the flywheel forces the clutch bearing to free wheel, which keeps the generator shaft turning.

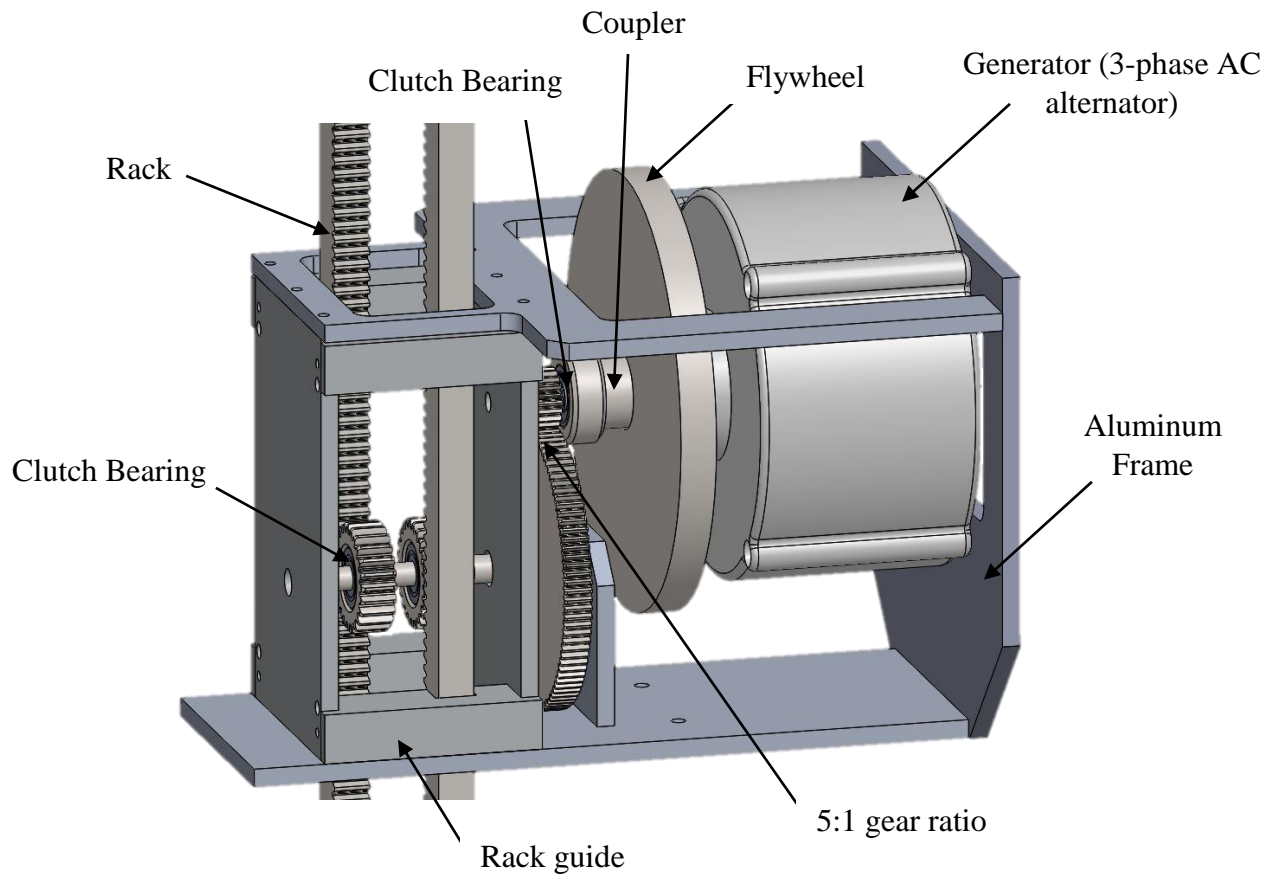


Figure 23: PTO design

Many improvements were made from the previous year. The new model was designed for maximum efficiency with an emphasis on minimizing frictional losses. Two bevel gears were eliminated to reduce the interaction of moving parts as an effort to reduce friction. This meant that the generator had to then be mounted horizontally instead of vertically which helped place the center of gravity in the center of the PTO unit. Higher quality gears and bearings were also used, again minimizing frictional losses. To reduce corrosion, all of the support frame of the PTO was machined out of 6061 aluminum.

# Data Acquisition

## Pressure Sensor Data

After the float and spar were designed and fabricated, the next step was to determine the water to wire efficiency. The “water-to-wire” efficiency is the ratio of the amount of power produced by the generator to the amount of available power from the waves. The energy of the waves was computed by knowing the wave height and frequency, but under normal conditions, the sea is random containing a summation of many different wave heights and frequencies. Wave energy can be accurately determined by using a pressure transducer to record the pressure field at the deployed site. The pressure results were converted to energy by using Linear Wave Theory and statistics. The pressure sensor was deployed in 69 feet of water and 10 ft. below the surface for about an hour, while it was secured by the mooring system. The pressure sensor stored the data in Hoboware, which was able to be transferred to MATLAB for analysis.

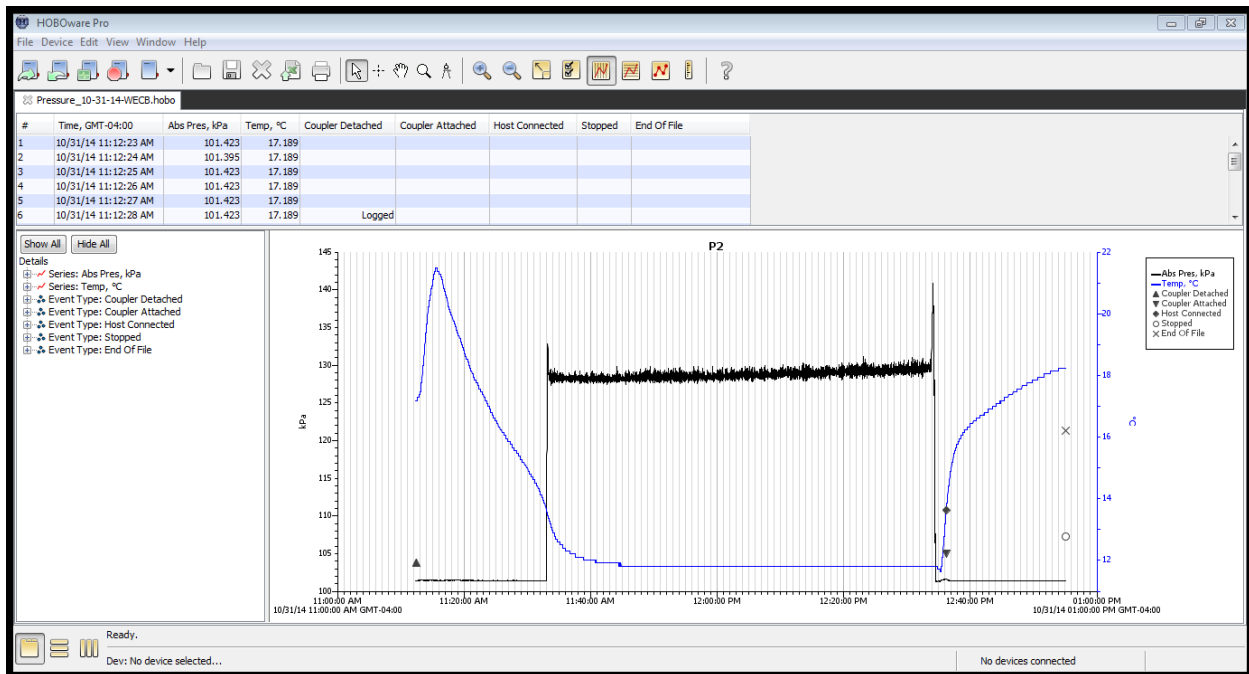


Figure 24: Data from Pressure Sensor Uploaded to Hoboware

The black line represents the pressure data while the blue line represents temperature. Since the pressure sensor begins to record once it is removed from a computer, the lowest temperatures correlate to when the sensor was in the ocean. Therefore the ocean pressure is the only area of concern. As Figure 24 shows, the time of analysis lasted approximately one hour while measuring absolute pressure in units of kPa.

In order to utilize the pressure data to obtain energy available within the waves, Hydrostatic Pressure equations were used to determine wave height as shown in equation 18.

$$P = P_{atm} + \rho gh \quad h = \frac{P - P_{atm}}{\rho g} \quad (18)$$

Where  $P$  is the pressure obtained from the sensor,  $P_{\text{atm}}$  is the atmospheric pressure,  $\rho$  is the density of salt water,  $g$  is the gravitational constant, and  $h$  being the wave height.

For a wave height to wavelength ratio of  $1/50^{\text{th}}$  or less, Linear Wave Theory can be used with excellent accuracy in predicting the kinematic properties of waves. Due to the dispersion relation as shown in *equation 19* it is appropriate to assume deep water conditions when the depth is greater than half the wavelength

$$\sigma^2 = gk \tanh(kh) \quad (19)$$

Where  $\sigma$  is angular frequency in rad/s,  $g$  is gravity,  $h$  is the water depth, and  $k$  is the wave number. In deep water,  $h$  becomes large which simplifies the hyperbolic tangent to one. Therefore, the wave number can be found knowing gravity and angular frequency. The wave number is important because it relates cycles to wavelength.

$$k = \frac{2\pi}{L} \quad (20)$$

The wave number is also used to determine the pressure response factor  $K_p$ .

$$K_p(z) = \frac{\cosh[k(h+z)]}{\cosh(kh)} \quad (21)$$

The pressure response factor is used to correct pressure data obtained from a pressure sensor. The  $z$  term is the vertical location of the pressure sensor, which is always negative because the origin is at the surface. When  $z$  is zero, the pressure response factor is one. If the pressure sensor was placed at the surface, there would be a perfect response. Pressure sensors cannot be placed at the surface because of the horizontal motion of the waves, which will cause the pressure sensor to pick up noise.

Due to the depth being much greater than the wavelength, deep water conditions can be assumed allowing for the calculations of wavelength  $L$  (also noted as  $\lambda$ ) and phase velocity  $C$ , given the wave period,  $T$ .

$$L = \frac{gT^2}{2\pi} \quad (22)$$

$$C = \frac{gT}{2\pi} \quad (23)$$

Based on the aforementioned theory, the total energy in a wave is obtained from *equation 24*

$$E_{\text{tot}} = E_p + E_k = \frac{\rho g H^2 L b}{8} \quad (24)$$

Where  $E_p$  is the wave potential energy,  $E_k$  is the wave kinetic energy,  $H$  is the wave height,  $b$  is the width of the crest. The mass density of saltwater is  $1025 \text{ kg/m}^3$ .

The transfer of wave energy from point to point in the direction of wave travel is characterized by the energy flux, or wave power based on *equation 25*

$$P = \frac{\rho g H^2 c_g b}{8} \quad (25)$$

Where  $c_g$  is the group velocity. When a group of waves are traveling in deep water, as shown above, the relationship between phase velocity and group velocity is shown by *equation 26*

$$c_g = \frac{c}{2} \quad (26)$$

Thus the total energy per unit crest width is shown by *equation 27*

$$\frac{E}{b} = \frac{\rho g H^2 L}{8} \quad (27)$$

Similarly for power per unit crest width,

$$\frac{P}{b} = \frac{\rho g H^2 c_g}{8} \quad (28)$$

The primary characteristics that determine wave energy are the height and frequency. A random sea may be thought of as the superposition of a large number of waves with different heights and frequencies traveling in many directions. Both the height and period of random seas can only be calculated through a statistical approach, thus the height data needed to be “ensembled”, implying the periods of the highest waves are separated out and averaged.

By Fourier analysis, complex waveforms can be considered as a sum of sinusoids of appropriate magnitude, frequency and phase, referred to as its spectrum as shown in *equation 29*. Before taking the Fourier transform we “detrended” the data to remove linear drift from the tides.

$$f(x) = a_0 + \sum_{n=1}^{\infty} \left( a_n \cos \frac{n\pi x}{L} + b_n \sin \frac{n\pi x}{L} \right) \quad (29)$$

Once the Fourier analysis was completed, the random sea was broken up into amplitudes that were tied to discrete wave frequencies. Since the total energy of random seas is the summation of all wave heights and frequencies, the energy obtained from the wave field is found from *equation 30*

$$\sum E_i = \frac{\rho g H_i^2 \lambda_i b}{8} \quad (30)$$

To evaluate the energy of all the component waves passing a point, the wave height term must be represented by *equation 31*

$$\frac{H_i^2}{8} = S_t(T_i) \delta T_i \quad (31)$$

Where  $S_t(T_i)$  is called the wave spectral density with units of  $m^2 \cdot s$  and  $\delta T_i$  is the elemental wave period.

The wave spectrum tells how much energy is carried by the various frequencies present in a random wave group. By integrating the wave spectral density over all periods the expression of the wave energy per unit width crest is shown below as *equation 32*. The raw Fast Fourier Transform of the field data is demonstrated in *figure 25*

$$\frac{E_i}{b} = \rho g \lambda \int_0^\infty S_t(T) dT \quad (32)$$

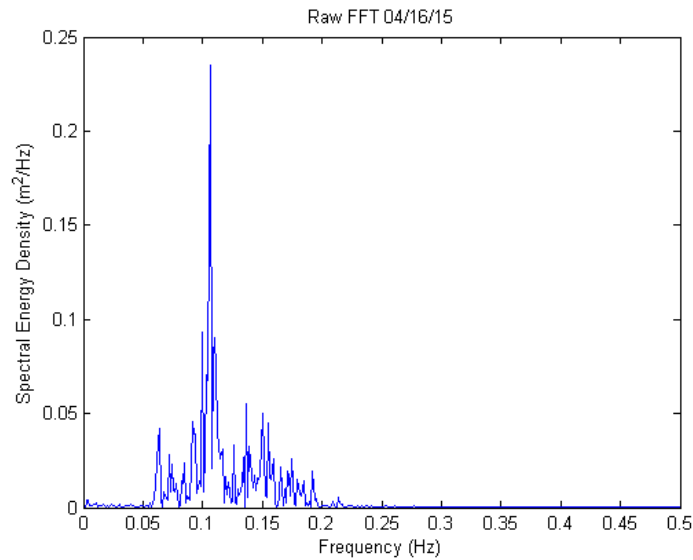


Figure 25: The Raw FFT derived from the previous equations

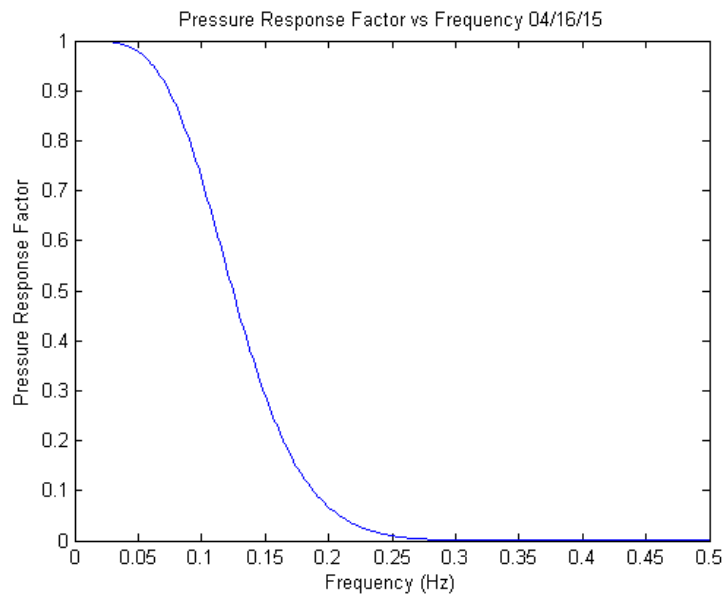


Figure 26: Pressure response of the waves as the frequency of the waves change

The pressure response factor is a unit less parameter that corrects a pressure reading for different frequency waves. *Figure 26* shows the pressure response factor vs frequency. When the frequency



increases, the pressure response factor decreases. This happens because at higher frequencies the wave's pressure does not penetrate very far below the surface.

The pressure response factor is affected by the depth of the pressure sensor. A smaller depth yields a response factor that stays closer to one at higher frequencies, which is desirable because a low response factor decreases accuracy. However, if the sensor is too close to the surface it will be affected by lateral sway from the waves, which will introduce inaccuracy as well. Our depth of approximately 10 feet was selected as a good compromise.

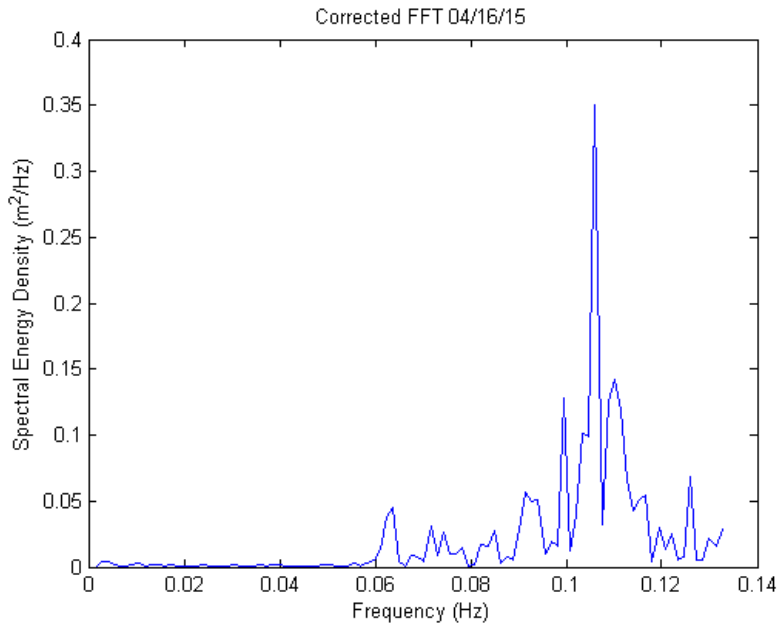


Figure 27: Spectral Energy Plot

Figure 27 shows the corrected FFT due to the pressure response factor. The dominant frequency of the spectrum is determined to be 0.125Hz from the plot, which translates to a dominant period of 8 seconds. The dominant wave height was determined to be 0.209 meters.

The area under the spectral energy curve, which is the energy flux, is the total available wave energy per unit length that is able to be extracted over the elapsed time the pressure sensor was recording data. By knowing the energy flux and the diameter of the buoy, the total available power from the waves can be determined. By using the dominant wave frequency and height, the available power of the buoy for one specific propagation of waves was determined to be 505.5Watts. This value is low because the wave heights were relatively small in the deployment site.

## **On-board Data Acquisition System**

One of the goals for the Wave Energy Buoy team this year was to design a reliable data acquisition system to monitor the performance of the buoy. The system that was designed was intended to monitor both generator output and the displacement of the buoy relative to the spar. It was also designed to log data to an SD card and to a web server over a GSM connection, which allowed the buoy to be monitored in real time. The primary design choices made were: choosing appropriate sensors, ensuring adequate power, designing reliable logging and communications, and choosing an enclosure.

The two sensors used were a voltage divider with analog to digital converter and a LIDAR displacement sensor. Previous years optimizations and this teams bench tests indicated that the optimum resistance for the generator/buoy/waves configuration was about 100 Ohms, with generator output of up to 60 volts. An Arduino Uno's analog to digital converter can handle voltages of up to 5 volts, so our system measured the voltage across 8 ohms in series with 92 ohms. This gave a total readable range of 0 to 62.5 volts. It was found that the best way to ensure an accurate "zero" reading was to connect the ground output of the rectifier circuit to the ground of the Arduino. Connecting ground to the Arduino AREF pin did not seem to work, and the Arduino was not harmed by tying the grounds together.

The second sensor was the LIDAR unit that sensed displacement between the float and the spar. This unit sends and receives a laser pulse and then outputs a digital pulse to the Arduino. The pulse length was then multiplied by a scaling factor and added to a constant to derive centimeters of displacement.

The SD shield was a Seedstudio v3.1 shield. It is somewhat picky about what SD card it will accept and also does not work with the standard Arduino SD library. The script that is included in the appendix leverages the SdFat library and creates a new data file every time the Arduino is turned on. General data processing for both sensors took about 5 milliseconds, which with a 20 millisecond delay yielded a ~40Hz sampling rate.

The GSM shield that was initially purchased was a TinySine shield using a SIM900 chip. It was found to be unreliable, and had very high power requirements. As a last resort a generic Arduino GSM shield was borrowed which worked satisfactorily. The Arduino connected to the GSM was programmed to cache voltage readings for 30 seconds at 10Hz, and then send those data points to the server in one HTTP GET request with the data as a single URL argument of comma separated values. Unfortunately, the request took about 5 seconds, during which time no data was collected.

The server was an Amazon Web Services EC2 t2.micro server instance running apache. An apache module called mod\_wsgi was installed to enable python WSGI scripting. A framework called Flask was used to build the web app. Sqlite3 was used for the database. Front-end plotting used a javascript library called Char.js. Initially the data for the chart was updated periodically via ajax requests using jQuery, but this seemed to make Chart.js behave erratically for large numbers of data-points, so a simple auto refresh every five seconds was used instead. This server/web app setup successfully handled logging requests and graphically exposed logged data to both desktop and mobile devices.

Powering the two Arduinos plus a GSM chip required relatively large amounts of power, mostly because of the GSM. It was difficult to calculate power requirements as the GSM draw was very erratic with signal strength/frequency of requests. Our system sent one request every ~35 seconds for 4-5 hours using three 9 volt batteries connected in parallel. Once the peak battery output was sufficiently reduced, the system would become unstable during network requests, and the Arduinos would start resetting themselves.

The housing for the data acquisition system was a pelican case with a hole drilled in the side for DC generator power lines, LIDAR power and communication lines, and a power switch line. All electronics as well as the power resistors were housed in the pelican case. If the buoy had operated as expected, there was a chance that the heat from the resistors could have become an issue.

During the most recent deployment the data acquisition system performed well. Both the SD card logging and GSM logging worked successfully, and our values seemed accurate. There were some erratic values from the LIDAR during towing, which is believed to have had to do with improper alignment of the sensor and sensing plate.

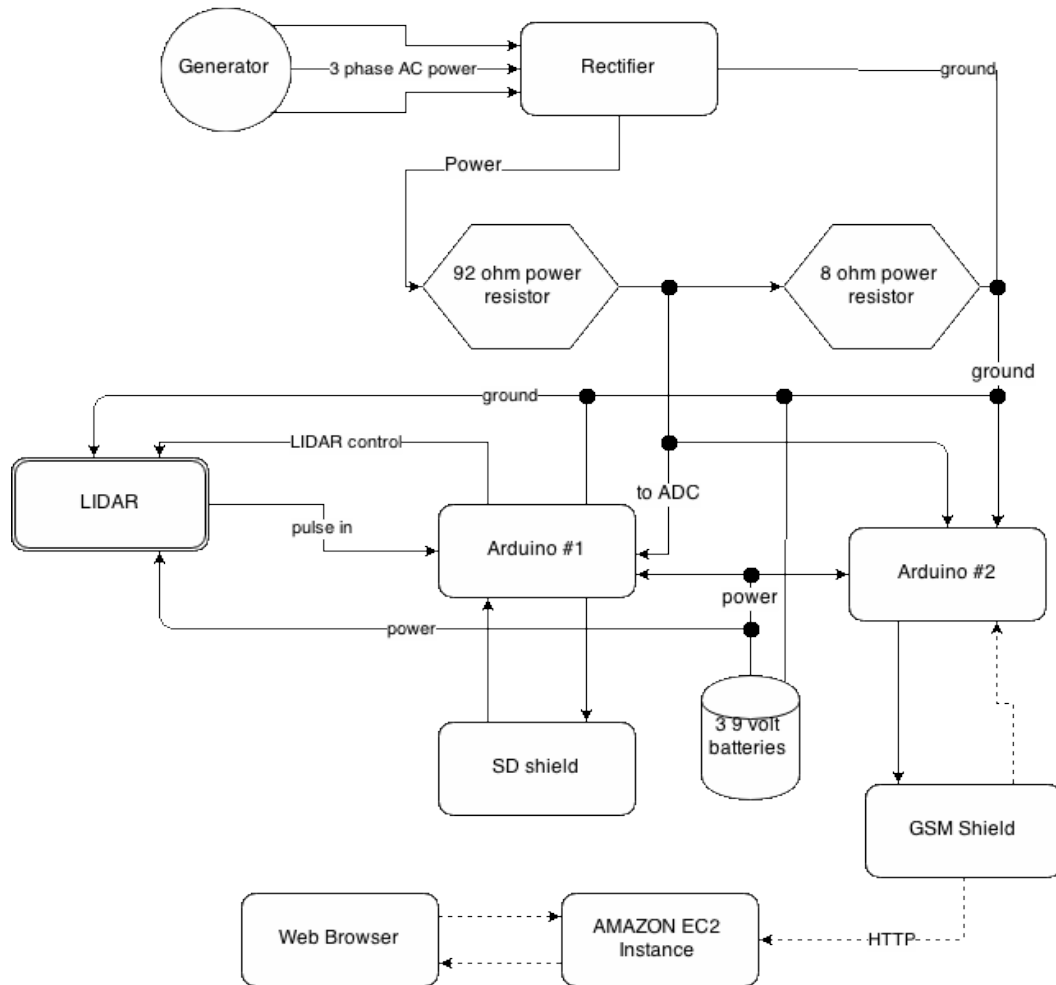


Figure 28: Block Diagram of the Data Acquisition System

## Final Design

A point source absorber buoy was chosen for the final design of this year's wave energy conversion buoy. The buoy is designed to extract power from the ocean waves it encounters using a mechanical system that relies on the principle of relative motion to turn a generator which in turn produces power. The diagram to the right (*figure 29*) shows all the components of the buoy along with the full scale dimensions.

To create the relative motion needed to generate power the buoy relies on two main floats, the spar buoy and the follower buoy (or the float). The spar is meant to remain motionless in the water as the follower buoy moves up and down relative to the spar. The follower buoy was designed to be very responsive (short natural period) to the waves whereas the spar is designed to be very unresponsive (long natural period). The spar must sit at a certain height out of the water in order to allow the buoy to produce power on both the up and down strokes. The racks of the power take off system will be at mid stroke when the spar sits at the correct height relative to the water surface. The reason for the length of the spar is that it needs to produce enough buoyancy force to achieve the proper height while accounting for all the weight acting on the spar.

If the spar sits too low in the water the follower cannot travel as far up before hitting stops in the same way that if the spar sits too high out of the water the follower buoy's down stroke is limited.

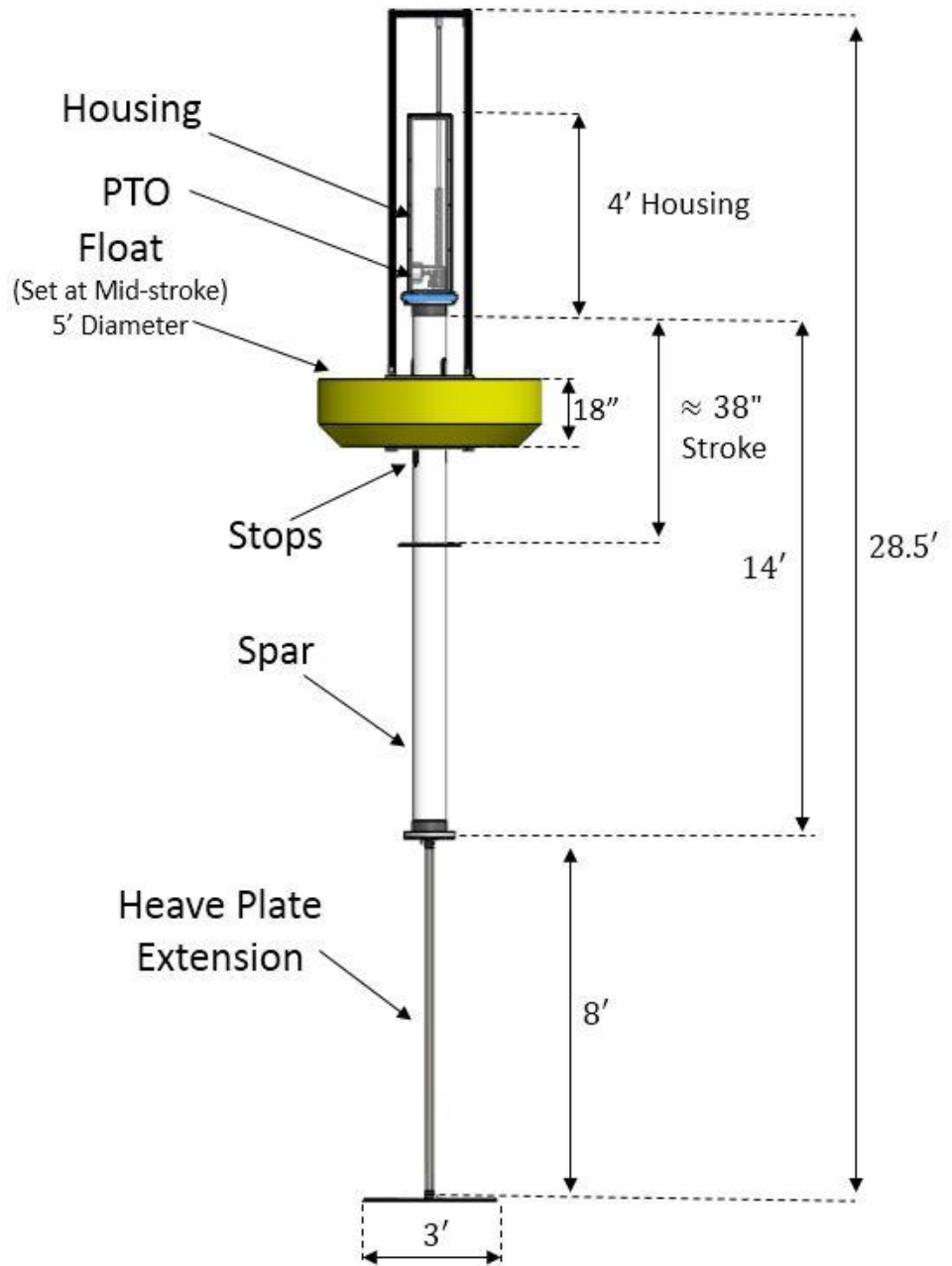
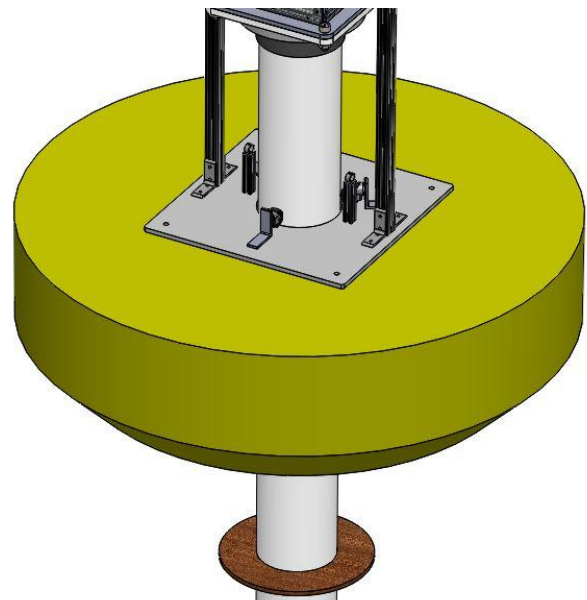
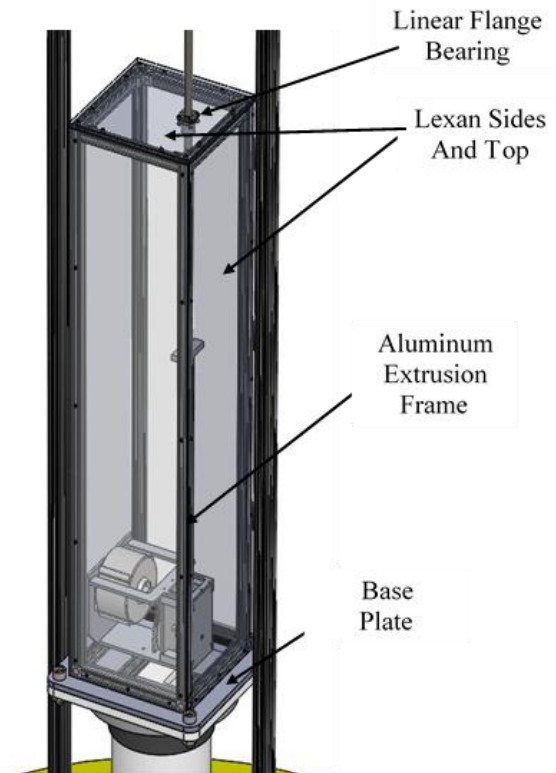


Figure 29: Final design

A 2'x2' HDPE plate sits on the top and bottom of the follower. They are pressed together through the buoy by 5/8" threaded rod and secured with lock washers and nuts. On each side of the follower casters are mounted to the HDPE plates with the wheels tangent to the spar. These casters help to guide the follower up and down the spar smoothly reducing friction between the spar and the plates themselves. Two pieces of aluminum extrusion are also mounted on the plates. Each piece of extrusion has a small bumper on the top that act as the stops for the float in the event that the buoy encounters too big of a wave (above the 38" stroke capability). On the upstroke the stops on the follower hit the bottom side of the PVC flange that mounts to the top of the spar. On the down stroke the stops on the bottom side of the follower hit a circular platform located on the spar that is held up by a large clamp. The clamp serves as both the bottom of the stroke and a picking point for deployment. The circular platform can be seen in *Figure 30*. The PVC flange that mounts to the top of the spar is held in place by three bolts that pass through the flange and the spar. This allows it to be removed so that the entire spar can be removed. One of the bolts used to hold the flange on is an eye hook that serves as the top picking point for the bridal system.



*Figure 30: Top view of follower buoy*



*Figure 31: Housing design*

The power take off unit for this buoy contains a data acquisition system as well as exposed wires for the generator, to keep all of these components dry a very water resistance housing was created. The housing cannot be called water proof due a small opening for a linear flange bearing in the top. The housing is comprised of an aluminum extrusion frame with Lexan side panels. The housing can be seen in *Figure 31* to the right. The side panels are drilled to allow clearance for t-nuts. The t-nuts slide in and out of the grooves in the extrusion. This allows the side panels to be held securely to the frame.

The housing was also sealed with Lexel a waterproof sealant. The top of the housing is made out of 1/4" Lexan that has the four cross members that connect the framing uprights attached to it. The reason for this is so that when the top comes off there is enough room to fit the PTO inside. T-nuts are also used to connect the top plate to the 4 cross members. To hold the top plate to the uprights a 1/4-20 bolt is threaded into the top of each upright. To improve water resistance a gasket is placed in between the top plate and the cross members. A linear flange bearing (see *Figure 31*) is mounted in the top plate to allow a rod, which drives the dual rack system, to pass in and out of the housing with as little friction as possible. There is an additional cross member that runs along the bottom of the housing on the inside where the PTO sits. Two holes have been drilled through the cross member to allow bolts to pass through and thread into the bottom of the PTO to hold it securely. The housing sits on a square base that has a large section cut out of it to allow room to thread in bolts to the PTO through the cross member from the bottom side. The cutout section also allows clearance for the racks to move up and down. T-nuts were also used to attach the framing to the base plate. This base plate is bolted to an adapter plate in each corner. The adapter plate simply attaches to the rectangular housing base plate and also bolts to a circular flange on top of the spar. A gasket material is in between the plates with a cutout for the racks to pass through. This provides a very water tight enclosure for the PTO.

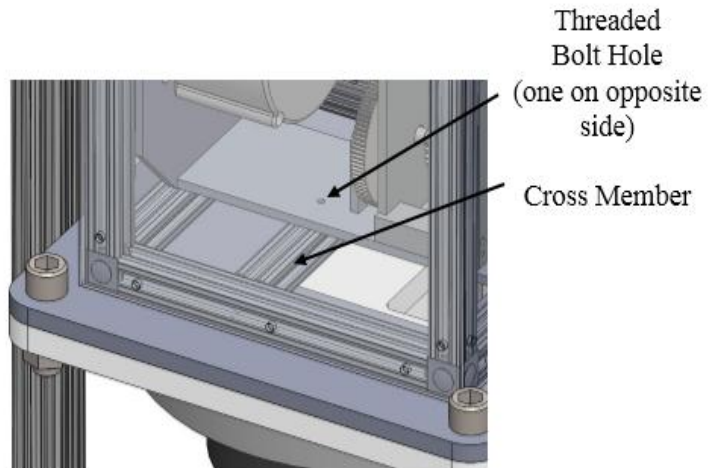


Figure 32: PTO mount

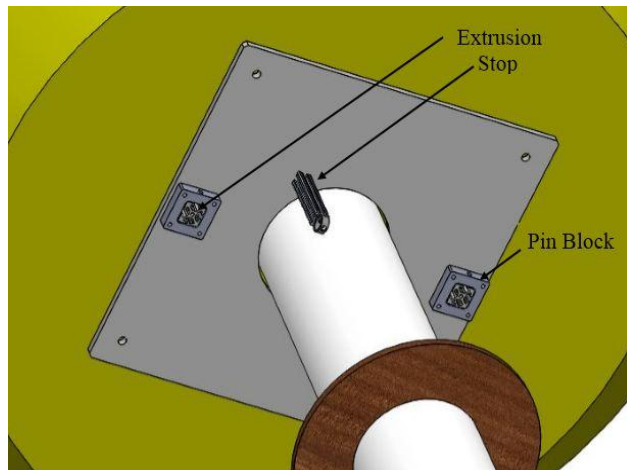


Figure 33: Bottom view of follower buoy

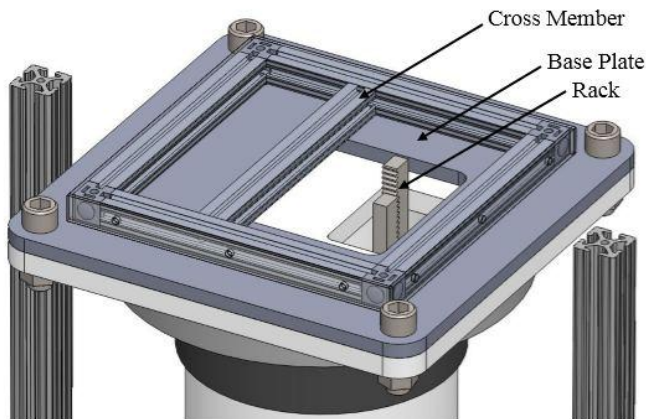


Figure 34: Section view of housing base

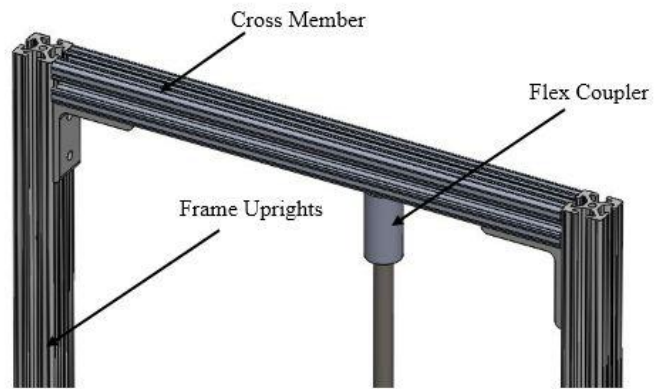


Figure 35: Flex coupler attachment

An aluminum extrusion frame is attached through the follower buoy with a cross member running across the top. The two uprights that run through the buoy are pinned through blocks that have been attached to the bottom HDPE plate. The PTO is driven by the follower buoy by connecting a rod from the top of the dual rack system to the frames cross member. The rod that connects the rack system to the frame is mounted to a flex coupling which accounts for any rotation in the spar during deployment as seen in *Figure 35*. As mentioned before as the follower moves up and down it moves the racks up and down. The racks then rotate two gears that are pressed on clutch bearings that turn a shaft. The way that the racks are orientated with the gears ensures that the shaft will be continuously spun in the same direction on both up and down stroke.

After a 5:1 gear ratio a smaller shaft spins the input shaft of the generator. The gear ratio is used to increase the angular velocity of the input shaft that turns the generator. A flywheel is attached to the input shaft of the generator and mounted to a coupler as shown in *Figure 36*. The coupler contains another one way bearing so that when the racks stop moving at the top and bottom of the stroke the flywheel can decouple from the rest of the mechanical system, which is motionless at this point, to continue to spin the generator until the next stroke using its stored momentum. The generator is a 3-phase AC alternator passes through a rectifier circuit to transform the energy into useful DC voltage.

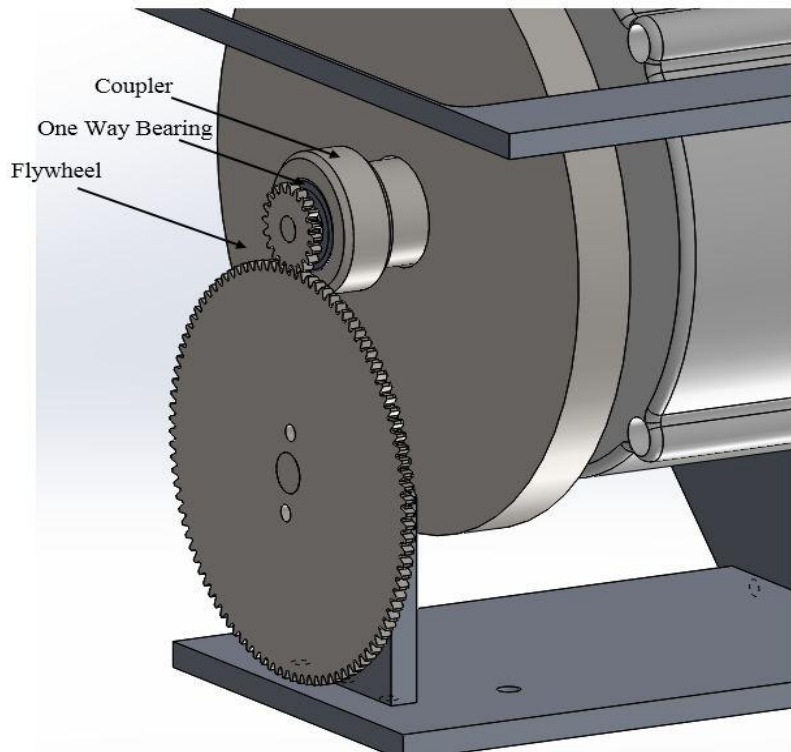


Figure 36: Section view of PTO

The final part of the buoy needed for the deployment is the heave plate. The heave plate is designed to resist motion through the water column. In doing so, it helps to keep the spar from traveling up and down in response to the waves. If the spar were to move it would take away the relative motion and therefore generate no power. The heave plate is attached to a spar extension which is a long rigid pipe. The reason for a rigid pipe down to the heave plate is to lower the center of gravity of the buoy which helps with stability.

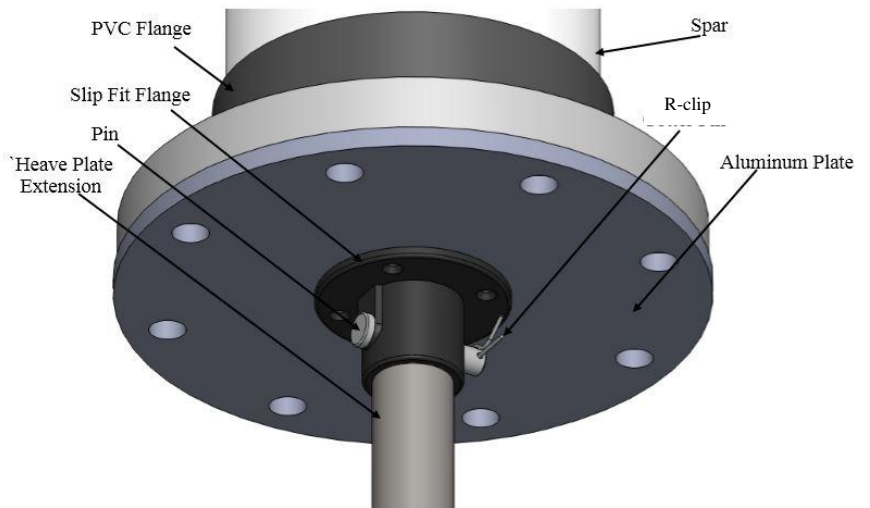


Figure 37: Heave plate extension attachment

The heave plate extension brings the plate down to a depth where the water particle motion is less than 10% of the motion seen at the surface. The deeper the heave plate sits in the water column the less motion there is and the more effective the heave plate will be in adding stability. There is a PVC pipe flange on the bottom of the spar, just like the top, where an aluminum plate has been bolted on with a gasket. This plate closes off the volume of the spar which provides the necessary buoyant force. A slip fit pipe flange for a 1.5” diameter pipe has been bolted onto the bottom aluminum plate as shown in *Figure 37*. The pipe flange has a hole drilled through the middle where a pin slides through. The heave plate extension pipe (8’ galvanized 1.5” diam. pipe) also has a hole drilled through it and when inserted into the flange a pin is placed through both and secured with a R clip. A pin connection allows for a quick way to attach the heave plate to the bottom of the spar when being deployed. On the heave plate side of the pipe the same pin connection is used. A threaded pipe flange is mounted to the back side of the heave plate which shares the same mounting bolts as the slip fit pipe flange on the other side. By “pancaking” the heave plate with the two flanges it ensures that the weight from the mooring will act on the pipe and the pin connections at the top and bottom of the extension pipe and not on the wooden heave plate. A male to male coupling is attached to the threaded pipe flange on the bottom side of the heave plate. A standard T connection is threaded onto the coupling with the ears shaved off so that the pin from a shackle can pass through it. A 45lb weight is attached to a chain which suspends from the shackle at the bottom of the heave plate. The length of the chain must be long enough so that it can be held on the deck of the boat as the buoy is deployed. The purpose of the weight is to lower the center of gravity. The rest of the mooring system is then attached to the other end of the weight.

The future goal of this buoy is to provide a hard wire connection to a battery bank located on Appledore Island to help power the Shoals Marine Laboratory. A data acquisition system was added to this year’s design to observe the power output of the buoy. Using the output from the generator along with the linear displacement of the rack and pinion system and an available energy spectrum acquired using a pressure transduce, a true experiment efficiency can be found.



## Field Test

To test the Wave Energy Conversion Buoy, facilities at the Jere A. Chase Ocean Engineering Laboratory were utilized, as well as an actual field deployment. Because of the increased size of the buoy, new techniques to transport, deploy and recover the buoy were implemented. These strategies are summarized in a deployment procedure that can be found in procedure section of the Appendix.

The buoy was put in the engineering tank at the Jere A. Chase Ocean Engineering Laboratory on multiple occasions to evaluate a lifting procedure, as well as to investigate hydrostatic characteristics. For use with the on-site crane, a bridal system to lift the buoy from a singular pick point was constructed. The bridal system comprises of a rope, with each end tied to a rigid point on the spar located below and above the follower buoy. A loop tied in this rope at different positions allows the buoy to be suspended at different angles. Through tests in the engineering tank, an angle of approximately  $15^\circ$  was determined to be best for deploying and recovering the buoy. This angle was restricted by the height of crane, length of the buoy and other spacial constraints. A guide rope is also used during the lifting of the buoy to prevent the any rotational movement to ensure a proper orientation. Tank testing was useful for understanding the behavior of the buoy when it is in water as well as suspended in air. These observations served as a starting point for designing a deployment strategy in open water.

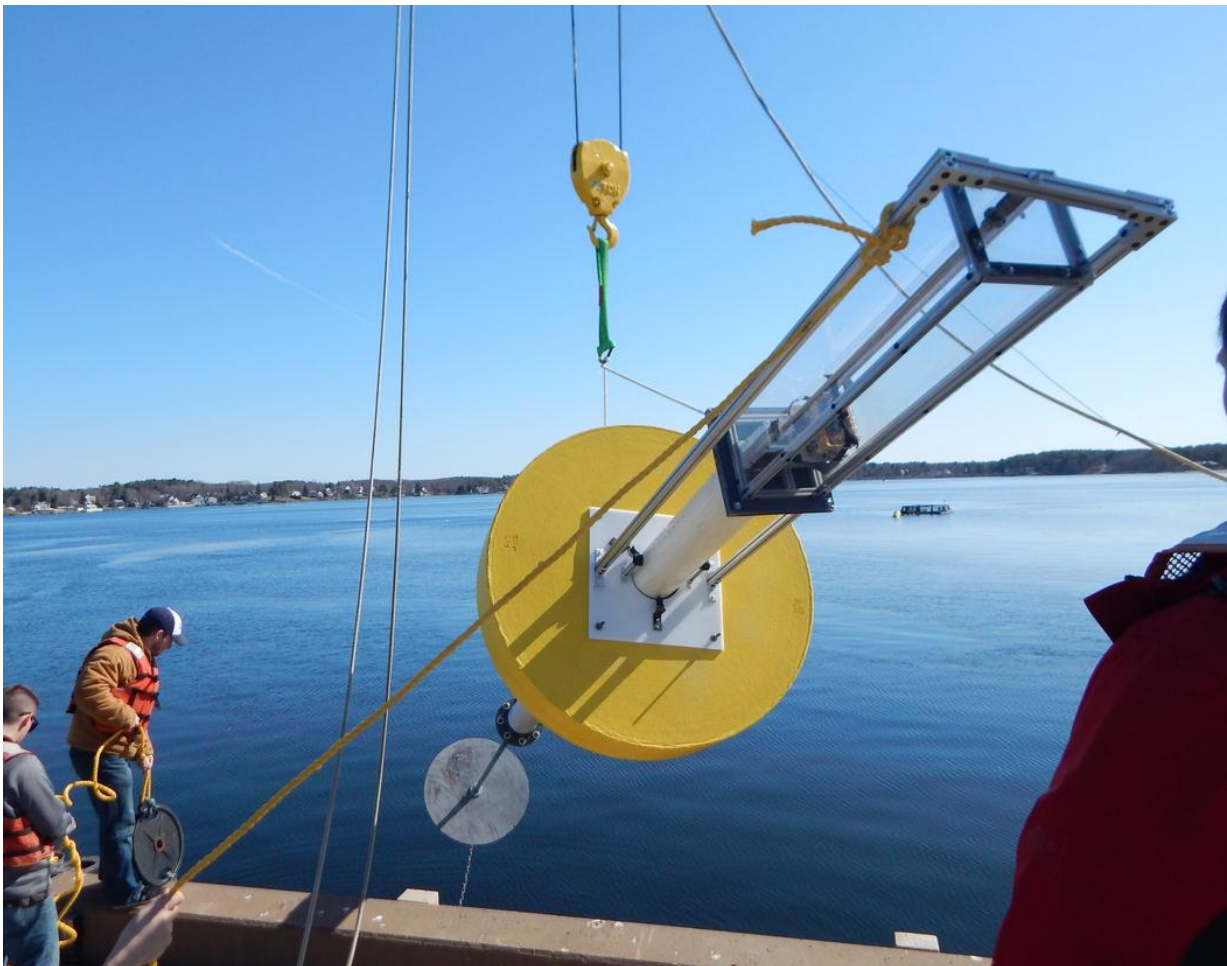


*Figure 38: The buoy being lifted into the water at the UNH pier in Newcastle. A custom bridal system was used to lift the buoy safely and consistently.*

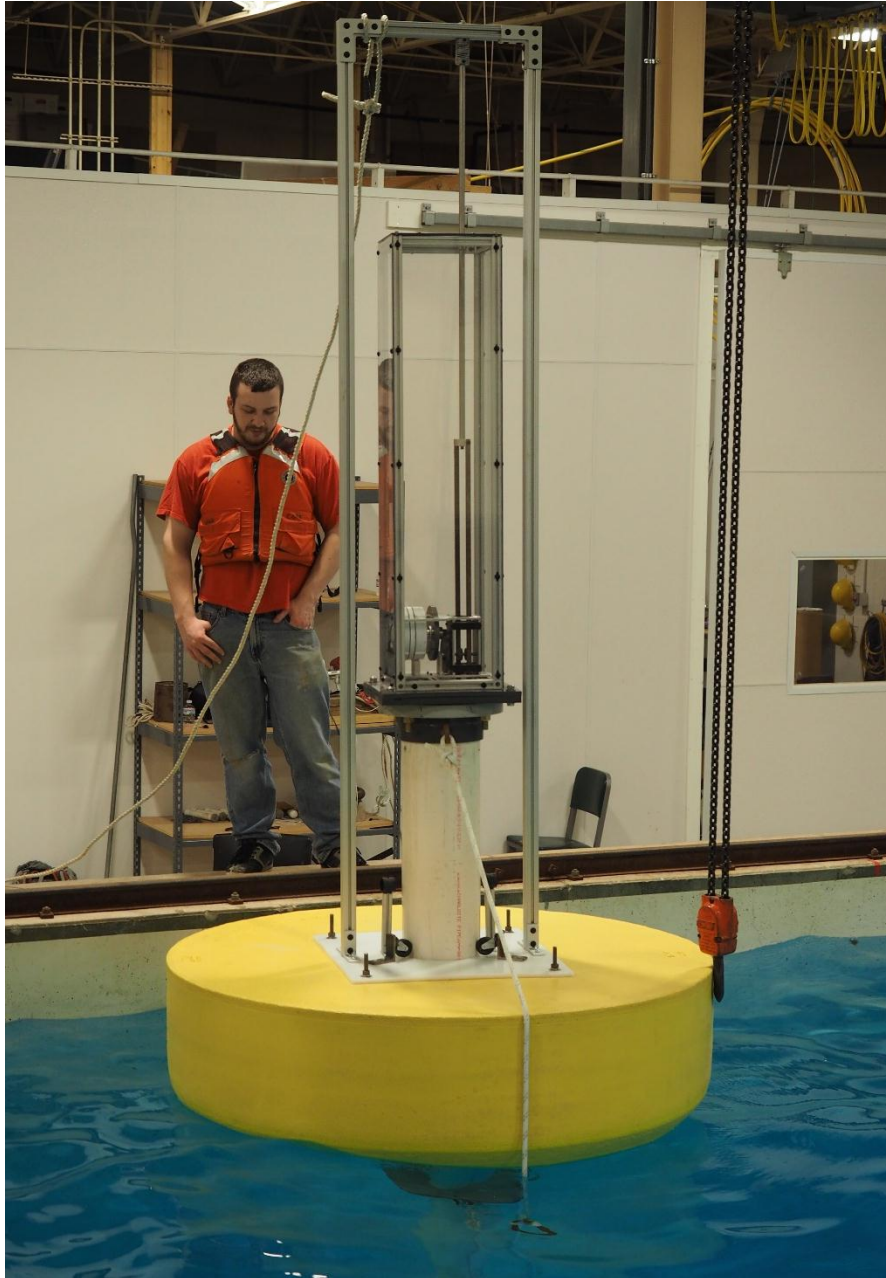


*Figure 39: The buoy in the engineering tank at the Jere A. Chase Ocean Engineering laboratory. Tank testing was important in evaluating the functionality and hydrostatics of the buoy.*

A procedure was developed for the transportation of the buoy to the Isle of Shoals with the UNH research vessel, the Gulf Challenger, docked at the UNH pier in Newcastle, NH. Similarly to the previous field deployment, this procedure called for the fully assembled buoy to be lifted from the dock to the deck of the Gulf Challenger using the on-site crane. The Gulf Challenger would then deploy the buoy and mooring at the Isle of Shoals test site using its A-frame mounted winch. After

allowing the buoy to collect data for some amount of time, the Gulf Challenger would pull the buoy and mooring aboard and return to shore. However, because of logistical issues with the use of the Gulf Challenger, a different vessel had to be utilized. Because there were no other boats with the capability to move the buoy on and off deck, it was decided that the buoy would be towed to open water. Another UNH research vessel, the Cocheco, was chosen for this and the buoy was deployed on April 16, 2015.

The buoy was transported semi-assembled on a flatbed truck and put together at the UNH pier. Data acquisition was activated and the buoy was lowered in to the water by the on-site crane. The mooring for this experiment was the same as the first deployment and was loaded on to the deck of the Cocheco (specifics on the mooring were discussed previously in Mooring section). The buoy was never designed to handle stresses associated with being pulled through water. There was a significant concern that the heave plate would be at risk of deformation because of the considerable resistance force associated with its large surface area, so it was towed at a slow velocity of roughly one knot. The intended location at the Isle of Shoals could not be reached in an appropriate time frame, so the buoy was towed until a temporary test site with adequate depth of 70' was found outside of Portsmouth Harbor.



*Figure 40: The buoy being towed to a temporary test site outside of Portsmouth Harbor*



*Figure 41: The buoy deployed at a temporary test site outside of Portsmouth Harbor*

At the temporary test site, the mooring was deployed and buoy's response to waves was observed. The buoy sat well in the water, but as the test progressed, the position of the spar fell in the water column. When the flex coupling that connects the motion of spar and follower buoy broke, the decision was made to recover the buoy. The mooring was pulled out of the water and the buoy was towed back to the UNH pier.

Upon further investigation, it was concluded that a clutch bearing in the power take off unit had failed due to the torques it experienced when being towed. The broken clutch bearing rendered the PTO inoperative. The broken bearing was only activated during the upstroke, and so the added resistance of this broken bearing explains why the spar was not able to move up to correct itself. Besides this failure, every other aspect of the buoy deployment was successful. Although the quality of the data was compromised because of the broken PTO, the data logging worked well. The follower buoy showed excellent wave responsiveness, and the spar showed little movement, as well as improved stability. The improved integrity of the buoy was certainly demonstrated, especially considering the

stresses associated with towing.

Although the deployment strategy called for the buoy being placed directly in the water at a specified test site, the test still yielded useful insight to the behavior of the buoy. For future tests of this buoy however, a deployment procedure using the Gulf Challenger is the ideal scenario, because the buoy is not designed to be towed. With a working PTO, the data can be used to further understand and improve the system. A water to wire efficiency can then be calculated and the damping of the system can be understood by comparing the dominant wave height calculated from the pressure sensor data and dominant stroke displacement recorded by the laser.

## Conclusion

Wave energy has a great potential to help alleviate the world's energy demand, due to the abundance of a clean, renewable energy source available within the ocean. In order to efficiently design a WECB, many parameters need to be efficiently optimized to extract the most energy while operating at an appropriate cost range. To begin the analysis of the previously designed WECB, an initial field test was conducted to understand the buoy's response to the motion of the waves. Upon testing, a plan was formulated to improve the hydrostatics of the system, increase the structural integrity, modify the power take off, and install a data acquisition system.

The follower's geometry was optimized through careful experimentation which led to a design that increased the surface planar area, as well as the system response. This allowed for the follower to extract more energy from the waves due to a decreased natural period. Since the follower had a higher buoyancy force compared to the previous design, the spar was lengthened to increase its buoyancy and achieve a design goal for the spar to naturally sit at mid stroke above the water surface level. The housing was constructed using Lexan panels to provide a more water resistant enclosure, thus protecting the power take off. Additionally, extruded aluminum was used for the support frame, which provided a rigid, strong structure at a reasonable cost. Through all the geometric modifications, during the hydrostatics test, the WECB was only 1 inch off of the desired goal of the buoy resting at mid stroke on the initial test. This was easily corrected by adding an additional amount of ballast weight to bring the spar down to sit 42" out of the water. This proved a successful hydrostatic design and allowed for the focus to shift on the power take off optimization.

To increase power generation, the sources of energy loss had to be reduced. Two bevel gears were eliminated, allowing for the generator to be installed parallel with the input shaft, thus decreasing friction loss. The gears, shafts, and guide blocks were re-machined to higher tolerances, allowing proper press fits to eliminate slippage that occurred during movement. Additionally, a flywheel was installed which acted as a mechanical filter stabilizing the intermittent voltage output, at the peak and base of the stroke.

In order to calculate the water-to-wire efficiency, the power output of the generator was required to be recorded to compare it to the amount of available energy the waves contained. Through the use of a GSM shield, the generator output was able to be remotely viewed from a server, and an SD card was used to record the data at a high resolution. A pressure sensor was used to translate wave height into a wave energy flux over the deployment time. Due to last minute cancellations of Gulf Challenger, the system had to be towed, which was not the intended purpose. During the tow, a clutch bearing broke which led to the mechanical system to fail. The location was also 4 miles closer to shore which led to inconclusive power results. The plan is to re-launch the buoy in the upcoming weeks to gather more results, but through the hydrostatics and bench testing, the buoy responded as designed and has a very probable chance of reaching efficiencies above 20%.

## References

- [1] Ogata, Katsuhiko. "Time-Domain Analysis of Dynamic Systems." *System Dynamics*. 4th ed. Upper Saddle River, N.J.: Prentice-Hall, 2004. 383-399. Print.
  
- [2] Sullivan, Corey, Carl Smith, and Joe Henderson. *WECB: Wave Energy Conversion Buoy*. Rep. 2014.:Tech. Durham: U of New Hampshire. Print.
  
- [3] Caron, Shaun, Paul Madea, and David Kurtz. *WESML – Wave Energy at the Shoals Marine Lab*.2013.:Tech. Durham: U of New Hampshire. Print
  
- [4] Berteaux, Henri O. *Coastal and Oceanic Follower buoy Engineering*. Woods Hole, MA (P.O. Box 182, Woods Hole 02543): H.O. Berteaux, 1991. Print.

## Appendix

### Future Work

To properly deploy the current buoy design it must be placed in the water at the deployment site with a boat equipped with an “A” frame. Before the next deployment of the WECB the heave plate extension should be redesigned. A “telescoping” design utilizing 3 pipes that can be retracted around the spar is recommended in order to shorten the buoy for easier deployment. Another area of concern is the unwanted torsion the racks can put on the gears when the spar rotates inside the float. Since the rod that connects the racks to the aluminum extrusion frame is not concentric with the spar, an axial load is placed on the clutch bearings potentially causing them to fail. Currently a flex coupler absorbs much of the torsion created however a pivoting arm design is more desirable.

Since the buoy is too long to be tested in the wave tank ocean tests are the only option. Once these design changes are made multiple ocean tests should be completed before other design changes are made.

It is recommended that the official Arduino shield be purchased if future groups want to do remote monitoring. In conjunction with the Arduino GSM library, this shield should have the capability to operate in an asynchronous mode. While this mode is more difficult to use and was never successfully operated, it would be very useful as it would eliminate the loss of data that occurs during the ~5 seconds it takes to perform a network request, and possibly eliminate the need for a second Arduino. Another option would be to cache the data on the Arduino connect to the SD card and have the Arduino connected to the GSM chip request a chunk of data over a serial connection periodically. This would allow the GSM chip to operate in the simpler synchronous mode without loss of data points.

It might be a good idea to use an off-the-shelf internet data logging solution rather than the custom web app used this year. Example services are PushingBox and Temboo.

In the future an excellent project would be to use a voltage regulator, charging circuit, and rechargeable battery to power the system off of the generator output. This would allow the buoy to operate for extended periods of time.

As the resistance is lowered, more current is forced through the generator creating more power. Based on different wave conditions, the follower buoy experiences different vertical velocities. As the vertical velocity increases, more torque is transferred through the system. At this time only 1 resistive load can be used during a deployment. Using an array of sensors to constantly monitor wave conditions could be used to have a dynamic resistance in order to maximize the power output of the generator.

## Budget

Item	Cost
Pelican Case	\$13.45
First Launch	\$546.00
9V Batteries	\$6.49
Resistors	\$7.49
SD Shield	\$13.99
Arduino Uno	\$29.99
4GB SD Card	\$9.99
GSM Shield	\$31.00
Accelerometer	\$4.58
SIM Card	\$0.99
H2O Activation Card	\$9.95
PTO materials	\$772.59
One bearing, lexan	\$42.32
Strapping	\$4.49
Bearing Pullers	\$30.82
Float	\$1,230.00
Spar Extension	\$240.14
Plastic Stock	\$155.34
Foam	\$38.06
Lexan, Hardware	\$46.40
One way bearing	\$110.25
Flywheel material, hardware	\$50.60
Pipe, screws	\$54.61
90 brackets	\$37.52
Laser	\$89.00
hardware, foam	\$44.54
foam,webbing, buckle	\$21.78
clear gorilla tape	\$6.98
hardware	\$113.20

Source	Total
ME Dept (initial)	\$2,200.00
ME 441	\$200.00
Accepted Students Day	\$200.00
OE Dept/Seagrant	\$1,000.00
Additional Funding	\$250.00
<b>Total</b>	<b>\$3,850.00</b>
<b>Remaining</b>	<b>\$87.44</b>



## Part Locations

### High Bay

- Spar/Float Assembly
  - Spar Assembly
    - Top PVC flange
      - 2x ½” bolts and nuts
      - 1 lifting eye and nut
    - Adapter plate
      - 4x ¾” bolts and nuts
    - Gasket
    - Bottom PVC flange (permanently mounted)
    - Aluminum mounting plate
      - 8x ¾” bolts, washers and nuts
      - Red gasket
      - Galvanized 1 ½” pipe flange
        - 4x ¼-20 bolts and expanding nuts
  - Float Assembly
    - Float
    - 6 casters
    - 4 stops
    - Aluminum extrusion frame and brackets
    - Pin blocks
    - 2x ¼” pins
- Heave Plate Extension Assembly
  - 1 m plywood heave plate
  - 2 flanges
  - 8’ 1 ½” galvanized pipe
    - 2 cotter pins

### Inside Chase on Shelving Unit

- Housing
- PTO
- Data Acquisition system (in yellow pelican case)

Note: All hardware used to assemble the buoy are located in the existing bolt holes. The float, spar and heave plate extension were stored assembled in the high bay as of date of the URC. The PTO and housing were also stored assembled on the shelving unit inside Chase. For a complete assemble procedure see below.

## Matlab Code

### PTO

```
% Nate Bent
% John Pauley
% Corin Craig
% ME 747
% Final Lab

% http://www.micromo.com/motor-calculations

close all;clc;
% import data
% column 1: resistance
% column 4: load cell voltage (delta)
% column 5: generator output voltage
% column 6: generator output current

D_60=xlsread('data','60');
D_98=xlsread('data','98');
D_117=xlsread('data','117');
D_151=xlsread('data','151');
D_188=xlsread('data','188');
D_247=xlsread('data','247');
D_302=xlsread('data','302');

% Determine Kb from back emf (79.4 ohm resistor)
E=xlsread('data','back_emf');
Kb=mean(E(:,2)./E(:,1))

figure
plot(E(:,1),E(:,2),'*')
ylabel('Back emf (V)')
xlabel('RPM')
title('Back emf vs RPM')
grid

%%
% Conversion to Force
v_excite=4.97; %volts dc
sens=3.25001; %mv/v
fullLoad=100; %lbf
gain=1000;

% %Calc Force
% force=(fullLoad.*D_117(:,5)*1000)/((v_excite*sens*gain));
%
% % Calc Torque
% r=7.800; % inchs
% T=r*force
%
% % Determine Ka (79.4 ohm resistor)
% Ka=T./D_117(:,6)
```

```

%%
% plot RPM vs T,power and current (100 ohm resistor)

R101=xlsread('data','R101.2');
omega=R101(:,1);
v_out=R101(:,3);
i_out=R101(:,4);
F=(fullLoad.*R101(:,2)*1000)/((v_excite*sens*gain));
r=7.8/12; % ft
T=r.*F;
r101=101.2;
P=v_out.^2./r101;

AAA=xlsread('data','R101.2');
current=AAA(:,4);
figure
plot(current,T,'*')
xlabel('Output Current (amps)')
ylabel('Torque (ft-lbs)')
title('Torque versus Curent')
grid

Ka=mean(T./current)

figure
[hAx,hLine1,hLine2]=plotyy(omega,T,omega,P)
%legend('Torque (lbf ft)','Power (watts)')
xlabel('RPM')
ylabel(hAx(1),'Torque (lbf ft)')
ylabel(hAx(2),'Power (watts)')
title('Torque and Power vs. RPM (100 ohm Resistor)')
grid

% plot RPM vs T,power and current (200 ohm resistor)

R200=xlsread('data','R200.5');
RPM=R200(:,1);
v_out=R200(:,3);
i_out=R200(:,4);
F=(fullLoad.*R200(:,2)*1000)/((v_excite*sens*gain));
r=7.8/12; % ft
T=r.*F;
r200=200.5;
P=v_out.^2./r200;

figure
[hAx,hLine1,hLine2]=plotyy(RPM,T,RPM,P)
%legend('Torque (lbf ft)','Power (watts)')
xlabel('RPM')
ylabel(hAx(1),'Torque (lbf ft)')
ylabel(hAx(2),'Power (watts)')
title('Torque and Power vs. RPM (200 ohm Resistor)')
set(gca, 'YTick', [0 0.05 0.1 0.15 0.2 0.25 0.3 0.35 0.4])
grid

```

```

% [hAx,hLine1,hLine2]=plotyy(t,V,t,displacement_int)
% % axis(hAx(2),[-0.1 -40 40]);
% % axis(hAx(1),[-0.1 .7 -2600 2600]);
% title('Acceleration vs Displacement')
% xlabel('time (s)')
% ylabel(hAx(2),'in/s^2')
% ylabel(hAx(1),'in')

%%
% column 1: resistance
% column 4: load cell voltage (delta)
% column 5: generator output voltage
% column 6: generator output current
[Pe_60,Pm_60,eff_60]=det_power(D_60(:,5),D_60(:,1),D_60(:,4),60);
[Pe_98,Pm_98,eff_98]=det_power(D_98(:,5),D_98(:,1),D_98(:,4),98);
[Pe_117,Pm_117,eff_117]=det_power(D_117(:,5),D_117(:,1),D_117(:,4),117);
[Pe_151,Pm_151,eff_151]=det_power(D_151(:,5),D_151(:,1),D_151(:,4),151);
[Pe_188,Pm_188,eff_188]=det_power(D_188(:,5),D_188(:,1),D_188(:,4),188);
[Pe_247,Pm_247,eff_247]=det_power(D_247(:,5),D_247(:,1),D_247(:,4),247);
[Pe_302,Pm_302,eff_302]=det_power(D_302(:,5),D_302(:,1),D_302(:,4),302);

figure
plot(D_60(:,1),eff_60,D_98(:,1),eff_98,D_117(:,1),eff_117,...
     D_151(:,1),eff_151,D_188(:,1),eff_188,D_247(:,1),eff_247,...
     D_302(:,1),eff_302)
xlabel('Resistance (ohms)')
ylabel('Efficiency (%)')
title('Efficiency vs. Resistance')
% ylim([0 100])
legend('60 RPM','98 RPM','117 RPM','151 RPM','188 RPM','247 RPM',...
      '302 RPM','location','northeast')
grid

figure
plot(D_60(:,1),Pe_60,D_98(:,1),Pe_98,D_117(:,1),Pe_117,...
     D_151(:,1),Pe_151,D_188(:,1),Pe_188,D_247(:,1),Pe_247,...
     D_302(:,1),Pe_302)
xlabel('Resistance (ohms)')
ylabel('Power (watts)')
title('Power vs. Resistance')
% ylim([0 100])
legend('60 RPM','98 RPM','117RPM','151 RPM','188 RPM','247 RPM',...
      '302 RPM','location','northeast')
Grid

close all;clear all;clc
T=2;
z=0;
h=80; % ft
g=32.17;
% t=24;
% t1=linspace(0,360*(t/T),360*(t/T));
% [u w]=velocity(H,T,z,h,t,g)
% figure,plot(t1,w)

```

```

H=linspace(.5,4,8)';
vert_vel=(H/T); % ft/s
r=2/12; % ft
ang_vel_g1=vert_vel/r;
gear_ratio=5.56;
omega_shaft=gear_ratio*ang_vel_g1*60/(2*pi);
figure,plot(H,omega_shaft,'*')
xlabel('Wave Height (4s period)')
ylabel('Average RPM')
xlim([0 4.5])
grid

% y=3.2^2X

```

## Pressure transducer analysis code

```

load wavedata2.txt

%-----
DataPoints=wavedata2(:,1);
Pressure=wavedata2(:,2);
Temperature=wavedata2(:,3);

plot(DataPoints,Temperature)
%-----

%Filtering Data
actualData=wavedata2(12813:13566);
%actualTemp=wavedata2(12813:13582,3);
actualPressure=wavedata2(12813:13566,2);

plot(actualData,actualPressure)
%-----

P=actualPressure.*.001; %Places Pressure Values in a Column (kPa)

%Given Info
g=9.81; % gravity (m/s^2)
rho=1020; % Density of Sea Water (kg/m^3)
z=-6.096; % Depth of Sensor (m)
h=21.0312; % Water Depth (m)
rate=1; % Sample Rate of Sensor (Hz)

%-----

%Converting Abs Pressure from Sensor to Gage Pressure
Pgage=P-101.325; % Gage Pressure (kPa)
Pgage1=Pgage.*1000; % Gage Pressure (Pa)
deltah=Pgage1./(rho.*g);

%Subtrating Hydrostatic Pressure From Measured Pressure
PD=Pgage1+(rho.*g.*z); %Equation 4.23 in Dean Text (Pa)
%Even though there is a plus sign, z is negative which causes it to
%be subtracted. There is a negative sign on the right hand side of

```

```

%eq 4.23, so we need to assume its being added.
%deltaH1=PD./(rho.*g);

%-----

%Obtain Raw FFT to obtain w(rad/s)
[Y,freq]=Guu_calc(deltaH,rate);
w=2.*pi.*freq;
f=freq;

%Plot of Raw FFT
plot(f,Y)
title('Raw FFT 04/16/15')
xlabel('Frequency (Hz)')
ylabel('Spectral Energy Density (m^2/Hz)')

%-----

%Determining Pressure Response Factor Kp
%Assume Deep Water Conditions due to Placement of Deep Water Buoy
%Dispersion Relation for Deep Water
k=w.*w./g; % Wave number at each frequency
Kp=1./cosh(k.*h); % Pressure Response Factor

NewY=Y';

figure, plot(f,Kp)
xlabel('Frequency (Hz)')
ylabel('Pressure Response Factor')
title('Pressure Response Factor vs Frequency 04/16/15')

%-----

% Corrected FFT
NewestY=NewY./Kp;
figure, plot(f(1:100),NewestY(1:100))
xlabel('Frequency (Hz)')
ylabel('Spectral Energy Density (m^2/Hz)')
title('Corrected FFT 04/16/15')

%-----

%Determining Significant Wave Height
HH=sqrt(f(1:100).*NewestY(1:100));
Hrms=rms(HH);
Hsig=1.35.*Hrms;
E=1030.*g.*(Hsig.^2)./8;
C=9.81.*8./(2.*pi);
FF=E.*5.*C.*1.589;

%Determining Available Wave Energy
EE=trapz(NewestY(1:100));

function [Guu,f] = Guu_calc(data,samp_freq)
t2 = detrend(data);

```

```

n2 = max(size(data));
y2 = fft(t2,n2);
Guu = 2*y2.* conj(y2)/(samp_freq*n2);
f = samp_freq*(1:n2)/n2;
b1 = round(length(Guu)/2);
b2 = round(length(f)/2);
  Guu = Guu(1:b1);
  f = f(1:b2);

```

## Arduino Code

```

/*
 * Simple data logger.
 */
#include <SPI.h>
#include <SdFat.h>
// SD chip select pin. Be sure to disable any other SPI devices such as Enet.
const uint8_t chipSelect = SS;
// Interval between data records in milliseconds.
// The interval must be greater than the maximum SD write latency plus the
// time to acquire and write data to the SD to avoid overrun errors.
// Run the bench example to check the quality of your SD card.
const uint32_t SAMPLE_INTERVAL_MS = 150;
// Log file base name. Must be six characters or less.
#define FILE_BASE_NAME "Data"
SdFat sd;    // File system object.
SdFile file; // Log file.
uint32_t logTime;// Time in micros for next data record.
// PIN ASSIGNMENTS
const int LIDAR_TRIGGER = 2;
const int LIDAR_MONITOR = 3;
const int VOLTAGE_MONITOR = A3;

//=====
// User functions. Edit writeHeader() and logData() for your requirements.
//-----

void set_leds(int reading);
void writeHeader() {
  file.print(F("millis"));
  file.print(F(",voltage"));
  file.print(F(", displacement"));
  file.println();
}

void logData() {
  int voltage = analogRead(VOLTAGE_MONITOR);
  int displacement = pulseIn(LIDAR_MONITOR, HIGH);
  //set_leds(voltage);

```

```

// Write data to file. Start with log time in micros.
file.print(millis());
file.write(',');
file.print(voltage);
file.print(", ");
file.println(displacement);

float power = pow(float(voltage) / 1023.0 * 5 * 99.6 / 7.9, 2) / 100;
float voltage_reading = voltage / 1023.0 * 5 * 99.6 / 7.9; // 5 / 1023.0 * 30 / 4
float displacement_reading = displacement / 10.0 - 9.33;
Serial.print(voltage);
Serial.print(" volts, ");
Serial.print(displacement_reading);
Serial.println(" cm.");
}
//=====
=====
// Error messages stored in flash.
#define error(msg) sd.errorHalt(F(msg))
//-----

void setup() {
  Serial.begin(9600);
  //-----
  //LIDAR
  //-----
  pinMode(LIDAR_TRIGGER, OUTPUT); // Set lidar trigger pin
  pinMode(LIDAR_MONITOR, INPUT); // Set lidar monitor pin
  pinMode(4, OUTPUT);
  pinMode(5, OUTPUT);
  pinMode(6, OUTPUT);
  pinMode(7, OUTPUT);
  pinMode(8, OUTPUT);
  pinMode(9, OUTPUT);
  digitalWrite(8, LOW);
  digitalWrite(9, LOW);

  digitalWrite(LIDAR_TRIGGER, LOW); // Set trigger LOW for continuous read
  //-----
  //SD shield setup
  //-----
  const uint8_t BASE_NAME_SIZE = sizeof(FILE_BASE_NAME) - 1;
  char fileName[13] = FILE_BASE_NAME "00.csv";
  // Initialize the SD card at SPI_HALF_SPEED to avoid bus errors with
  // breadboards. use SPI_FULL_SPEED for better performance.
  if (!sd.begin(chipSelect, SPI_HALF_SPEED)) {
    digitalWrite(8, HIGH);
    sd.initErrorHalt();
  }
}

```



```

}

// Find an unused file name.
if (BASE_NAME_SIZE > 6) {
  error("FILE_BASE_NAME too long");
}
while (sd.exists(fileName)) {
  if (fileName[BASE_NAME_SIZE + 1] != '9') {
    fileName[BASE_NAME_SIZE + 1]++;
  } else if (fileName[BASE_NAME_SIZE] != '9') {
    fileName[BASE_NAME_SIZE + 1] = '0';
    fileName[BASE_NAME_SIZE]++;
  } else {
    digitalWrite(8, HIGH);
    error("Can't create file name");
  }
}
if (!file.open(fileName, O_CREAT | O_WRITE | O_EXCL)) {
  error("file.open");
  digitalWrite(8, HIGH);
}
Serial.print(F("Logging to: "));
Serial.println(fileName);
// Write data header.
digitalWrite(9, HIGH);
digitalWrite(8, LOW);
writeHeader();
//-----
}
//-----

void loop() {
  logData();
  // Force data to SD and update the directory entry to avoid data loss.
  if (!file.sync() || file.getWriteError()) {
    error("write error");
  }
  delay(20);
}

void set_leds(int reading){
  if (reading > 25)
    digitalWrite(4, HIGH);
  else
    digitalWrite(4, LOW);
  if (reading > 275)
    digitalWrite(5, HIGH);
  else
    digitalWrite(5, LOW);
}

```

```

if (reading > 525)
  digitalWrite(6, HIGH);
else
  digitalWrite(6, LOW);
if (reading > 775)
  digitalWrite(7, HIGH);
else
  digitalWrite(7, LOW);
}
#include "SIM900.h"
#include <SoftwareSerial.h>
#include "inetGSM.h"
// #include "sms.h"
// #include "call.h"

// To change pins for Software Serial, use the two lines in GSM.cpp.

// GSM Shield for Arduino
// www.open-electronics.org
// this code is based on the example of Arduino Labs.

// Simple sketch to start a connection as client.

InetGSM inet;
// CallGSM call;
// SMSGSM sms;

char msg[50];
int numdata;
char inSerial[50];
int i=0;
boolean started=false;

void setup()
{
  // Serial connection.
  Serial.begin(9600);
  Serial.println("GSM Shield testing.");
  // Start configuration of shield with baudrate.
  // For http uses is recommended to use 4800 or slower.
  if (gsm.begin(2400)) {
    Serial.println("\nstatus=READY");
    started=true;
  } else Serial.println("\nstatus=IDLE");

  if(started) {
    // GPRS attach, put in order APN, username and password.

```

```

//If no needed auth let them blank.
while (!inet.attachGPRS("att.mvno", "", "")){
  Serial.println("status=ERROR, trying again");
  delay(1000);
}
Serial.println("status=ATTACHED");
delay(1000);

//Read IP address.
gsm.SimpleWriteLn("AT+CIFSR");
delay(5000);
//Read until serial buffer is empty.
gsm.WhileSimpleRead();

//TCP Client GET, send a GET request to the server and
//save the reply.

}
};

void loop()
{
  msg[0] = '\0';
  numdata=inet.httpGET("tzero.com", 80, "/", msg, 50);
  //Print the results.
  Serial.println("\nNumber of data received:");
  Serial.println(numdata);
  Serial.println("\nData received:");
  Serial.println(msg);
  //Read for new byte on serial hardware,
  //and write them on NewSoftSerial.
  serialhwread();
  //Read for new byte on NewSoftSerial.
  serialswread();
  delay(1000);
};

void serialhwread()
{
  i=0;
  if (Serial.available() > 0) {
    while (Serial.available() > 0) {
      inSerial[i]=(Serial.read());
      delay(10);
      i++;
    }
  }
}

```

```

inSerial[i]='\0';
if(!strcmp(inSerial, "/END")) {
    Serial.println("_");
    inSerial[0]=0x1a;
    inSerial[1]='\0';
    gsm.SimpleWriteln(inSerial);
}
//Send a saved AT command using serial port.
if(!strcmp(inSerial, "TEST")) {
    Serial.println("SIGNAL QUALITY");
    gsm.SimpleWriteln("AT+CSQ");
}
//Read last message saved.
if(!strcmp(inSerial, "MSG")) {
    Serial.println(msg);
} else {
    Serial.println(inSerial);
    gsm.SimpleWriteln(inSerial);
}
inSerial[0]='\0';
}
}

void serialswread()
{
    gsm.SimpleRead();
}

```

## Procedures

### Assembly Procedure

- Spar Assembly
  - Bolt on aluminum plate w/ 1 ½” galvanized flange with red gasket in place to the bottom of the spar making sure washers are placed under bolt heads
  - Insert spar into float
  - Mount PVC flange onto the top of the spar aligning the bolt pattern and fasten with 2x ½” bolts and 1 lifting eye ensuring that the lifting eye lines up with the other lifting point on the metal bracket fastened to the spar (heads of bolts are inside of spar)
  - Bolt adapter plate onto PVC flange with 4x ¾” bolts
- PTO/Housing Assembly
  - Mount PTO inside housing with 2x ¼-20 bolts through the cross member on the bottom of the housing (racks pass through slotted hole in housing
  - \*Note – once the PTO is mounted inside the housing the racks must extend through the bottom of the housing in order to fasten the top on the housing
  - Bolt 5/8” rod onto the end of the racks placing small of sheet metal in between rack end and rod (sheet metal is for laser to reflect off of)
  - Mount top onto housing using 4x ¼-20 bolts by passing the rod through the linear flange bearing first
- Mount PTO/Housing onto spar using 4x ½” bolts and washers ensuring that the racks also pass through the hole in the adapter plate
- Insert 5/8” rod into flex coupler which is already mounted to the top of the aluminum extrusion frame
- Heave Plate Extension Assembly
  - Insert cotter pin through the pipe and flange on the aluminum plate
  - Insert cotter pin through pipe and flange on heave plate



# University of New Hampshire

## Wave Energy Buoy

### **Mobilization – Deployment – Recovery Procedures UNH-WEB-DOC-01**

Prepared by: Pedro Damasceno

Approved by: WEB Team - Prof. Rob Swift - Matthew Rowell - Gulf Challenger Captain

<b>2.0</b>	<b>Issued for Revision</b>	<b>Feb.27.15</b>	<b>PDA</b>	<b>WEB</b>
Version	Reason for Issue	Issue Date	Prepared by	Approved by



# Content

1. General.....	3
2. Objective .....	3
3. Abbreviations and Definitions.....	3
4. Specifications .....	3
5. Procedures .....	5
a. Mobilization Procedure.....	5
b. Deployment Procedure.....	8
c. Recovery Procedure .....	10
6. Attachments.....	12



## 1. General

This document describes the steps and actions that shall be followed to a safe, efficient and successful operation with the UNH – Wave Energy Buoy.

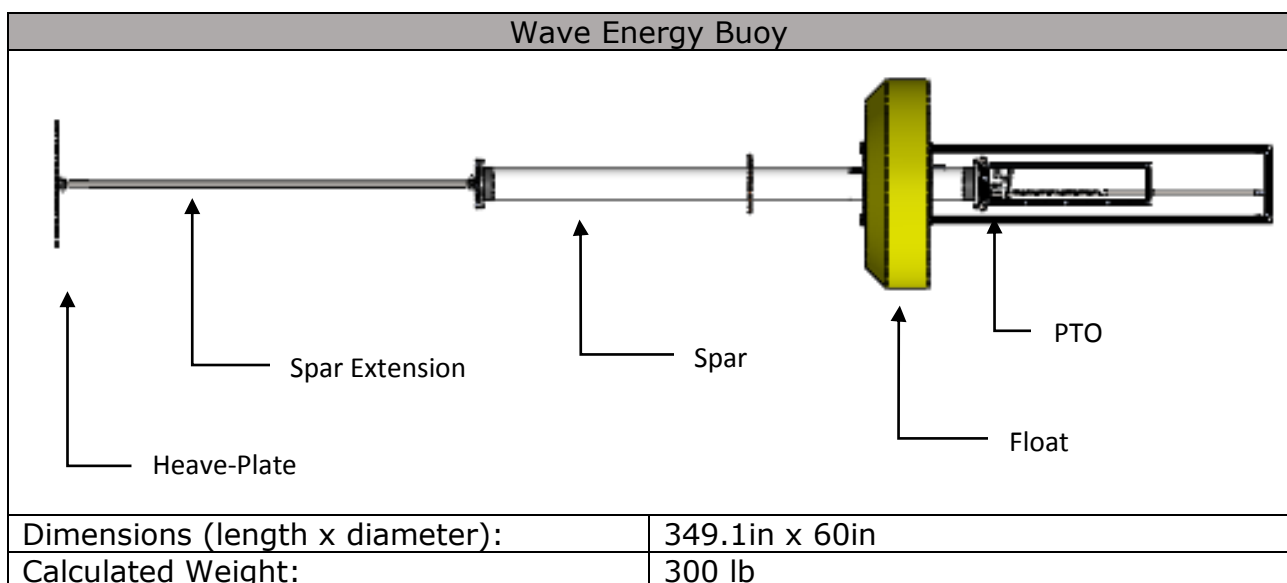
## 2. Objective

The objective of this procedure is to provide all relevant personnel with a clear understanding of the different steps for the planning and execution of Wave Energy Buoy operations.

## 3. Abbreviations and Definitions

Abbreviations	Definition
A-Fr. Op.	A-Frame Operator
Capt.	Captain
Crane Op.	Crane Operator
G.C.	R/V Gulf Challenger – UNH Vessel
UNH	University of New Hampshire
WEB	Wave Energy Buoy
Winch Op.	Winch Operator

## 4. Specifications



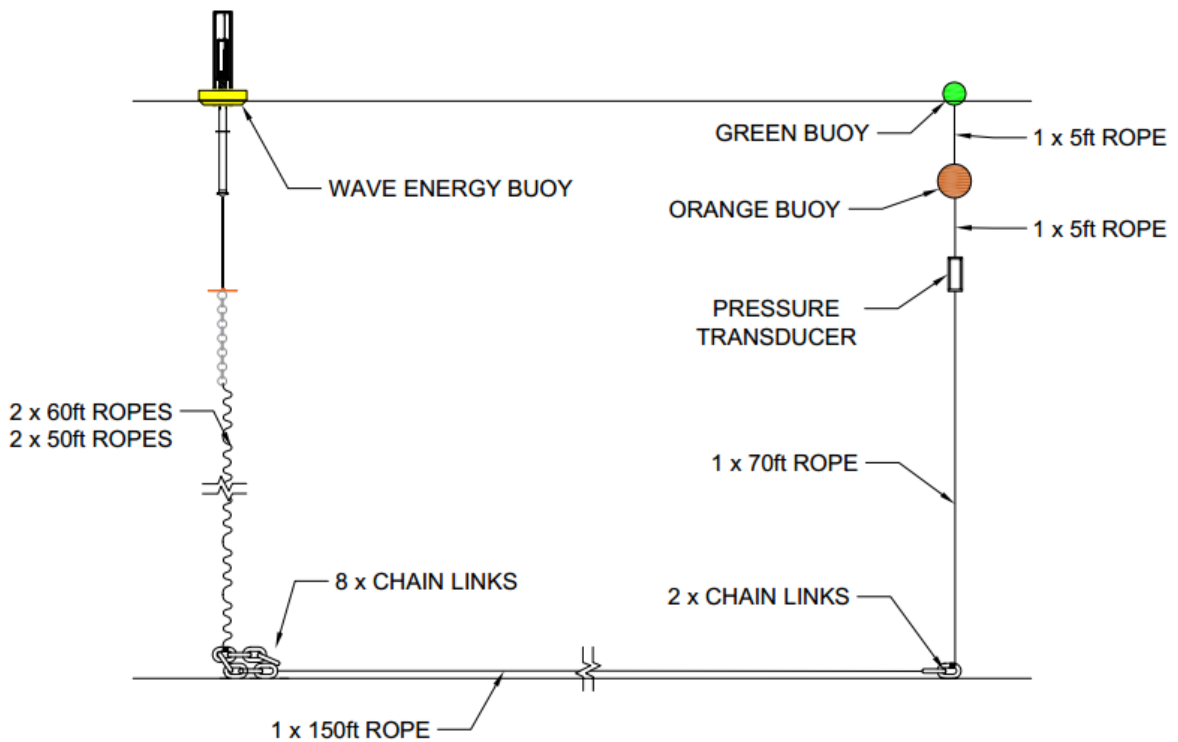




**Deployment Location**

Location:	Isle of Shoals Area
Estimated Water Depth:	80ft




**Mooring Schematic**







Items	Qty.:
35ft x 40' White Rope	1
Pear Link	1
50' Yellow Rope	2
60' White Rope	2
25lb Chain Link	10 (1 set of 8 & 1 set of 2)
100ft x 150' White Rope	1
70ft x 90' Black Rope	1
Pressure Transducer	1
Orange Buoy	1
Green/Red Buoy	1
5ft Rope	2


## 5. Procedures

### a. Mobilization Procedure



UNH – Wave Energy Buoy Mobilization, Deployment and Recovery Procedure			
Mobilization Procedure			
Item	Action	Responsible	Check
	Safety Concern.1: Always be careful with your hands and fingers for pitching points. DO IT SAFE OR NOT AT ALL!	INFO	
	Safety Concern.2: Anyone should STOP the operations if note any dangerous condition. DO IT SAFE OR NOT AT ALL!	INFO	
1.	Use the Chase Lab Crane to load the WEB on the trailer;	WEB Team	
2.	Attach 2 pieces of wood to avoid the buoy movement;	WEB Team	
3.	Tie a rope on the pieces of wood in order to facilitate its removal during the deployment ops;	WEB Team	
4.	Use cargo ratchets and ropes to firmly secure the buoy on the trailer;	WEB Team	
5.	Attach the trailer to the car hitch;	WEB Team	
	Safety Concern.3: Before start to tow the trailer, ensure that there are <b>NO</b> loosen items that can fall during the transportation route; DO IT SAFE OR NOT AT ALL!	INFO	
6.	Ensure that all items required for the deployment and recovery operations were previously segregated, checked and are ready to go; [see materials check list attached]; <ul style="list-style-type: none"> <li>• Ropes;</li> <li>• Small Buoys (Green and Orange);</li> <li>• Pressure Transducer;</li> <li>• Pear Link;</li> <li>• Chains</li> </ul>	WEB Team	
7.	Load all the items on the truck/cars and close the checklist;	WEB Team	
8.	Drive to UNH Pier;	WEB Team	
9.	Arrive at UNH Pier;	WEB Team	

10.	Assemble the data acquisition, PTO housing and PTO;	WEB Team	
11.	Park the trailer next to the Pier Crane, according Crane Operator instructions;	WEB Team	
	Safety Concern.4: Check the lifting rigging before connect it to the Pier Crane hook; DO IT SAFE OR NOT AT ALL!	INFO	
12.	Connect the Pier Crane hook's to the lifting rigging;	Crane Op. / WEB Team	
13.	Attach ropes as tag lines to control the WEB movements during the lifting;;	WEB Team	
14.	Check if the: <ul style="list-style-type: none"> <li>• G.C. Deck is clear of non-essential personnel;</li> <li>• The A-Frame is not on the lifting route;</li> <li>• Deck space is sufficient to land the WEB;</li> <li>• All personnel is aware that the lifting is ready to start;</li> </ul>	Crane Op. / WEB Team	
15.	Wait Captain authorization to start the lift;	Crane Op.	
	Safety Concern.5: <b>NEVER</b> stay under the load during the lifting operations. DO IT SAFE OR NOT AT ALL!	INFO	
16.	Start to lift the Buoy from the trailer;	Crane Op.	
17.	Rotate the Crane and lower the WEB until it gently land on the G.C. deck;	Crane Op.	
18.	Use ropes and wooden stoppers to securely seafastening the WEB on deck;	WEB Team	
19.	Captain to check if the seafastening is ok;	Capt.	
20.	Stretch and organize the ropes on the deck to ensure that there are no knots and facilitate the deployment order;	WEB Team	
21.	Pre-assemble the mooring system, ropes, transducers and buoys, as per drawing UNH-WEB-DWG-01, ref [01];	WEB Team	
22.	Connect the heave plate to the chain;	WEB Team	
23.	Connect the heave plate + chain to the spar extension;	WEB Team	
24.	Attach the spar extension on the spar;	WEB Team	
	Safety Concern.6: Be sure that the 2 x R-Clips are securely in place; DO IT SAFE OR NOT AT ALL!	INFO	


	<b>Wave Energy Buoy</b>  <b>Mobilization – Deployment – Recovery Procedures</b>	<b>Page 7</b>
---	---	---------------

	<b>Safety Concern.7: Before start the transit all personnel aboard shall wear life jackets (PFD); DO IT SAFE OR NOT AT ALL!</b>	<b>INFO</b>	
<b>25.</b>	<b>Start transit to deployment location (WD~80ft).</b>	<b>Capt.</b>	

## b. Deployment Procedure



Deployment Procedure			
Item	Action	Responsible	Check
1.	Finish transit and arrive at deployment location;	Capt.	
	Safety Concern.8: Before start the Deployment Operation everyone should: <ul style="list-style-type: none"> <li>• Be aware of the operation risks;</li> <li>• Know where to stay and his/her function on the operation;</li> <li>• Know the deployment order, starts on the WEB end.</li> </ul> DO IT SAFE OR NOT AT ALL!	INFO	
2.	After Captain authorization, start to remove the WEB seafastening;	WEB Team	
3.	Connect the A-Frame hook to the lifting rigging;	WEB Team	
4.	Start to pay-in on the A-Frame winch (lift) the WEB;	A-Fr Op.	
5.	Extend the A-Frame in stern direction;	A-Fr Op.	
6.	As soon the WEB is clear of the deck, start to gently pay-out the A Frame winch until the buoy touch the water and start to float by itself;	A-Fr Op.	
7.	Continue to pay-out on the winch until the lifting rigging is slacked;	A-Fr Op.	
8.	Disconnect the lifting rigging from the A-Frame;	WEB Team	
9.	Retract the A-Frame in bow direction;		
10.	Pull the ropes (see Mobilization Procedure step #3) to remove the buoy wooden stoppers;	WEB Team	
11.	Prepare to lower the mooring lines;	WEB Team	
	Safety Concern.9: Be sure that all the knots are tight; DO IT SAFE OR NOT AT ALL!	INFO	
12.	Deploy and start to gently lower the chain + 45lb weight, connected to the bottom of the heave plate;	WEB Team	
13.	Deploy the first set of mooring lines (1 x 35ft 40' white rope, 2 x 50' yellow rope, 2 x 60' yellow rope) until the end is close to the G.C. bulwark;	WEB Team	
14.	Be ready to deploy the second set of the mooring lines;	WEB Team	
15.	Tie the yellow rope end on the 8 x chain links;	WEB Team	
16.	Tie the 100ft rope on the 8 x chain links;	WEB Team	





17.	Use the winch to deploy the chain links and start to lower it until the 8 x chain links are inside the water;	WEB Team / Winch Op.	
18.	Captain to record the actual position;	Capt.	
19.	Captain to move the G.C. 100ft forward while the chain is lowered;	Capt.	
20.	Continue to lower the chain;	Winch Op.	
21.	All stop once it is time to tie the 2 x chain links;	ALL	
22.	Tie the white rope end on the 2 x chain links;	WEB Team	
23.	Tie the 70ft Black Rope on the 2 x chain links;	WEB Team	
24.	Captain to slowly move G.C. on the same heading until complete 100ft transit;	Capt.	
25.	Restart to lower the 100ft white rope;	WEB Team	
26.	Deploy 2 x chain links + Black Rope;	WEB Team	
27.	Stop once the C.G had moved 100ft from position recorded on step #18;	Capt.	
28.	Restart to lower the chain links and the black rope, using the winch;	WEB Team	
29.	Continue to lower the rope until the end of the black rope is close to the G.C. bulwark;	WEB Team	
30.	Use zip-ties to attach the pressure transducer to the end of the black rope;	WEB Team	
	Safety Concern.10: Be sure that the zip ties are <b>NOT</b> supporting the mooring lines, its function is only to hang the pressure transducer on the mooring lines; DO IT SAFE OR NOT AT ALL!	INFO	
31.	Tie a 10ft rope on the end of the black rope close to the pressure transducer;	WEB Team	
32.	All stop after lower 5ft of the rope;	WEB Team	
33.	Use a short piece of rope to attach the orange buoy on the mooring line;	WEB Team	
34.	Restart to lower the 10ft rope part that is on the deck;	WEB Team	
35.	Tie a green/red buoy at the end of the 10ft rope;	WEB Team	
36.	Captain to move G.C. to a clear area;	Capt.	
37.	Deploy the buoy;		
38.	Standby for 2 hours or until WEB Team decision.	All	



## c. Recovery Procedure

Recovery Procedure			
Item	Action	Responsible	Check
	<p>Safety Concern.11: Before start the Recovery Operation everyone should:</p> <ul style="list-style-type: none"> <li>• Be aware of the operation risks;</li> <li>• Know where to stay and your function on the operation;</li> <li>• Know that the recover order starts on the buoy end.</li> </ul> <p>DO IT SAFE OR NOT AT ALL!</p>	INFO	
1.	Captain to place G.C. close to the green/red buoy;	Capt.	
2.	Wait for Captain authorization to commence the recovery operations;	ALL	
3.	Use the long hook to bring the buoy aboard;	WEB Team	
	<p>Safety Concern.12: After start to pull the ropes aboard be careful to keep an organize deck in order to avoid slips, trips and falls;</p> <p>DO IT SAFE OR NOT AT ALL!</p>	INFO	
4.	Use the winch to start to recover the 10ft rope aboard;	Winch Op.	
5.	Recover the Orange buoy;	WEB Team	
6.	Continue to use the winch to pull the 10ft rope aboard;	Winch Op.	
7.	Recover the pressure transducer;	WEB Team	
8.	Continue to use the winch to pull the 70ft rope aboard;	Winch Op.	
9.	Be ready to recover the 2 x chain links;	WEB Team	
10.	All stop when the 2 x chain links are on the water line;	ALL	
11.	Gently bring the 2 x chain links aboard;	WEB Team	
12.	Captain to move the vessel backwards while the 100ft rope is recovered;	Capt.	
13.	Continue to use the winch to pull the 100ft rope aboard;	Winch Op.	
14.	Be ready to recover the 8 x chain links;	WEB Team	
15.	All stop when the 8 x chain links are on the water line;	ALL	
16.	Gently bring the 8 x chain links aboard;	WEB Team	



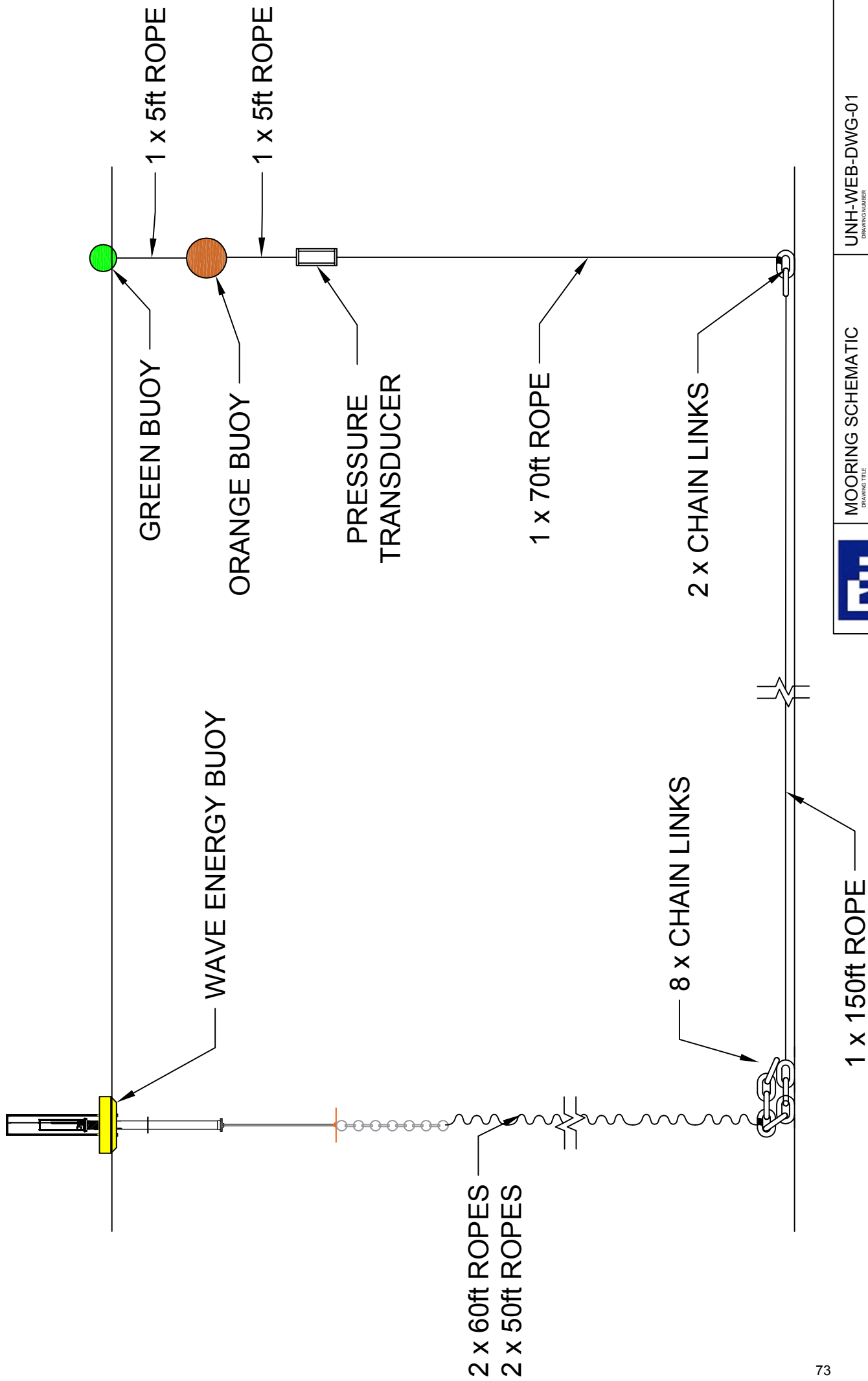
17.	Continue to use the winch to pull the 220ft rope aboard;	Winch Op.	
18.	Recover all the rope;	WEB Team	
19.	Continue to use the winch to pull the 35ft rope aboard;	Winch Op.	
20.	Note that the buoy starts to tilt, it means that the 45lb weight is close to the water line;	INFO	
21.	Be ready to recover the 45lb weight;	WEB Team	
22.	All stop when the 45lb weight is on the water line;	ALL	
23.	Gently bring the 45lb weight aboard;	WEB Team	
24.	Disconnect the 45lb weight from the chain;	WEB Team	
25.	Pull the chain in order to move the buoy closer to the stern;	WEB Team	
26.	Use the long hook to recover the masterlink on the top of the lifting rigging;	WEB Team	
27.	Extend the A-Frame in stern direction;	A-Fr. Op.	
28.	Pay-Out on the A-Frame Winch in order to connect the masterlink on the A-Frame hook;	WEB Team	
	Safety Concern.13: Before start the lift all non-essential personnel shall leave the deck; DO IT SAFE OR NOT AT ALL!	INFO	
	Safety Concern.14: Check if the deck is clear and have enough space to land the WEB; DO IT SAFE OR NOT AT ALL!	INFO	
29.	Wait for Captain authorization to bring the WEB aboard;	Capt.	
30.	Start to lift the buoy;	A-Fr. Op.	
31.	Once the buoy is at the deck level retract the A-Frame in the bow direction;	A-Fr. Op.	
32.	Gently land the buoy on the deck;	A-Fr. Op.	
33.	Use ropes and wooden stoppers to securely seafastening the WEB on deck;	WEB Team	
34.	Disconnect the lift rigging from the A-Frame;	WEB Team	
35.	Captain to check if the seafastening is ok;	Capt.	
36.	Organize the deck and prepare to start the transit;	WEB Team	
37.	Start the transit back to the UNH Pier.	Capt.	






## 6. Attachments

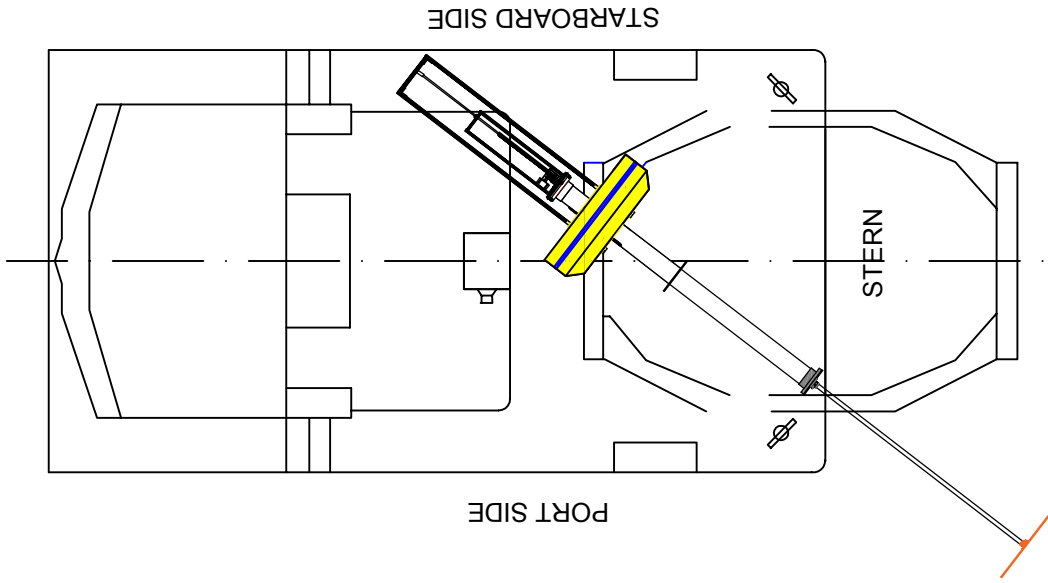
Document Number	Document Title
UNH-WEB-DWG-01	Mooring Schematic Drawing
UNH-WEB-DWG-02	Deployment Storyboard
UNH-WEB-DWG-03	Recovery Storyboard
UNH-WEB-DWG-04	Wave Energy Buoy
UNH-WEB-DWG-05	Lifting Rigging
UNH-WEB-DWG-06	Gulf Challenger Deck Plan



	MOORING SCHEMATIC	UNH-WEB-DWG-01
	<small>DRAWING TITLE</small>	<small>DRAWING NUMBER</small>
WAVE ENERGY BUOY PROJECT		
<small>PROJECT NAME</small>		
UNIVERSITY OF NEW HAMPSHIRE	PDA	04/23/15
	<small>PREPARED BY</small>	<small>DATE</small>
		2 0
		<small>REVISION</small>

STEP BY STEP:

1. CONNECT THE A-FRAME HOOK TO THE LIFTING RIGGING;
2. START TO LIFT THE WEB;

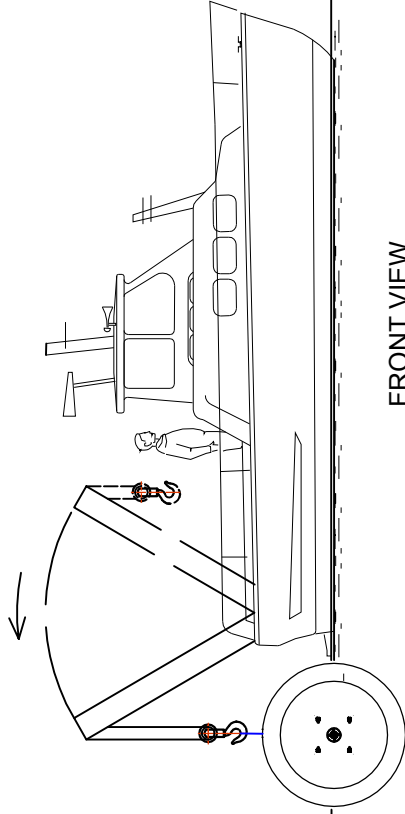


NOTES:

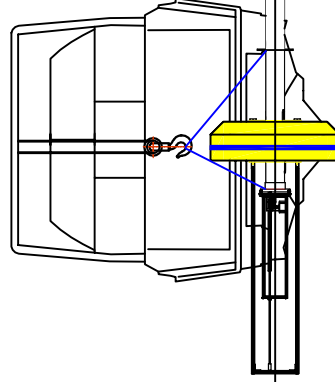
1. DRAWING NOT TO SCALE;

STEP BY STEP:

3. EXTEND THE A-FRAME IN THE STERN DIRECTION;
4. LOWER THE WEB;
5. DISCONNECT THE LIFTING RIGGING;



FRONT VIEW



LEFT VIEW



DEPLOYMENT STORYBOARD

DRAWING NUMBER

UNH-WEB-DWG-02 - Page 01

WAVE ENERGY BUOY PROJECT

PROJECT NAME

UNIVERSITY OF NEW HAMPSHIRE

PREPARED BY

PDA

DATE

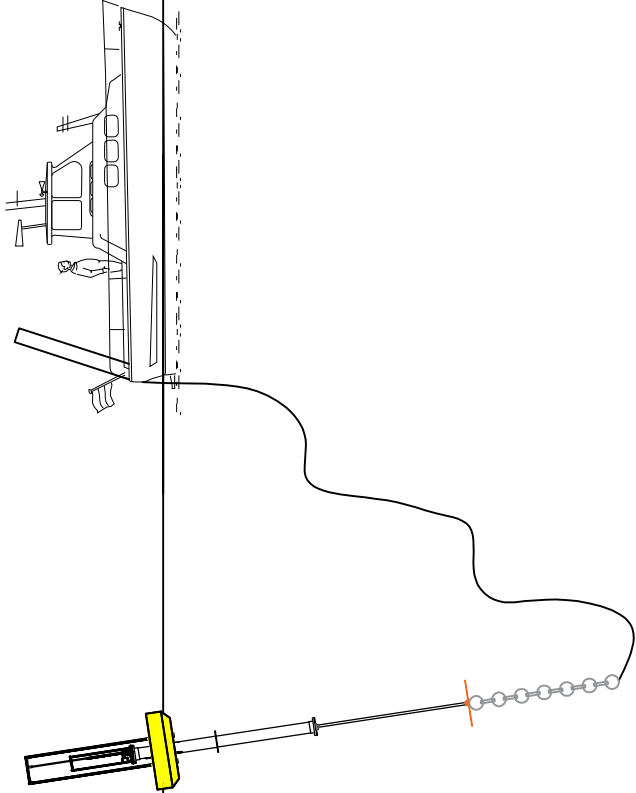
04/23/15

REVISION

1.0

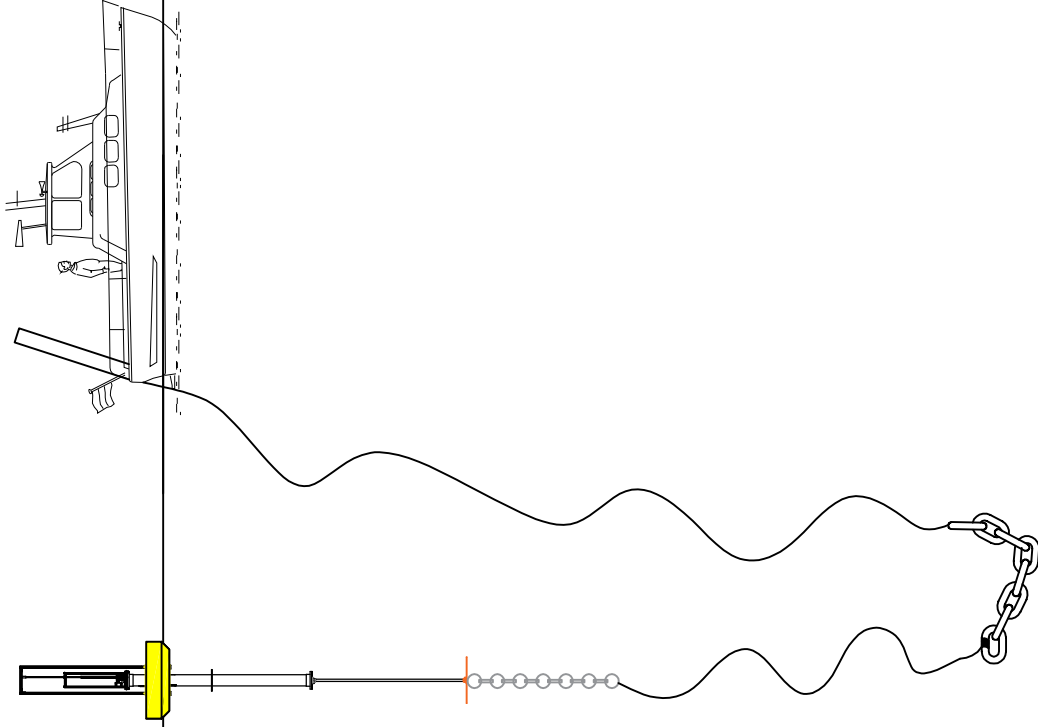
STEP BY STEP:

- 6. DEPLOY 1st SET OF ROPE;
- 7. PREPARE 8 x CHAIN LINKS;



STEP BY STEP:

- 8. DEPLOY 8 x CHAIN LINKS;
- 9. DEPLOY BOTTOM MOORING ROPE;



NOTES:

- 1. DRAWING NOT TO SCALE;



DEPLOYMENT SCHEMATIC  
DRAWING TITLE

WAVE ENERGY BUOY PROJECT  
PROJECT NAME

UNIVERSITY OF NEW HAMPSHIRE  
PREPARED BY

PDA  
DATE

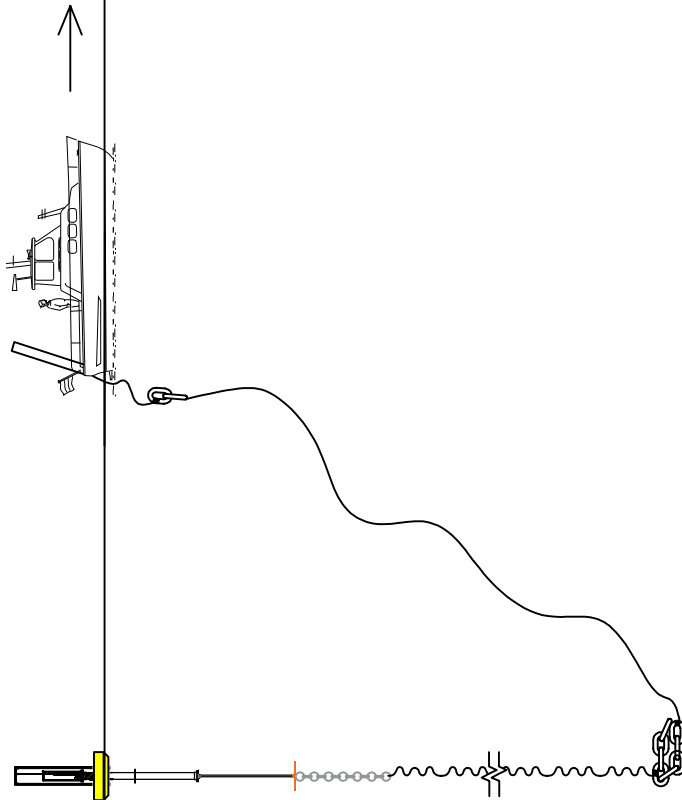
03/03/15  
DATE

1.0  
REVISION

UNH-WEB-DWG-02 - Page 02  
DRAWING NUMBER

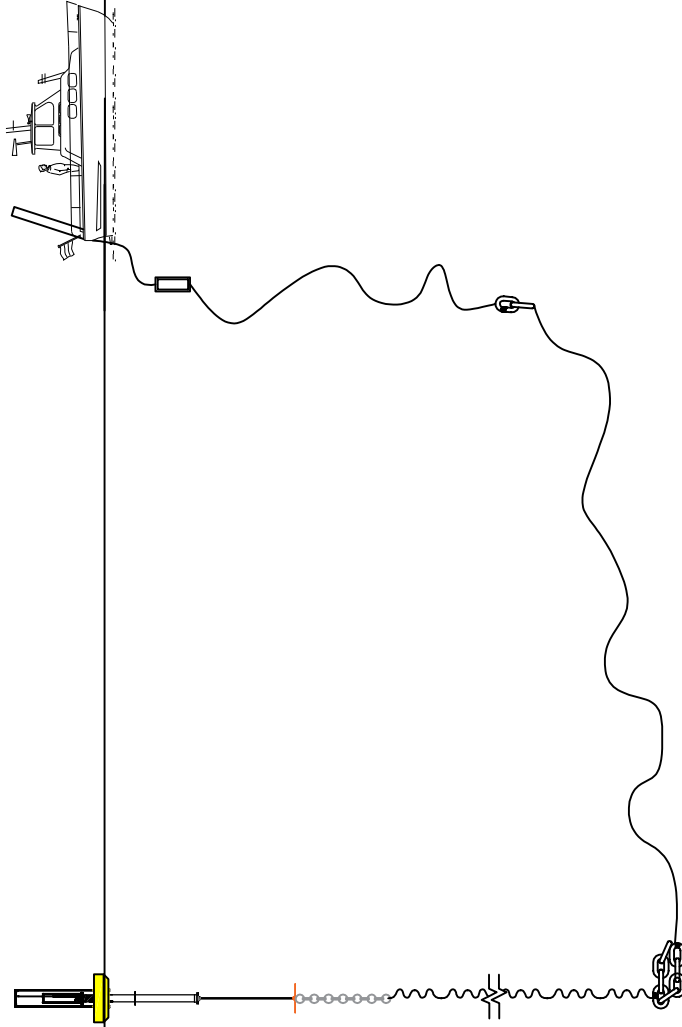
STEP BY STEP:

- 10. DEPLOY 2 x CHAIN LINKS;
- 11. PREPARE THE 2nd SET ROPE;



STEP BY STEP:

- 12. DEPLOY THE PRESSURE TRANSDUCER;
- 13. PREPARE THE NEXT ROPE;



NOTES:

- 1. DRAWING NOT TO SCALE;



DEPLOYMENT SCHEMATIC

UNH-WEB-DWG-02 - Page 03

WAVE ENERGY BUOY PROJECT

UNIVERSITY OF NEW HAMPSHIRE

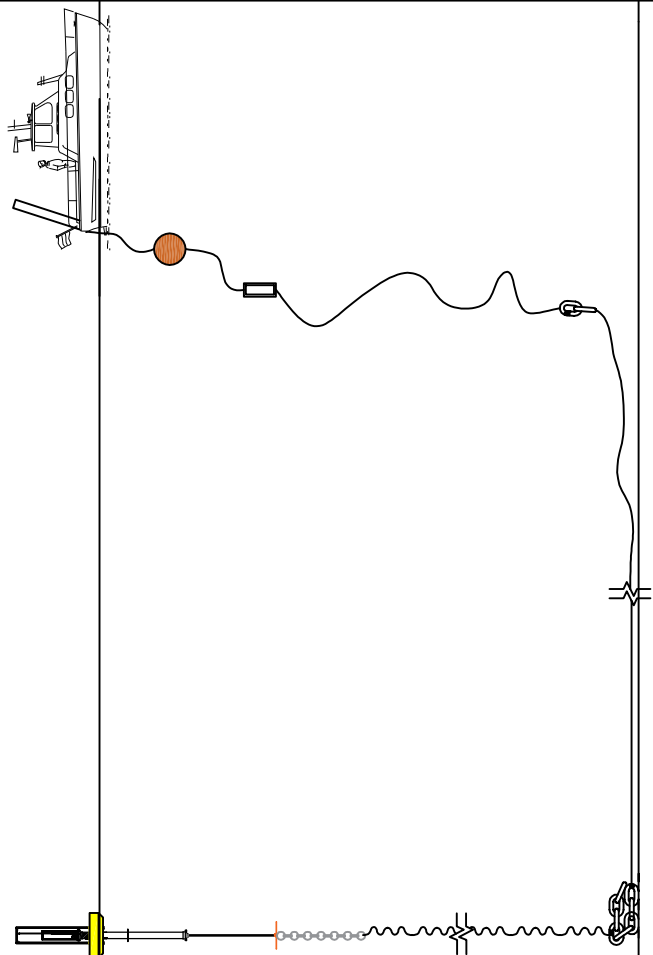
PREPARED BY  
PDA

DATE  
03/03/15

REVISION  
1.0

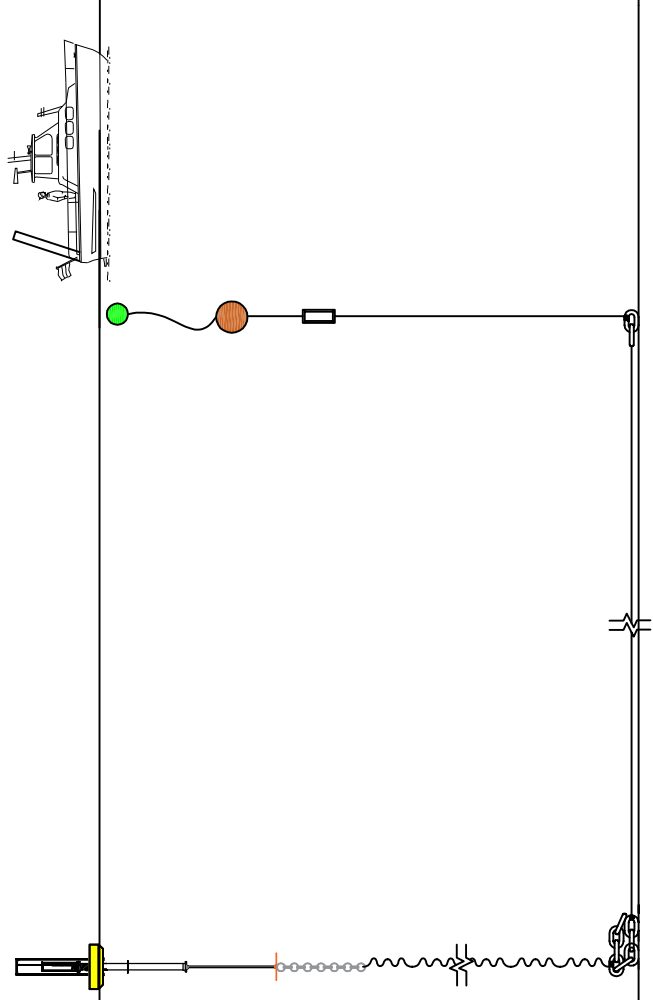
STEP BY STEP:

- 14. DEPLOY THE ORANGE BUOY;
- 15. PREPARE THE NEXT ROPE;



STEP BY STEP:

- 16. DEPLOY THE GREEN BUOY;
- 17. CAPTAIN TO MOVE GULF CHALLENGER TO A SAFE AREA.



NOTES:

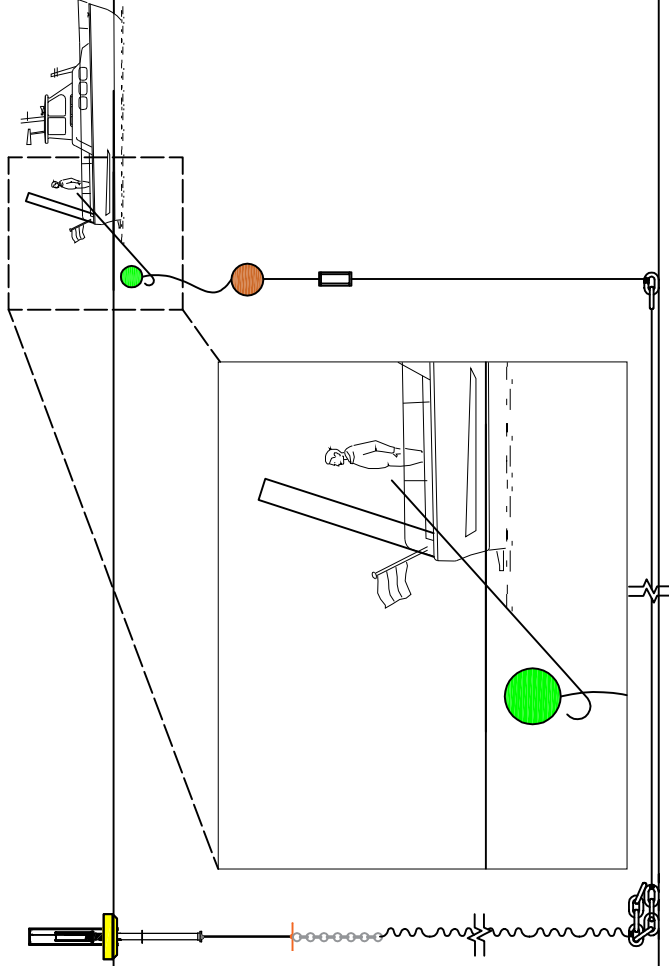
- 1. DRAWING NOT TO SCALE;



DEPLOYMENT SCHEMATIC	UNH-WEB-DWG-02 - Page 04
<small>DRAWING TITLE</small>	<small>DRAWING NUMBER</small>
WAVE ENERGY BUOY PROJECT	
<small>PROJECT NAME</small>	
UNIVERSITY OF NEW HAMPSHIRE	PDA
<small>PREPARED BY</small>	03/03/15
	<small>DATE</small>
	1.0
	<small>REVISION</small>

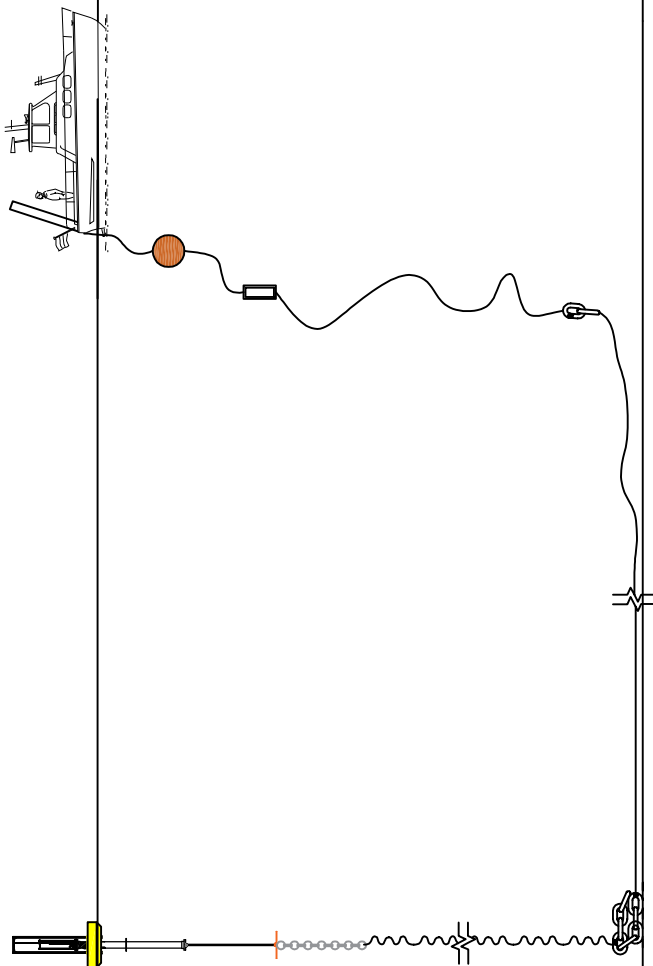
STEP BY STEP:

1. CAPTAIN TO MOVE GULF CHALLENGER TO A POSITION CLOSE TO THE SMALL GREEN BUOY;
2. CREW TO USE THE LONG HOOK TO RECOVER THE GREEN BUOY ABOARD;;



STEP BY STEP:

3. CREW TO USE RECOVERY THE ROPES;
4. CREW TO RECOVER THE ORANGE BUOY;



NOTES:

1. DRAWING NOT TO SCALE;



RECOVERY STORYBOARD

UNH-WEB-DWG-03 - Page 01

WAVE ENERGY BUOY PROJECT

UNIVERSITY OF NEW HAMPSHIRE

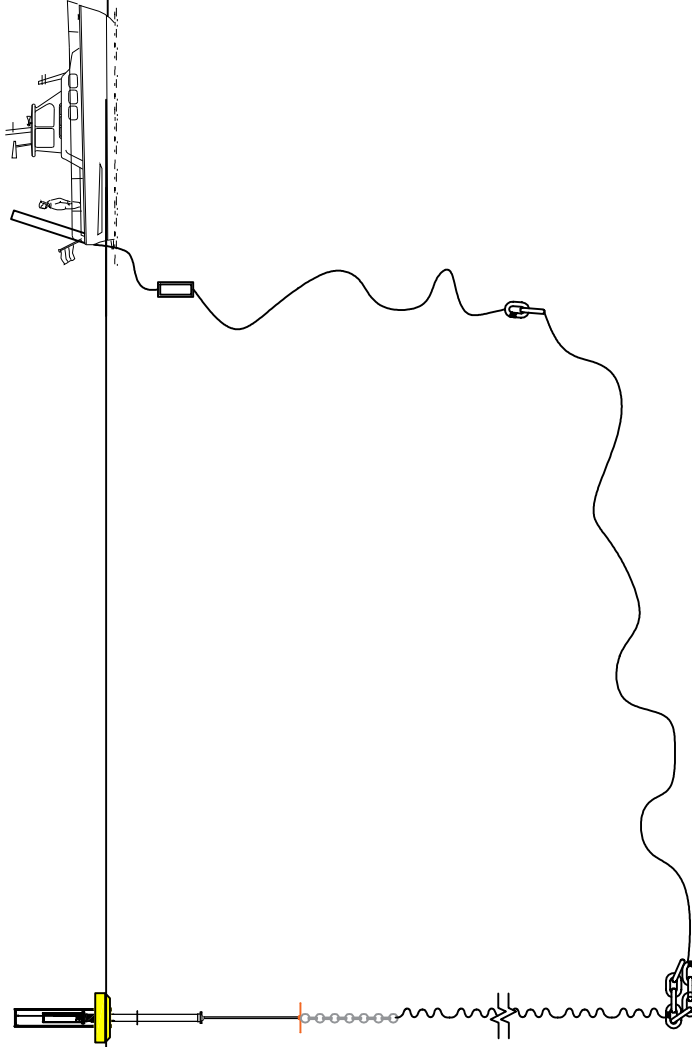
PDA

03/05/15

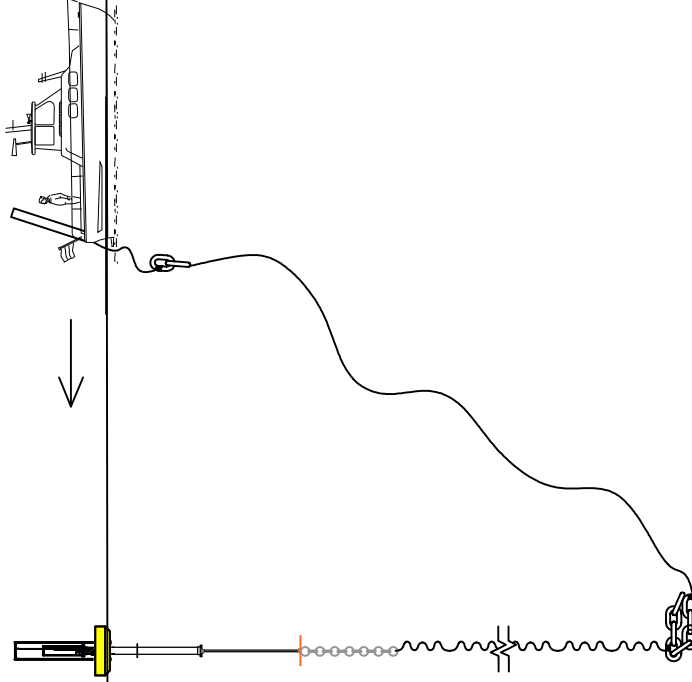
1.0

REVISION

STEP BY STEP:  
 5. RECOVER THE MOORING ROPE  
 6. RECOVER THE PRESSURE TRANSDUCER;



STEP BY STEP:  
 7. RECOVER THE MOORING ROPE;  
 8. RECOVER THE 2 x CHAIN LINKS;  
 9. CAPTAIN TO MOVE GULF CHALLENGER BACKWARDS  
 IN ORDER TO FACILITATE THE RECOVERY OF THE  
 BOTTOM MOORING ROPE;



NOTES:  
 1. DRAWING NOT TO SCALE;



RECOVERY STORYBOARD  
DRAWING TITLE

UNH-WEB-DWG-03 - Page 02  
DRAWING NUMBER

WAVE ENERGY BUOY PROJECT  
PROJECT NAME

UNIVERSITY OF NEW HAMPSHIRE  
PREPARED BY

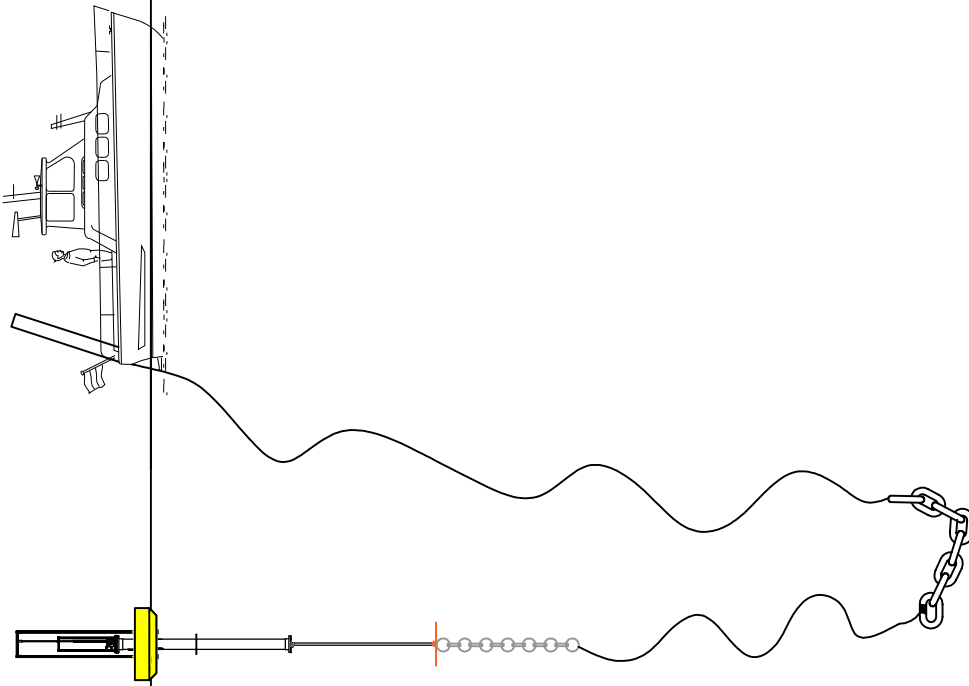
PDA  
DATE

1.0  
REVISION



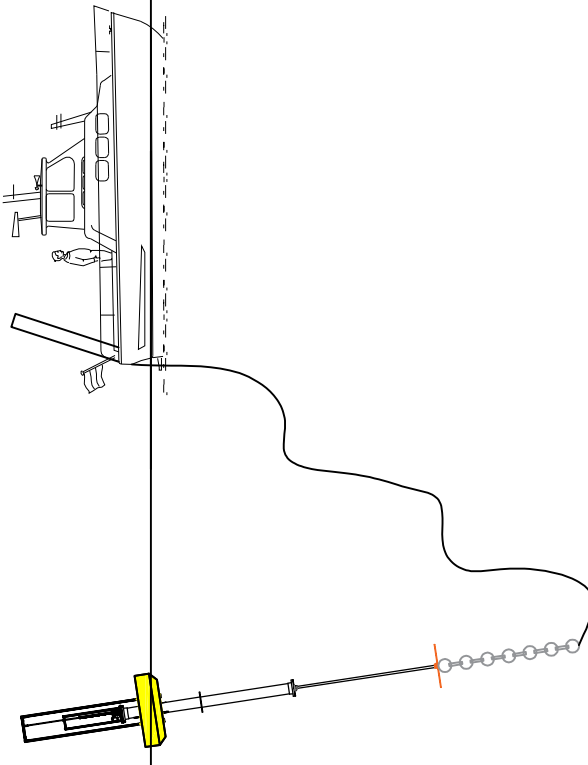
STEP BY STEP:

- 10. CONTINUE TO RECOVER THE BOTTOM MOORING ROPE;
- 11. RECOVER THE 8 x CHAIN LINKS;



STEP BY STEP:

- 12. RECOVER THE ROPE;
- 13. NOTE THAT THE BUOY STARTS TO TILT;
- 14. RECOVER THE 40 lb WEIGHT AND THE CHAIN;



NOTES:

- 1. DRAWING NOT TO SCALE;



RECOVERY STORYBOARD  
DRAWING TITLE

UNH-WEB-DWG-03 - Page 03  
DRAWING NUMBER

WAVE ENERGY BUOY PROJECT  
PROJECT NAME

UNIVERSITY OF NEW HAMPSHIRE  
PREPARED BY

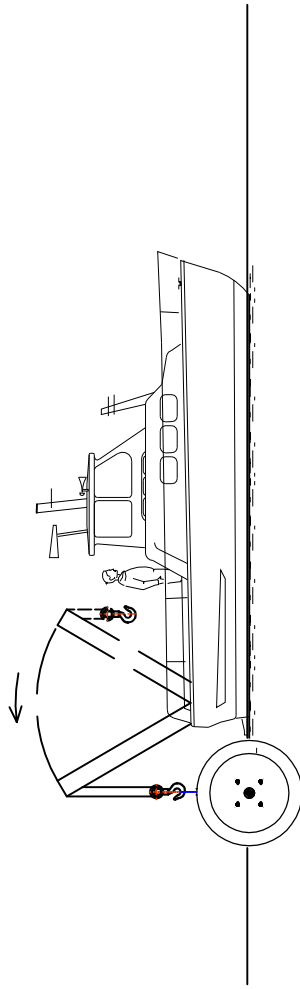
PDA  
DATE

03/03/15  
DATE

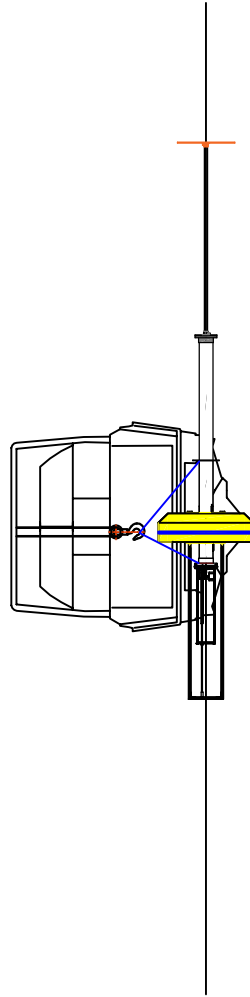
1.0  
REVISION

STEP BY STEP:

- 15. CONNECT THE A-FRAME HOOK TO THE LIFTING RIGGING;
- 16. START TO LIFT;
- 17. RETRACT THE A-FRAME IN THE BOW DIRECTION;



FRONT VIEW



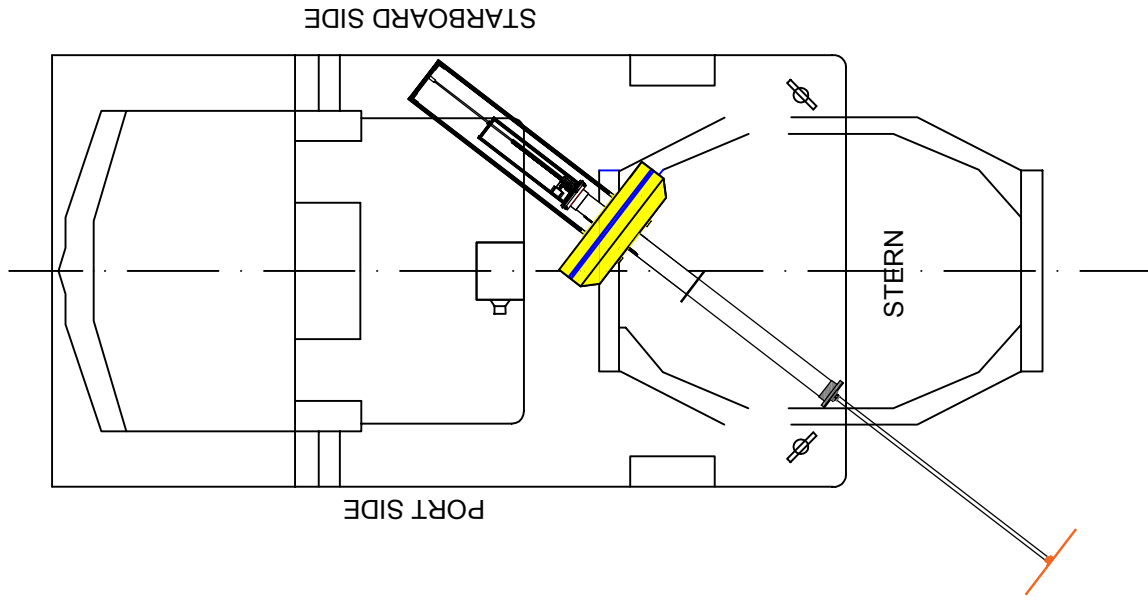
LEFT VIEW

NOTES:

- 1. DRAWING NOT TO SCALE;

STEP BY STEP:

- 18. LAND THE BUOY ON THE DECK;
- 19. DISCONNECT THE LIFTING RIGGING;
- 20. USE ROPES AND WOODEN STOPPERS TO SEAFASTEN THE BUOY;



RECOVERY STORYBOARD

UNH-WEB-DWG-03 - Page 04

WAVE ENERGY BUOY PROJECT

DRAWING NUMBER

UNIVERSITY OF NEW HAMPSHIRE

PROJECT NAME

PDA

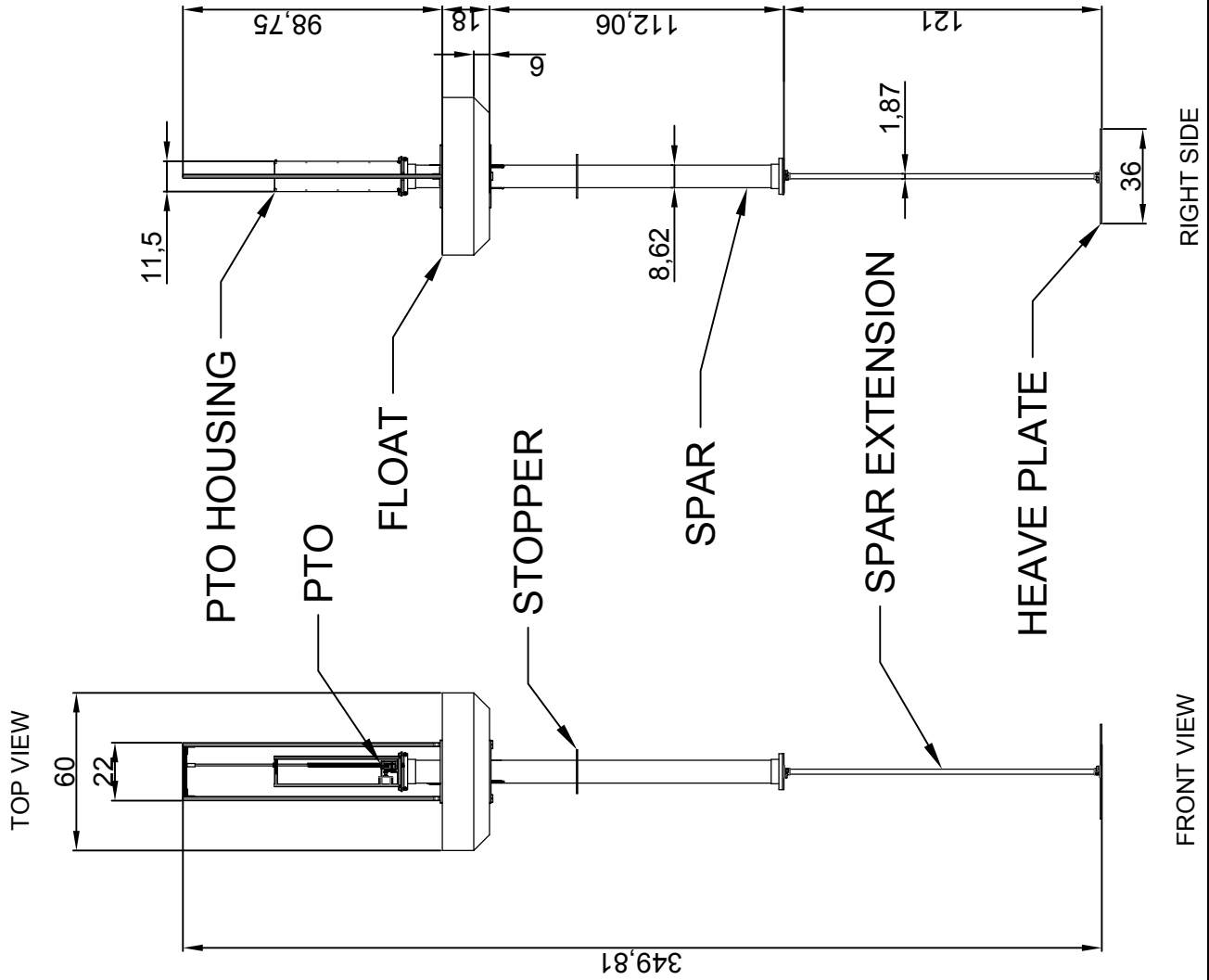
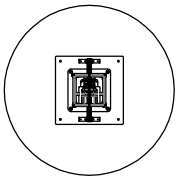
PREPARED BY

04/23/15

DATE

2.0

REVISION

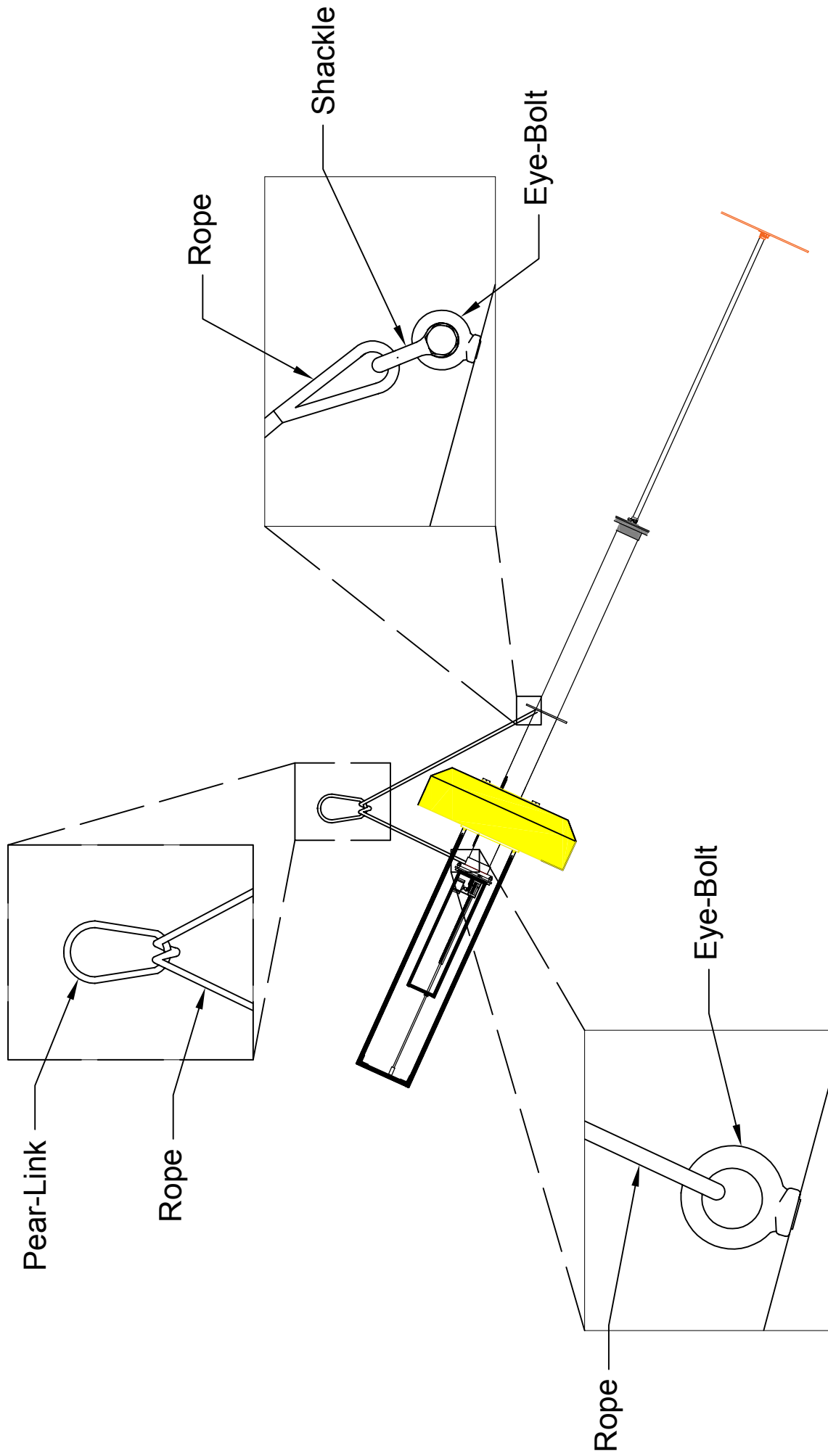


**NOTES:**

1. DRAWINGS NOT TO SCALE;
2. UNITS IN INCHES;
3. OVERALL DIMENSIONS:  
HEIGHT: 349.81in;  
DIAMETER: 60in;
4. WEIGHT:  
CALCULATED: 300 lb;  
MEASURED: TBC lb
5. DRAWING CONVERTED FROM "FULL BUOY.SLDASM"  
FILE
6. FOR FURTHER INFORMATION, DETAILED DRAWINGS  
AND DIMENSIONS SEE SOLIDWORKS MODELS;

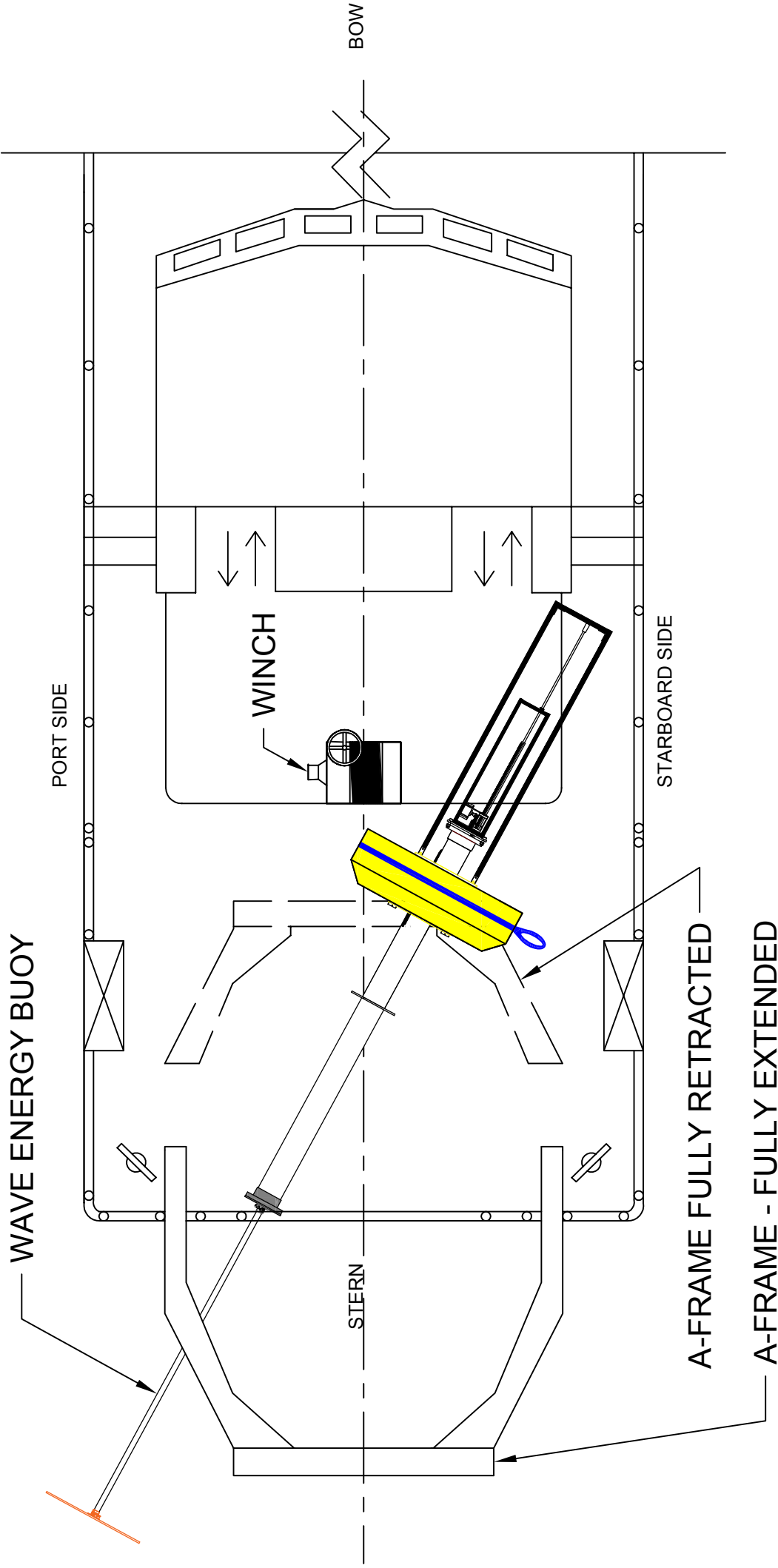


WAVE ENERGY BUOY <small>DRAWING TITLE</small>	UNH-WEB-DWG-04 <small>DRAWING NUMBER</small>
WAVE ENERGY BUOY PROJECT <small>PROJECT NAME</small>	
UNIVERSITY OF NEW HAMPSHIRE	PDA <small>PREPARED BY</small>
04/23/15 <small>DATE</small>	2.0 <small>REVISION</small>



NOTES:  
 1. DRAWING NOT TO SCALE;

	LIFTING RIGGING	UNH-WEB-DWG-05
	<small>DRAWING TITLE</small>	<small>DRAWING NUMBER</small>
WAVE ENERGY BUOY PROJECT		
<small>PROJECT NAME</small>		
UNIVERSITY OF NEW HAMPSHIRE	PDA	04/23/15
	<small>PREPARED BY</small>	<small>DATE</small>
		1.0
		<small>REVISION</small>



**NOTES:**

1. DRAWING NOT TO SCALE;
2. GULF CHALLENGER DRAWING DOWNLOAD FROM UNH SCHOOL OF MARINE SCIENCE AND OCEAN ENGINEERING WEBSITE '<http://marine.unh.edu/specifications-and-drawings>';
3. MAIN DECK COMPONENTS ARE ILLUSTRATED ON THE DRAWING FOR FURTHER DETAILS SEE DRAWING DESCRIBE ON STEP 2;
4. FOR WAVE ENERGY BUOY DETAILS SEE DRAWING - UNH-WEB-DWG-04

84



UNH CHALLENGER DECK PLAN <small>DRAWING TITLE</small>		UNH-WEB-DWG-06 <small>DRAWING NUMBER</small>
WAVE ENERGY BUOY PROJECT <small>PROJECT NAME</small>		
UNIVERSITY OF NEW HAMPSHIRE		
PDA <small>PREPARED BY</small>	03/30/15 <small>DATE</small>	1.0 <small>REVISION</small>